FUNCTIONAL ANALYSIS OF THE *PLG1* GENE FROM *MAGNAPORTHE ORYZAE*

A Dissertation

by

KATHRINA DIZON CASTILLO

Submitted to the Office of Graduate and Professional Studies of
Texas A&M University
in partial fulfillment of the requirements for the degree of

DOCTOR OF PHILOSOPHY

Chair of Committee,	Terry L. Thomas
Committee Members,	Deborah Bell-Pedersen
	Daniel J. Ebbole
	Wayne K. Versaw
Head of Department,	Thomas D. McKnight

August 2015

Major Subject: Biology

ABSTRACT

Magnaporthe oryzae is the causative agent of blast disease, which destroys economically important crops such as rice, wheat and barley. Successful infection relies on the ability of the fungus to sense both environmental and host surface signals at different stages of the disease cycle. Surface sensing is carried out in part by G protein-coupled receptors. This project is focused on the functional analysis of PLG1, a member of the *M. oryzae* PTH11 class of GPCR-like proteins.

Targeted deletion of *PLG1* generated a mutant that is unable to infect intact rice and barley plants, but is capable of invasive growth on wounded leaves. *M. oryzae* requires a hard and hydrophobic surface to develop necessary infection structures. Infection-related morphogenesis assays on a hydrophobic membrane showed that germ tube hooking and apical swelling occurred in the Δ*plg1* mutant, but appressoria formed at only 10% of the wild type frequency. To assess its signaling role, cAMP and diacylglycerol (DAG) were exogenously added to the developing Δ*plg1* spores. On a hydrophobic surface, addition of cAMP alone, DAG alone, and both cAMP and DAG resulted in appressorium formation frequencies of 55%, 39% and 58%, respectively. When similar treatments were done for the Δ*plg1* mutant on a hydrophilic surface, almost no appressoria were observed upon addition of either cAMP or DAG, but appressoria formed up to 17% when both inducers were present. Moreover, evident disease symptoms on barley were observed upon DAG-treatment of the Δ*plg1* mutant.

Also, the transcript level of *PKC*, a gene that is downstream of the DAG-related pathway was found to be significantly reduced in the Δ*plg1* mutant at 24 hours post exposure on Teflon. Taken together, these data suggest a potential role for PLG1 as a major activator of the signaling pathways related to DAG. The last 46 amino acids in the cytoplasmic region of PLG1 weakly interacts with the Gα subunit MagB in a yeast two hybrid assay, strengthening the possibility that PLG1 could be a *M. oryzae* GPCR.

Overall, this body of work contributed to a better understanding of *M. oryzae* appressorium development by defining a good GPCR candidate for transducing signals via the DAG-mediated pathway.

DEDICATION

I dedicate this work to Noelle, Nanay, Ian, and in loving memory of Tatay and Yichun Yang; and to Aldrin, the best motivator and critic rolled into one.

ACKNOWLEDGEMENTS

I would like to express my sincerest gratitude towards my adviser, Dr. Terry L. Thomas, for allowing me to develop into an independent research scientist in his laboratory, for his constant guidance and support in all aspects of my graduate work, and for emphasizing that biology is not merely a course of study but a way of understanding oneself and the things that are happening around. I would like to thank my committee members, Dr. Deborah Bell-Pedersen, Dr. Daniel Ebbole, and Dr. Wayne Versaw. They have asked questions which allowed me to think more thoughtfully about my project and suggested relevant experiments to make sure that I haven't wandered too "far into the woods."

I am grateful for the training I had in the Thomas Lab with Dr. Andrew Tag and Dr. Phillip Beremand. I cannot thank Dr. Tag enough for patiently teaching me the basic molecular biology skills and fungal-related experiments when I was just starting out. He had been very helpful as my constant go-to person for both research and computer issues. I thank Dr. Beremand for all his suggestions to make experiments work better, for his useful comments during practice presentations, and for the stimulating discussions concerning graduate life and teaching. Thanks also go to Chenyu Wang for the company, for asking relevant questions about *M. oryzae* that fostered a better understanding of concepts, and for finding ways to improve our current protocols in studying *M. oryzae*. Life in the lab was easier for the last several years because of them.

I am indebted to Dr. Mark Zoran and Dr. Alisa Womac for teaching me how to use the microscope available at the Shared Instrument Facility in the department. A great part of this research work had been addressed because of their assistance. I also thank Dr. Rigzin Dekhang, Dr. Teresa Lamb, Dr. Xiaorong Lin, Dr. Kathryn Ryan, Dr. Matthew Sachs, Dr. Ana Suescun, Dr. Cheng Wu, and Dr. Ying Zhang for providing methods and resources so I can carry out my experiments, particularly the RNA and protein assays. I also thank Dr. Steve Lockless for addressing questions I had about GPCRs and ion channels. Thanks also go to all friends and colleagues in the department, especially Parul Agrawal, Dr. Bing Zhai, Maria Guevara, past and current members of the Lin, McKnight and Versaw labs for making my time in the department a wonderful experience. I would also like to thank Dr. Brian Shaw from the Plant Pathology Department and Dr. Stansilav Vitha from the MIC for assisting me with microscopy issues in the past.

I am thankful to these people who made graduate life more bearable and living in College Station more enjoyable: Samae and JC Reyes, Joan Hernandez, Madz Maglinao, Roy and Faye Estrada, Jewel Capunitan, Monet Maguyon, Kristian Saguin, Fred Briones, Gally Veluz, Rene Arazo, Ruel Mojica, Ligaya Rubas, Paul Narciso, Bjorn Santos, Noah Badayos, Froilan Aquino, Greg Cubio, KC Canales, Abigail Peralta, and Maritess Arancillo. Special thanks go to Jesselyn and Alnald Javier for hosting the fun events we had and for welcoming Noelle into your home when we needed assistance. Maraming salamat!

TABLE OF CONTENTS

Page

LIST OF FIGURES

Page

LIST OF TABLES

Page

CHAPTER I

INTRODUCTION AND LITERATURE REVIEW

The rice blast disease, considered as the most destructive disease of rice worldwide, is caused by the filamentous ascomycete fungus, *Magnaporthe oryzae* (*M. oryzae*) (Ou, 1980). Recently, the *Molecular Plant Pathology* journal conducted a survey of the Top 10 fungal plant pathogens on the basis of their perceived scientific and economic importance. *M. oryzae* landed in first place, which was hardly surprising, as the fungal pathogen persists in destroying rice (*Oryza sativa*), a staple food for more than half of the world's population (Dean et al., 2012). In several rice growing regions of the world such as North America, Asian countries including India, Korea, Japan, Indonesia and the Philippines, yield losses due to rice blast are estimated to reach up to 50-70% (Widawsky and O'Toole, 1990; Zeigler et al., 1994; Cho et al., 2009; Endo et al., 2009). As with any typical pathogen, the levels of infection are dependent on the following: susceptibilities of the planted cultivars, environmental conditions such as humidity, temperature and soil composition, and the disease management strategies employed by the farmers (McBeath et al., 2010).

M. oryzae attacks not only rice but other economically significant grasses like barley (*Hordeum vulgare*), wheat (*Triticum aestivum*), finger millet *(Elusine coracana*),

oats (*Avena sativa*), Italian millet (*Setaria italica*), weeping lovegrass (*Eragrostis curvula*), and perennial ryegrass (*Lolium perenne*) (Kato et al., 2000; Xu et al., 2007). Wheat blast, for example, is also caused by *M. oryzae*, but its causal agent is a distinct population o f *M. oryzae* called the *Triticum* population which does not infect rice (http://www.k-state.edu/wheatblast/). Nonetheless, wheat blast is an important crop disease across central and southern Brazil, and in some regions in Bolivia, Argentina and Paraguay. Thus far, there is no reported presence of wheat blast outside South America. However, since it remains a threat to wheat crops in the United States, because of possible long distance migration of fungal spores or movement of infected seeds, measures are currently being put in place for a comprehensive wheat blast preparedness plan. (Castroagudín et al., 2014) (http://www.k-state.edu/wheatblast/).

The varying host specialization of *M. oryzae* infection within the Poaceae family which includes rice, wheat, oat, barley and millet, and more than 50 other grass species, clearly suggests that *M. oryzae* belongs to a species complex of fungal populations (Couch et al., 2005). It is for this reason that multilocus phylogenetic studies were done recently, and it revealed that *Magnaporthe* is a polyphyletic genus where *M. oryzae* forms the basal clade that is separated from other species in the family (Zhang et al., 2011). Previously, the asexual stage of the rice blast fungus found in the field was known as *Pyricularia oryzae*. It was then changed to *Pyricularia grisea*, since the rice pathogen was not morphologically distinct from pathogens of related grasses (Rossman et al., 1990). On the other hand, the sexual stage of the rice blast fungus was named

Magnaporthe grisea, until phylogenetic analysis and fertility tests among different strains showed that the *Magnaporthe* isolates should be divided into *M. grisea*, the species that infect Digitaria spp. (crab grass) and *M. oryzae*, the species that infects other isolates, including rice (Couch and Kohn, 2002).

Genetic and molecular tools have allowed researchers to gain a better understanding of the biology of *M. oryzae*. The availability of its genome sequence, coupled with its tractability allowed the hemiobiotrophic *M. oryzae* to evolve as a fungal model for plant-phytopathogen interactions (Dean et al., 2005; Jeon et al., 2013). Such recognition was important, to encourage more efforts into the development of effective strategies for rice blast epidemic prevention and treatment. To date, developing blast resistant crop cultivars still remains as the most economically feasible and environmentally-safe method for controlling the disease. However, cultivars become ineffective within 2 to 3 years, as the fungus overcomes the resistance (Ou, 1980). In order to build a better framework for a long-term and more durable resistance against rice blast, a clearer understanding of its pathogenic activity is required. This chapter discusses the current knowledge about the biology of *M. oryzae*, and the research areas that can be further explored, as potential avenues for preventing *M. oryzae* development on its host plants.

The Pathogenic Lifestyle of *M. oryzae*

Initiation of the rice blast disease cycle, as seen in Figure 1a, occurs when the three-celled *M. oryzae* asexual spores or conidia attach themselves to leaf surfaces via a special adhesive released from the spore tip, called the spore tip mucilage (Hamer and Talbot, 1998). Signaling between the fungus and the plant begins when conidial attachment takes place on the leaf surface (Kolattukudy et al., 1995). After about 2 h post infection (hpi) (Figure 1b), the conidium then germinates and produces a single polarized germ tube from the terminal cell. The germ tube represents the site and developmental stage for perception of the host surface (Figure 1c) (Bourett and Howard, 1990; Mendgen et al., 1996; Beckerman and Ebbole, 1996). Once the germ tube contacts an appropriate inductive surface (i.e. a hard and hydrophobic surface), and it perceives the required physical and chemical signals, it differentiates into a specialized infection structure called an appressorium (Figures 1c-f). Simultaneous to the formation of appressorium, a closed mitotic division takes place within the germ tube or the terminal cell of the conidium. A daughter nucleus then migrates into the incipient appressorium, while another nucleus moves back to the original conidial cell (Howard et al., 1991). A septum then forms between the germ tube and appressorium at around 6-8 hpi (Figure 1e). This completes the mitotic division during the infection cycle. It has been shown that a mass transfer of spore carbohydrates and lipid bodies into the incipient appressorium takes place, and that relocation of these storage products is accompanied by the autophagic cell death of the conidium (Figure 1g).

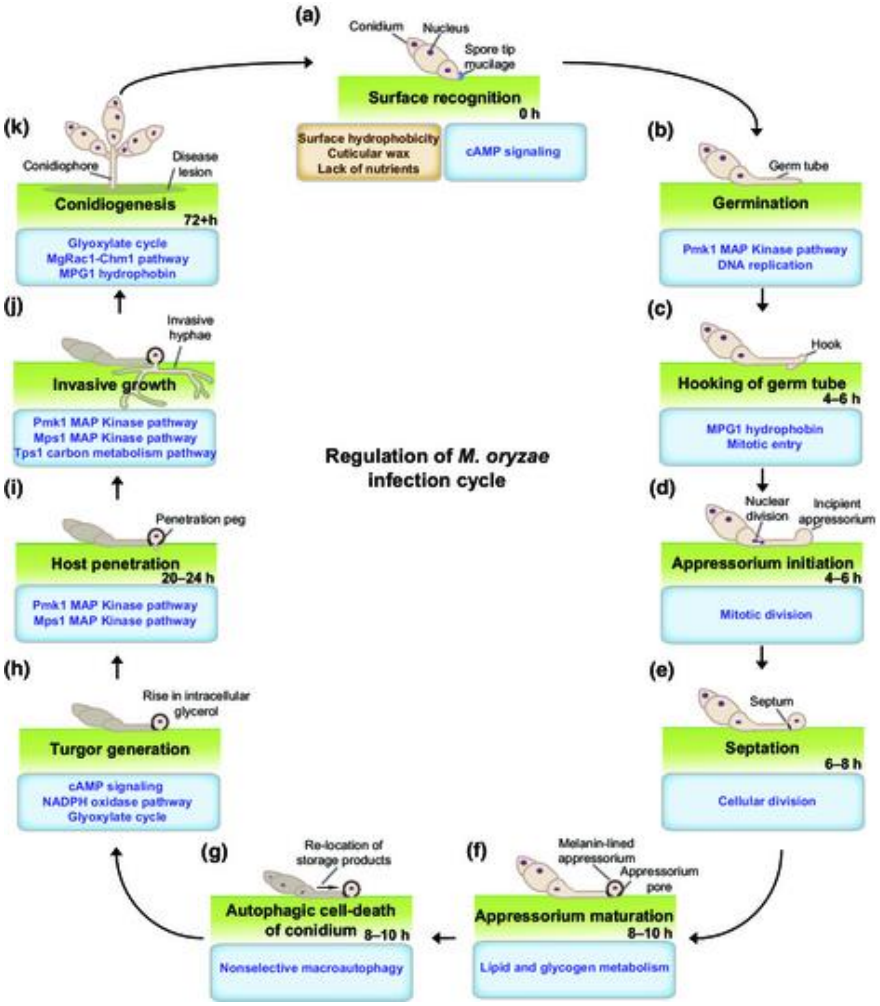

Figure 1. *M. oryzae* Infection Cycle and its Underlying Mechanisms

The *M. oryzae* infection cycle consists of elaborate developmental processes initiated when a viable conidium lands on a plant surface, and progresses when there is a compatible interaction between the fungus and plant host. The green boxes indicate the key processes in the cycle, and the approximate times they occur, following fungal inoculation. The blue boxes specify the hallmark features in each of the process and the characterized genetic components or signaling pathways involved. (Reprinted with permission from Saunders, D.G.O., 2015.)

Subsequent breakdown of the mobilized carbohydrates and lipids results in a large increase in glycerol, the major solute inside the appressorium. (Thines et al., 2000; Veneault-Fourrey et al., 2006). Leakage of glycerol from the appressorium is prevented by the deposition of melanin. Melanin provides a differential permeability barrier in order to generate turgor pressure, up to 8 MPa, within the appressorium. Hence, the mature appressorium is a melanized, dome-shaped structure; and the high turgor pressure translates into a mechanical force that is strong enough to breach the plant surface through the penetration peg (Figure 1h-i) (Talbot, 1995). If all conditions are favorable, appressorium maturation is completed between 15 hpi – 24 hpi.

The penetration peg then develops and it becomes a channel for the translocation of the nucleus and cytoplasmic contents from the appressoria into the growing primary hypha. After about 2 days, a single cell is colonized by the bulbous invasive hyphae (Figure 1j). Live cell imaging showed that the invasive hyphae appeared to scan the plant cell walls before moving into a neighboring cell. It was also observed that the hyphae appeared to constrict as it moves from one cell to another. The hyphal behavior and the level of hyphal constriction are consistent with the idea that hyphae seek out openings in the plant cell wall for cell-to-cell movement, and they utilize the plasmodesmata for such purpose (Kankanala et al., 2007). After 7 days, blast symptoms appear on the leaves. The lesions appear as elliptical spots with gray-colored centers and reddish brown edges, giving a blasted or a burnt appearance to the leaves. From these lesions, new

conidiophores carrying conidia can form and spread to nearby plants via dewdrops, wind or rain (Figure 1k) (Hamer and Talbot, 1998).

In a broader sense, the development of *M. oryzae* on its plant host is two-part due to the fungus' hemibiotrophic nature. It begins with the biotrophic phase where *M. oryzae* requires a close interaction with the host plant as described earlier, and where the plant cells appear healthy as the fungus performs early cell invasion (Kankanala et al., 2007). Then, the fungus switches to a necrotrophic phase, where it takes control of the host defense by deploying effector proteins. These effector proteins are thought to either completely turn off plant defense, or to help the fungus avoid being recognized by the plant resistance proteins (Khang et al., 2010).

In recent years, several studies came out focusing on effector proteins and elegant methods were designed to follow the movement of these fungal proteins in the plant cells. One outcome of these studies of great impact is the discovery of the biotrophic interfacial complex (BIC) where fungal secreted cytoplasmic proteins accumulate and the extra invasive hyphal membrane (EIHM), where secreted apoplastic effectors are found (Khang et al., 2010). These two structures were seen at the interface between the host plasma membrane and the fungal hypha. Such findings shed light on the biotrophic nature of the *M. oryzae*, as it appears to be dependent on some plant signaling processes to initiate pathogenicity. In a highly susceptible interaction, there wasn't a clear switch from biotrophy to necrotrophy. It was observed that the invaded plant cells appeared to

die, by the time the hyphae were ready to move into the next cell (Kankanala et al., 2007; Mosquera et al., 2009; Khang et al., 2010; Valent and Khang, 2010; Zhang and Xu, 2014).

Although there have been significant advancements on the stages in which *M. oryzae* has colonized the plant cells, a comprehensive model on the pre-penetration phase, where signaling between the plant and the fungus plays a key role, has yet to be established. In the next sections, the recognized genetic components and signaling pathways in *M. oryzae* prior to plant penetration will be discussed. By understanding what is currently known and by studying a predicted cell-surface receptor in *M. oryzae*, I hope to shed light on the potential roles of the expanded family of putative receptors found in *M. oryzae*.

Signaling and Transduction Pathways in *M. oryzae* Pathogenesis

Adhesion of Fungal Spores

The first important step for successful infection by *M. oryzae* and for most pathogenic fungi is the attachment of the conidia to the host's surface. In the environment, there are various environmental conditions which cause dislodgment of spores. Hence, it is important for a fungus to develop mechanisms by which its conidia will adhere effectively on its target host (Mendgen and Deising, 1993). *M.* oryzae is known to

release the spore tip mucilage (STM) from the spore apex, which allows it to stick to the plant (Howard and Valent, 1996). It appears to stick better to hydrophobic surfaces than hydrophilic surfaces. STM is pre-formed and stored in the periplasmic regions of the apical conidial cell. A humid condition was found to be necessary for the rapid release of the STM once the conidium encounters the plant surface. This is essentially a passive and energetically-favorable mechanism for the fungus, as the fungus does not have to instantly expend metabolic energy when it needed to secure its position on the plant surface (Hamer et al., 1988). This was demonstrated by the addition of cycloheximide, which is a protein biosynthesis inhibitor in eukaryotes. With cycloheximide treatment, spores were still able to produce STM, suggesting that *de novo* protein synthesis is not required (Breth et al., 2013). However, the adhesion was perturbed with the addition of the lectin concanavalin A (ConA), and degrading enzymes such as α-glucosidase, α-mannosidase and proteases. These findings suggest that STM may have both α-mannosyl and proteinaceous moieties which allow it to work as an adhesive (Hamer et al., 1988; Xiao et al., 1994).

To date, the exact composition of STM remains unidentified, and there are no reports about the genes required for its biosynthesis. It is known however that STM production is dependent on culture age, incubation conditions and isolate type which were determined under standard laboratory conditions. How the variation in the amount of STM affects pathogenicity in the field, is something that is yet to be addressed in the

future (Howard and Valent, 1996). Also, no adhesive glycoproteins have been cloned from any *Magnaporthe* species so far (Osherov and May, 2001).

There are also some genes which are important in the early stages of fungal development on the plant host. A transcription factor encoding gene *TRA1*, which was dependent on the Con7p regulator for its transcription was found to be important in *M. oryzae*, as its deletion led to a significant reduction in conidial adhesion, germination and virulence (Breth et al., 2013). Tra1p-dependent genes were identified from aerial structures and conidia via microarray analysis. Four out of the 11 mutated Tra1p-dependent genes showed promising significance in the biology of *M.* oryzae. First, the transcription factor encoding gene *TDG2* was found to be required for normal adhesion and virulence; and genes *TDG7* and *TDG4* are required for normal sporulation, while gene *TDG6* is required for wild type levels of spore adhesion (Odenbach et al., 2007; Breth et al., 2013).

In other fungal pathogens like *Colletotrichum* spp., the fungal extracellular matrix (ECM) plays a role in adhesion to the host (Hoch and Staples, 1987). In mammalian systems, fibronectin is known to act as an ECM adhesive for several pathogenic bacteria and yeast. The extracellular signals for such interactions are transduced via dimeric transmembrane glycoproteins called integrins. One approach to studying the activity of integrins is through masking or modification of the external integrin domain with antibodies such as the human fibronectin antibody (HGA) or with the tripeptide Arg-

Gly-Asp (RGD). The antibody or the tripeptide have strong affinities to integrins, and thus inhibit the function of integrins in transducing the signals (Klotz and Smith, 1991; Gruenheid and Finlay, 2003; Kwon et al., 2006; Bae et al., 2007). One project studied the effect of HFA and RGD peptide on conidial adhesion and appressorium formation. Both molecules inhibited conidial adhesion and appressorium formation in a dose-dependent manner. The inhibition due to the RGD peptides were rescued by the addition of adenosine 3',5'-cyclic monophosphate (cAMP). Overall, their results indicate that ECM proteins are involved in the early stages of fungal development, mediated by integrin-like receptors and presumably modulated by the cAMP-dependent pathway (Bae et al., 2007).

Spore Germination

Once the spore has attached to the plant surface, germination ensues even in the absence of exogenous nutrients. In *M. oryzae*, a single polarized germ tube typically emerges from the apical and/or basal cell of the spore, while the middle cell rarely germinates and functions as the reservoir for the cellular materials required for appressorial turgor generation. Examination of the germ tubes showed that they are surrounded by an ECM, which ensures close contact between the fungus and its host (Jelitto et al., 1994; Xiao et al., 1994). When a drop of *M. oryzae* conidial suspension was inoculated on a polycarbonate film, conidia settled and some of them were seen to adhere to the surface within 30 min before germ tube formation. They were then allowed to germinate and

germling adhesion was tested by rotating in water for 2 min or even overnight. The experiment resulted in germlings which were resistant to surface removal (Xiao et al., 1994). Moreover, enzymatic treatments similar to the ones described for the STM composition analysis, was performed for the germlings. Once again, α-glucosidase, α-mannosidase and proteases strongly inhibited germling adhesion, suggesting the presence of a glycoprotein mucilage surrounding the conidia and germ tubes (Xiao et al., 1994).

Unlike the release of the STM, formation of germ tubes require active metabolic activities, and thus, may require expenditure of energy from the cells. This also means that some metabolic and signaling pathways may regulate spore germination. In some filamentous fungi like *Fusarium solani* (*F. solani*) and *Aspergillus nidulans* (*A. nidulans*), the cAMP signaling and the mitogen-activated protein (MAP) kinase pathways are thought to mediate conidium germination, respectively (Osherov and May, 2001). In *M. oryzae*, the players in such pathways such as protein kinase A (PKA) or MAP kinase (MAPK) genes such as *PMK1*, *MPS1* or *OSM1* have already been identified, and conidium germination did not appear to be defective in the mutant strains deleted for the aforementioned genes. The results thus downplayed the involvement of either the cAMP or the MAPK pathways in germ tube formation (Xu, 2000).

Interestingly, no mutants that are completely defective in forming the germ tubes have been isolated in *M. oryzae*. A study in *A. nidulans* was performed in which an

enrichment procedure based on the fungicide nystatin was designed to increase the number of heat-sensitive germination-deficient conidia (Osherov and May, 2000). They were able to isolate mutants whose conidia were completely abolished of its ability to form germ tubes, in a germination-inducing media at a restrictive temperature. They defined and identified five of the eight genes lacking in the mutants. Four genes were directly involved in protein synthesis and folding, while the fifth showed a high degree of similarity to malonyl CoA synthetase. They also implicated the Ras signaling pathway involving small GTPases, because conidia with a mutant-activated form of rasA still germinate in the absence of a germination-inducing carbon source. For a model, they proposed that the first essential step in *A. nidulans* conidial germination is the uptake and breakdown of a carbon source, which activates the Ras signaling pathway. This specific pathway or other pathways activate the translation of proteins that initiate a cascade of morphological changes leading to entry into the cell cycle, conidial swelling, and hyphal growth (Osherov and May, 2000). It would be interesting to know too if *M. oryzae* employs the Ras signaling pathway for conidial germination.

Although no mutants blocked in germination were identified for *M. oryzae*, there are several mutants that exhibit delay in germination. Some examples of genes that were found to be important for normal conidial germination are *cdc42*, a member of the Rho family GTP-binding proteins; *MgAGT1* which encodes a serine/threonine kinase; and *MTP1* which encodes a type III integral membrane protein (Liu et al., 2007b; Lu et al., 2008; Zheng et al., 2009; Chen et al., 2014).

It was reported in the early 1970s that fungal conidia in dense populations often do not germinate because of chemicals on the conidia that lead to a phenomenon called self-inhibition. The first identified self-inhibitory chemical was methyl cis-3,4-dimethoxycinnamante and was found in the stripe rust fungus, *Puccinia striiformis* (Macko et al., 1971). The self-inhibitors are characterized to be small, lipophilic molecules that allow the conidia to germinate under favorable conditions. In a study conducted by Hedge and Kolattukudy, they reported that rice leaf surface wax and other plant surface waxes stimulated germination and appressoria formation in *M. oryzae*. They observed that when the conidial concentration was low, there was no wax requirement for germination. However, as the conidial density increases, there is also a greater requirement for the amount of wax to complete germination and subsequent appressorium formation. They proposed that the plant waxes relieved the self-inhibition caused by the conidia, and that in *M. oryzae*, the requirement for any hydrophobic surface, and not necessarily a host-specific wax, is precisely for counteracting the inhibitory molecules from the conidia. Although the nature of the conidia surface molecules in *M. oryzae* is not clear, the researchers proposed that the use of these lipophilic self-inhibitors most likely evolved in the successful phytopathogenic fungi, so they can adapt to the lipophilic nature of the plant surface (Hegde and Kolattukudy, 1997). As the plant surface wax is the first host component that the fungus encounters, undoubtedly, it serves as a communicator in the plant-pathogen interactions, which triggers pathways related to fungal development.

Appressorium Formation

Surface Cues for Appressorium Formation

Appressorium formation in fungal pathogens is triggered by thigmotropic cues on host surfaces (Hoch and Staples, 1991; Gilbert et al., 1996). Thigmotropism refers to the movement or orientation of an organism or a single cell with respect to the topography, shape and physical features of the surface where it is developing (Brand and Gow, 2012). As an example, the germ tubes of the bean rust fungus, *Uromyces appendiculatus* sense the height of the stomatal guard cells as a signal for forming the appressorium directly over the stomata (Hoch and Staples, 1987). The cereal pathogen *Bipolaris sorokiniana*, which causes foliar lesions similar to *M. oryzae*, is known for the thigmotropic growth of its hyphae along the grooves of barley epidermal cells. The appressoria they formed were also frequently found in those grooves (Jansson and Åkesson, 2003). In the case of *M. oryzae*, the fungus directly penetrates the host cuticle via an appressorial peg rather than entering into natural openings.

Surface hydrophobicity and hardness are considered to be the important surface cues for appressorium formation in *M. oryzae* (Jelitto et al., 1994; Xiao et al., 1994; Liu et al., 2007a). Several studies have shown that the frequency of appressorium formation is strongly correlated with the degree of surface hydrophobicity (Howard et al., 1991; Lee and Dean, 1993; Beckerman and Ebbole, 1996).

In the past, it was not clear if surface hydrophobicity was necessary and sufficient in triggering appressorium formation. The conundrum is due to results showing that appressorium formation does not occur even on some artificial hydrophobic surfaces with varying physicochemical properties, such as hardness (Xiao et al., 1994). Moreover, it was reported that variability among strains exists and that a clear relationship between surface hydrophobicity and appressorium formation cannot be established (Hardham, 1992; Jelitto et al., 1994). In 2007, the mutant Δ*rgs1* that is deficient of an RGS domain-containing protein, was characterized and was shown to form appressoria even on non-inductive surfaces (Liu et al., 2007a). It appears that the signaling for appressorium development was constitutively active in the Δ*rgs1* mutant. However, when the Δ*rgs1* mutant was tested on soft surfaces regardless of hydrophobicity, they failed to form appressoria. This suggested that surface hydrophobicity alone is not sufficient for appressorium differentiation, and that hardness (surface rigidity of about 150 kilopascals) was also an important and necessary requirement for such process to take place (Liu et al., 2007a).

Chemical Cues for Appressorium Formation

In addition to surface hardness and hydrophobicity, it can be imagined that the components of the host plant cuticle themselves, can trigger appressorium formation. Surface waxes and a hydroxy fatty acid polymer called cutin, are the major components of the cuticle layer (Kolattukudy, 1980). Cutin is known to be degraded into its

monomeric units, consisting of C_{16} and C_{18} aliphatic chains, by hydrolytic enzymes called cutinases. Cutinases have been identified in some fungal pathogens, and were shown to be important for the early stages of infection such as germination (Kolattukudy, 1985).

It has been proposed that the products of cutin degradation may also induce appressorium formation, so synthetic analogs of the cutin monomers were tested to verify such ideas (Gilbert et al., 1996). Some of the compounds that were found to selectively induce appressorium formation of *M. oryzae* on artificial substrates were 1,16-hexadecanedial, 1,16-hexadecanediol, cis-9,10-epoxy-18-hydroxyoctadecanoic acid, and cis-9-octadecen-1-ol. When the hydrophobicity indices of artificial substrates were tested upon addition of such chemicals, they remained unchanged. This implied that the biological response of the germ tubes to the cutin monomers was chemical in nature, rather than a thigmotropic one (Gilbert et al., 2006).

In addition to cutin, the plant surface is also composed of waxes that are made up of primary and secondary alcohols, alkyl esters, alkyl aldehydes, long chain fatty acids and alkanes (Uchiyama and Okuyama, 1990). When hydrophilic surfaces were coated with fractions of these waxes, the primary alcohols 1-octacosanol (C28) and 1-triacontanol (C30), and the long chain alkanes nonacosane (C29) and hentricacontane (C31) were shown to induce appressorium formation in *M. oryzae* (Liu et al., 2011b).

Fungal-Based Cues for Appressorium Formation

Fungal secretions or cell wall components are also known to either trigger or enhance appressorium differentiation. Hydrophobins are examples of fungal cell wall proteins which mediate surface dependency and fungal development (Wösten et al., 1994). In *M. oryzae*, the hydrophobin encoding gene *MPG1* was knocked out and its deletion led to reduced appressorium formation (Talbot et al., 1993; Beckerman and Ebbole, 1996). Hydrophobins are known to coat the conidia and other aerial structures of the fungus. A mutant that is deficient in hydrophobin production is characterized to be easily wettable, i.e. when the growing fungal culture on a plate is flooded with water, the hyphae soak up the water rather than repel it, and mutant conidia is easily suspended in water. The ability of the hydrophobin protein to self-assemble led to the idea that its accumulation might provide a sensing mechanism for surface hydrophobicity and allows the germlings to adhere properly to the hydrophobic surface (Talbot et al., 1993; Beckerman and Ebbole, 1996; Talbot et al., 1996). This idea was reinforced by the results in which the appressorium formation defect of the Δ*mpg1* mutant was rescued upon co-inoculation with wild type cells. Furthermore, when substrates such as the hydrophobic side of GelBond was tested, it can also support appressorium formation in the Δ*mpg1* mutant. Hence, *MPG1* is most likely not involved in appressorium morphogenesis per se, but is required to signal the presence of an inductive host surface (Beckerman and Ebbole, 1996; Kershaw et al., 1998).

It is also believed that the appressoria adhere tightly to the hydrophobic surface due to a ring of appressorium mucilage (Howard et al., 1991). Similar to the STM from the conidia, the appressorium mucilage is suggested to contain lipids, proteins and sugars. Treatment of appressoria with proteases and lipid or glycoprotein synthesis inhibitors led to a reduced bonding strength between the appressoria and the hydrophobic surface (Ebata et al., 1998).

Intracellular Signaling Pathways Involved in Appressorium Formation

Several genes and signaling transduction pathways leading to appressorium formation have been identified in *M. oryzae*. Due to the availability of background information from other model organisms, most of the molecular approaches in *M. oryzae* have focused on the intracellular signaling cascades (Lee and Dean, 1993). These highly conserved signaling pathways are not only necessary during fungal growth and development, but are also important in modulating host-pathogen interactions. In *M. oryzae*, signaling mechanisms implicated in appressorium formation include the cAMP, MAPK, and to a lesser extent the Ca^{2+} signaling pathways (Xu and Hamer, 1996; Choi and Dean, 1997; Dean, 1997; Adachi and Hamer, 1998; Lee and Lee, 1998).

In eukaryotes, the cAMP signaling pathway is initiated when the perceived signal drives the conversion of ATP to cAMP via adenylate cyclase, and subsequent activation of protein kinase A by cAMP binding to its regulatory subunit. Such binding changes the

conformation of the kinase, allowing the release of its catalytic subunit, which then phosphorylates downstream target proteins. In *M.* oryzae, the adenlyate cyclase, protein kinase A, and the catalytic subunit of protein kinase A are MAC1, PKA, and cPKA, respectively. When the *MAC1* was targeted for deletion, it resulted in mutants which cannot form appressoria, and were non-pathogenic. There were also pleiotropic effects which include reduction in conidiation, hyphal growth, and sexual development (Choi and Dean, 1997). Appressorium formation was restored in the Δ*mac1* mutants through addition of cAMP or by a bypass suppressor of the Δ*mac1* phenotype, *SUM1* arising from a mutation in the regulatory subunit gene of PKA that caused constitutive PKA activation (Choi and Dean, 1997; Adachi and Hamer, 1998). Moreover, hyphal growth, and sexual and asexual development were restored in the *SUM1* strain. However, the *sum1* mutation only partially suppressed the pathogenicity defect of the Δ*mac1* mutant. When PKA assays were performed, results revealed that the catalytic subunit gene, *CPKA*, is the only gene which encodes detectable PKA activity in *M. oryzae*. The *cpkA* deletion mutants showed reduced pathogenicity on host leaves. They were delayed in appressorium formation but nonetheless formed appressoria at wild type levels at 24 h. Although they formed melanized appressoria, they were unable to penetrate the plant cells. When inoculated on wounded leaves however, they formed lesions. They had no defects on hyphal growth, and sexual and asexual morphogenesis. Taken together, these results indicate the presence of divergent cAMP signaling pathways specific for either fungal cell development or pathogenesis (Xu and Hamer, 1996). The non-pathogenic phenotype despite the formation of what appears like normal appressoria, points to the

idea that the required turgor pressure is not achieved in the Δ*cpkA* mutant appressoria. This was confirmed by a study showing that the glycerol content of the Δ*cpkA* mutant appressoria was not sufficient to reach the required turgor pressure, because of the delay in lipid and glycogen degradation leading to glycerol accumulation (Thines et al., 2000).

In addition to genetic analysis, the role of cAMP in appressorium morphogenesis was confirmed by direct measurement of cellular cAMP in germ tubes developing on either an inductive or non-inductive surface for appressorium formation. It has been observed that cAMP levels were higher in *M. oryzae* growing on an inductive surface, rather than a non-inductive surface (Liu et al., 2007a). Overall, the cAMP studies in *M. oryzae* allowed for a straightforward assay in looking at placement of genes in signaling pathways, through the addition of exogenous cAMP or its analogs. They also paved the way for cAMP signaling-related studies in other pathogenic fungi like *Blumeria, Colletotricum*, *Fusarium*, and *Sclerotinia* species (Oh et al., 2008).

Aside from the cAMP pathway, the MAPK signaling pathway is also well-studied in *M. oryzae* (Xu and Hamer, 1996). MAPK stands for mitogen-activated protein kinase, and is part of the highly conserved serine/threonine protein kinases in eukaryotes, involved in several cellular processes like cell proliferation, differentiation, locomotion, stress response, regulated cell death and survival (Cargnello and Roux, 2011). The conventional MAPK signaling begins with the stimulus activating one or more MAPKK kinases (MAPKKKs) receptor-dependent and -independent mechanisms. The

MAPKKKs then phosphorylate a downstream MAPK kinase (MAPKK), which subsequently phosphorylates and activates MAPKs. The activated MAPKs then phosphorylate target proteins with specific biological processes (Plotnikov et al., 2011). In *M. oryzae*, the PMK1 protein exhibits extensive similarity to the *S. cerevisiae* MAPKs Fus3 and Kss1. In fact, it complements the mating defect of the Δ*fus3*Δ*kss1* double mutant. Deletion of *PMK1* led to mutants incapable of forming appressoria and were non-pathogenic on either intact or wounded host leaves. Interestingly, addition of cAMP to the Δ*pmk1*mutants only restored germ tube hooking and swelling, which are the early phases of appressorium formation (Xu and Hamer, 1996). Thus, it has been proposed that PMK1 lies downstream of the cAMP signaling pathway. However, the direct interacting components of each pathway remains to be identified (Choi and Dean, 1997; Xu, 2000).

In addition to *PMK1*, another MAP kinase homolog in *M. oryzae* is *MPS1*. *MPS1* is not required for appressorium formation, but is essential for host penetration, cell wall integrity and invasive growth. It was also found to regulate the accumulation of α-1,3-glucan, a sugar comprising the outer cell wall layer, which is thought to protect phytopathogenic fungi against chitinases as they infect the plants (Xu et al., 1998). Consistent with its function after the penetration phase, it was shown to interact with two transcription factors, MIG1 and MoSWI6 which are required for invasive growth and oxidative stress response, respectively (Mehrabi et al., 2008; Qi et al., 2012).

As introduced earlier, *M. oryzae* should generate appressorial turgor pressure to drive the penetration peg into the plant. Upon investigation of the genetic control of cellular turgor, another MAP kinase-encoding gene, OSM1 was identified, upon assaying for the response of *M. oryzae* to hyperosmotic stress. Disruption of the *OSM1* gene resulted in mutants that still had normal glycerol content and turgor in the appressoria, and hence were still pathogenic. However, the Δ*osm1* mutants showed hyphal defects upon exposure to hyperosmotic conditions. Such results suggest that separate signaling pathways are involved in cellular turgor during hyperosmotic stress, and turgor associated with appressorium-mediated plant infection (Dixon et al., 1999). One of the characterized downstream targets of OSM1 is the basic leucine zipper (bZIP) transcription factor MoATF1, which is responsible for modulating response to reactive oxygen species (ROS). The Δ*Moatf1*is defective in plant infection and this defect is rescued by addition of ROS scavenging compounds (Guo et al., 2010).

One of the less studied signaling pathways in filamentous fungi, including *M. oryzae* is the one mediated by calcium (Nguyen et al., 2008). In calcium signaling, Ca^{2+} pumps and transporters play a major role in keeping the resting cytosolic free Ca^{2+} concentration, $[Ca^{2+}]_c$ at extremely low levels in eukaryotic cells. When relevant stimuli are perceived by G protein-coupled receptors (GPCRs), phospholipase C (PLC) is then activated by the G protein. PLC hydrolyzes membrane-bound phospholipid phosphatidylinositol 4,5-bisphosphate (PIP_2) into diacylglycerol (DAG) and inositol 1,4,5-trisphosphate (IP_3). DAG remains bound to the membrane, while IP_3 is released

and diffuses into the cytosol to bind with receptors, which include calcium channels in the smooth endoplasmic reticulum. This activation leads to a transient increase in $[Ca^{2+}]_c$ and Ca^{2+} ions serve as secondary messengers that trigger downstream pathways mediated by protein kinase C (PKC) and Ca^{2+}/calmodulin (CAM)-binding kinases. Such pathways are important to processes involving circadian timing, cell cycle, cellular morphogenesis and stress responses (Bush, 1993; Stull, 2001).

Most of the studies implicating calcium signaling in filamentous fungi were done using imaging analysis or with the addition of pharmacological agents that disrupt Ca^{2+} fluxes or interfere with calcium-binding proteins. For example, the addition of extracellular Ca^{2+} and DAG had been shown to induce appressorium formation, in *U. appendiculatus* and *M. oryza*e, respectively (Hoch and Staples, 1987; Thines et al., 1997).

To further explore the relationship between calcium signaling and fungal development in *M. oryzae*, a study reported the effects of calcium chelators such as EGTA (ethylene glycol tetraacetic acid) and A23187 (a calcium ionophore), antagonists of the potent calcium binding protein calmodulin which inhibit calcium signaling, and the PLC inhibitor neomycin. Upon addition of EGTA and A23187 on wild type spores, appressorium formation was inhibited on both non-inductive and inductive surfaces, but not conidia germination. The appressorium differentiation defect was rescued by the exogenous addition of Ca^{2+} on inductive surfaces, but not on a non-inductive surface. This suggested that Ca^{2+} influx is necessary but not sufficient in appressorium formation,

and that a sustained level of cytosolic Ca^{2+} is most likely required throughout differentiation (Lee and Lee, 1998). Sodium and potassium ionophores were also tested, but they didn't appear to have roles in conidial germination and appressorium formation, since both processes were not affected. Neomycin also inhibited appressorium formation, but not conidia germination, suggesting the importance of PLC in appressorium formation (Lee and Lee, 1998). Several years later, a targeted gene deletion of the *MoPLC1* gene was done and results showed suppressed calcium flux via imaging of the intracellular calcium levels, which led to mutants which were delayed in appressorium formation and were non-pathogenic on rice. Moreover, the appressorium formation defect of the Δ*MoPLC1* mutant was rescued by the addition of either Ca^{2+} or DAG, or both, but still not to wild type levels (Rho et al., 2009)

In 2008, an extensive functional analysis of calcium-signaling proteins in *M. oryzae* was reported, arising from gene knockdowns using a high-throughput RNA silencing system (Nguyen et al., 2008). The genes targeted for silencing encoded calcium-related signaling proteins such as Ca^{2+} permeable channels, pumps and transporters, phospholipase C, calcineurin, calnexin and other calcium-binding proteins. Although the authors recognize the possible off-target effects of the RNA silencing system, their results first demonstrated the involvement of Ca^{2+} pumps calreticulin and calpactin in *M. oryzae* pathogenicity. Moreover, out of the 37 genes they examined, 35 appeared to be involved in sporulation, while 22 were associated with appressorium formation. Interestingly, defects in the mutants did not necessarily translate to reduction in fungal

virulence. Their results indicate that calcium homeostasis is most likely essential to pathogenesis-related development on the host surface, but may not play a big role once the fungus has invaded the host cell (Nguyen et al., 2008). However, as mentioned earlier, when the phospholipase gene *MoPLC1* was knocked out, fungal virulence was affected (Rho et al., 2009). Perhaps, the knockdown using RNA silencing did not completely eliminate the *PLC* gene expression required for virulence, or a different *PLC* version had been knocked down instead.

More recently, further involvement of the pathways mediated by DAG has been reported (Sadat et al., 2014). DAG is actually not a single molecular species but several molecules with varying acyl chain lengths and saturation levels (Deacon et al., 2002). The involvement of DAG in *M. oryzae* appressorium formation was first reported by Thines et al., where they tested different DAGs including 1,2-dioctanoyl-*sn*-glycerol (*sn*-DOG), 1,2-dioctanoyl-*rac*-glycerol (*rac*-DOG), 1-oleoyl-2-acetyl-*sn*-glycerol (*sn*-OAG) and 1-oleoyl-2-acetyl-*rac*-glycerol (*rac*-OAG). When these were tested on spores, only *sn*-OAG and *sn*-DOG were shown to be the effective in inducing appressorium formation on hydrophilic surfaces (Thines et al., 1997). Hence, in addition to cAMP and its more water-soluble analog 8-Bromo-cAMP, either *sn*-OAG or *sn*-DOG which will be simply called DAG throughout this thesis, can be used to place genes under different signaling pathways.

DAGs are synthesized either *de novo* or through the activation of GPCRs as mentioned earlier. A recent study suggested that *de novo* synthesis of DAG via the activity of lipid phosphate phosphatases, is important for pathogenesis. Targeted disruption of five genes encoding putative lipid phosphate phosphatases resulted in two mutants, *MoLPP3* and *MoLPP5*, which were defective in plant infection. Fungal virulence defects of the mutants were rescued with the addition of DAG.

Putative Sensors of Extracellular Signals for Appressorium Formation

The *CBP1* gene encodes a putative extracellular chitin-binding protein, and it was shown to be involved in appressorium formation, as the *CBP1* null mutant formed normal appressoria on the plant leaf surface, but not on artificial hydrophobic surfaces (Kamakura et al., 2002). The addition of known appressorium inducers such as cAMP, DAG and 1,16-hexadecanediol rescued the appressorium differentiation defect on the artificial surfaces. As a consequence of appressorium formation on the plant surface, the *CBP1* null mutant was pathogenic on rice leaves. CBP1 is a hydrophilic protein with no obvious transmembrane domains, but its C-terminal region contains chitin-binding domains with serine/threonine (Ser/Thr)-rich regions. It is proposed to be localized to the cell wall where the Ser/Thr cluster may act as a sensor. CBP1 appeared to be important for the recognition of physical factors on solid surfaces (Kamakura et al., 2002).

PTH11 was previously identified as a plasma membrane protein which was proposed to act as a GPCR in sensing hydrophobicity. Mutants lacking *PTH11* formed between 10-15% appressoria of the wild type frequency on an inductive surface. This finding indicated that *PTH11* is not required for appressorium morphogenesis per se, but may be involved in the completion of appressorium differentiation in response to surface recognition (DeZwaan et al., 1999). Although it has not been shown biochemically to interact with G proteins to be classified as a GPCR, it is currently the receptor depicted in models to be sensing hydrophobicity and transducing signals via heterotrimeric G protein signaling (Ramanujam et al., 2013).

The originally annotated GPCRs in filamentous fungi fall into five classes namely, cAMP receptor-like proteins, carbon sensors, microbial opsins, putative nitrogen sensors and pheromone receptors (Li et al., 2007). The classical seven transmembrane (7-TM) GPCR signaling begins when a ligand binds to the N-terminal region of the GPCR, leading to a GDP (guanosine diphosphate) to GTP (guanosine triphosphate) exchange on the Gα protein subunit, and dissociation of the Gα and the Gβγ subunits (Neves et al., 2002). Either subunit can regulate downstream pathways. When GTP is hydrolyzed, the GDP-bound Gα reassociates with the Gβγ dimer. RGS (regulator of G protein signaling) proteins are known to increase the rate of GTP hydrolysis, and thus modulate signal perception and downstream pathway activation (Neves et al., 2002). Because of the availability of genome sequences, it has been possible to identify more putative GPCR-

like proteins in filamentous fungi. However, some GPCR-like proteins do not appear to have 7-TM helices, perhaps due to annotation or sequence errors (Li et al., 2007). In *M. oryzae*, there is limited information about the functions of transmembrane receptors of various classes. In a comprehensive review by Li et al., homologs of functionally characterized receptors in other filamentous fungi, had been identified in *M. oryzae*. Pheromone receptors include MGG06452 and MGG04711; cAMP receptors include MGG11962, MGG06257 and MGG06738; carbon sensors include MGG08803 and MGG00258; nitrogen sensors include MGG04698 and MGG02855; and one opsin MGG09015 (Li et al., 2007). None of these possible paralogs have been characterized in *M. oryzae*.

After the release of the *M. oryzae* genome for the wild type strain 70-15, Kulkarni et al. annotated three new classes of predicted GPCRs in *M. oryzae*, namely PTH11-like GPCRs, proteins related to the *Homo sapiens* mPR steroid receptor and a protein with weak sequence similarity to the rat growth hormone releasing factor (Kulkarni et al., 2005). Of particular interest were the PTH11-related proteins because of their possible involvement in appressorium formation. Remarkably, no genes encoding PTH11-like proteins were identified in the annotated genomes of basidiomycetes *U. maydis* and *C. neoformans*, but some homologs were identified in some ascomycetes such as *N. crassa* and *A. nidulans*, suggesting possible pathogenicity roles. Moreover, the PTH11-like proteins containing the extracellular fungal-specific CFEM domain (eight cysteine-containing domain) appears to be highly represented in *M. oryzae* (Kulkarni et al., 2005).

Although not much is known about the transmembrane receptors in *M. oryzae,* the G protein subunits have been characterized in detail. Most filamentous fungi possess three Gα subunits that are members of distinct classes. *M. oryzae* has the Gα subunits MagA, MagB and MagC. Of the three Gα subunits, only MagB was shown to be required for growth, conidiation, appressorium formation, and sexual reproduction while, MagA and MagC only appeared to be involved in post-fertilization events (Liu and Dean, 1997). All three Gα subunits however, were shown to interact with the identified RGS in *M. oryzae,* RGS1. The phenotype of the Δ*rgs1* mutants had been described in earlier, in the section discussing the requirement for a hard surface for appressorium formation (Liu et al., 2007a). In addition to the Gα subunits, PTH11 was also shown to interact with RGS1 during infection-related development. This provides further evidence on the involvement of PTH11 in GPCR signaling (Ramanujam et al., 2013).

There are two Gβ subunits in *M. oryzae* namely Mgb1 and Mgb2. The deletion of Mgb1 led to mutants which have reduced conidiation, lacked appressoria, and were defective in penetration. Addition of cAMP rescued appressoria formation, but the appressoria looked abnormal in shape, and could still not penetrate. Elevated Mgb1 protein levels promoted appressoria formation, even on non-inductive surfaces (Nishimura et al., 2003). Similarly, disruption of the gene encoding the Gγ subunit Mgg1 via T-DNA insertional mutagenesis, also led to mutants which were defective in appressorium formation, penetration and infectious growth. Addition of cAMP led to results similar to those in Mgb1. Also, mating appears to be incapacitated in the *mgg1* mutants because

only a few perithecia or fruiting bodies were observed after mating assays with an appropriate mating type strains (Liang et al., 2006).

With the wealth of information available for the various genes involved in initiating infection, a model depicting their roles in the conserved eukaryotic signaling pathways seems necessary. The most recent model is presented in Figure 2, where some additional upstream and downstream genes are shown. One simplification that is noticeable in this model, is the perceived interaction between PTH11 and any of the Gα subunits. Thus far, there is no biochemical evidence regarding such interactions, although PTH11 was indeed shown to interact with RGS1 (Ramanujam et al., 2013).

Although it appears that these pathways function in parallel and independent of each other, it has long been proposed that extensive crosstalk takes place among the *M. oryzae* signaling transduction pathways. However, most of the genes and proteins linking these pathways, specifically with regards to surface recognition and appressorium morphogenesis, are yet to be examined in detail to establish relationships at the DNA and protein levels. Crosstalk is a consequence of second messengers in multiple signaling pathways. Since cAMP, DAG and Ca^{2+} act as second messengers in *M. oryzae* signaling, there is a high probability that inputs from one pathway affect downstream effectors in other pathways, either through a linear or feedback fashion. Interaction between pathways allows for better fine tuning of how the cell regulates its activities (Smékalová et al., 2014).

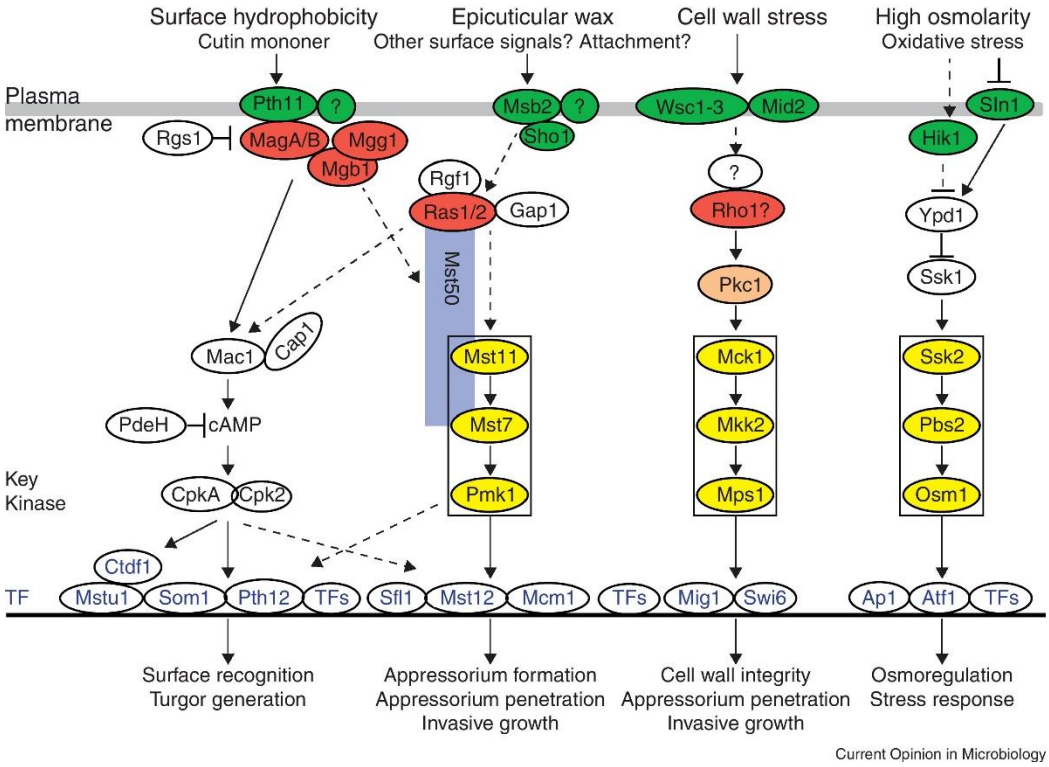

Figure 2. Signaling Pathways Involved in Infection-Related Morphogenesis in *M. oryzae*

The elaborate developmental processes in the *M. oryzae* infection cycle is supported by a number of gene products assigned under different conserved eukaryotic signaling pathways. Detection of surface signals or ligands is the role of transmembrane receptors (green), which are classified either as a GPCR or an ion channel. Signals relayed via GPCRs involve G protein subunits or small GTPases (red). The three MAP kinase cascades (yellow) and cAMP-related proteins (black text and unshaded) are well-characterized as a result of homology studies with other characterized cAMP and MAP kinase-related proteins in other eukaryotes. The sole characterized protein kinase C is shown in orange. The downstream effectors of the signaling cascades are transcription factors (blue text and unshaded). (Reprinted with permission from Li et al., 2012.)

Functional Analysis of the BIP1 Transcription Factor in *M. oryzae*

In an unpublished study conducted by Tag et al. (in preparation), restriction enzyme-mediated integration or REMI was utilized to identify non-pathogenic mutants in *M. oryzae* wild type strain P1.2. In the screen, mutant M763 was selected for further analysis, as it showed reduced penetration efficiency and infectious growth. The gene disrupted in M763 encodes a basic leucine zipper (bZIP) transcription factor, named BIP1 for B-ZIP Involved in Pathogenesis1. BIP1 is proposed to control a novel gene regulatory network involved in a "shock and awe" mechanism that overwhelms the plant host's physical and biological defenses during the early stages of infection. Deletion of *BIP1* by targeted gene replacement resulted in Δ*bip1* mutants which developed melanized appressoria but were unable to penetrate detached or wounded host leaves (Tag et al., in preparation).

Upon analysis of BIP1 transcript levels using qRT-PCR, results showed that the *BIP1* mRNA was expressed at about the same levels in spores and 24 h appressoria, while lower levels (15 fold) were seen in mycelia. When the kinetics of expression was analyzed by collecting RNA from different time points at which Guy11 spore suspensions were inoculated on barley leaves, maximum expression of *BIP1* transcript was found at 17 hpi, although significant expression was already detected as early as 8 h (Tag et al., in preparation). Further studies confirmed that *BIP1* controls expression of a distinct set of *M. oryzae* genes in the appressorium. Microarray analysis using total RNA isolated from

wild type P1.2 and Δ*bip1:hph* appressoria differentiated on Teflon membrane at 24 h, identified 44 significantly downregulated genes and surprisingly, no upregulated genes. Four of the BIP1 down-regulated genes encode PTH11-like GPCRs. Electrophoretic mobility shift assays (EMSA) showed that BIP1 specifically binds to the promoter elements of three of the four genes encoding PTH11-like GPCRs. These are *MGG01884.6*, *MGG03584.6* and *MGG06535.6*. So far, the proteins encoded by *MGG01884.6*, *MGG03584.6* and *MGG06535.6* are described only as putative signaling molecules which may be involved in detecting the presence of the plant plasma membrane and may signal the initiation of the penetration phase (Tag et al., in preparation). The specific functions of these four BIP1-regulated PTH11-like GPCRs are yet to be determined.

Research Aims

This project will analyze the function of *MGG03584.6* which encodes a PTH11-related protein, and is one of the downregulated genes in the Δ*bip1*strain. This gene had been named *PLG1* (PTH11-like GPCR 1). In Chapter II, a comparison between PLG1 and PTH11 based on *in silico* analysis will be presented. The major hypothesis is that similar to PTH11, loss of *PLG1* from the genome will preempt or limit initiation of host penetration and further infection. As a receptor, PLG1 is predicted to interact with one or more ligands enabling it to recognize the plant host. These ligands may be associated with surface cues for properties such as hydrophobicity and hardness, or other

environmental cues such as nutrients, humidity, light or temperature. Alternatively, the ligand may also be fungal-based, as a result of fungal response to host surface interaction. The kinetics of *PLG1* gene expression on Teflon membrane, an inductive surface for appressorium formation, determined through qRT-PCR experiments will also be discussed in the following chapter.

Functional analysis of PLG1 may increase our knowledge of the possible roles that the numerous transmembrane receptors predicted to be in the *M. oryzae* proteome have, and will yield additional insights into the downstream targets of the signaling pathways involved in the pre-penetration stage. If PLG1 is shown to be important for infection-related morphogenesis, it is also a goal to discover possible crosstalk mechanisms between the known intracellular signaling pathways. These studies are presented in Chapters III and IV. Since PLG1 is a predicted GPCR, it is also of interest to confirm whether or not it behaves as a canonical GPCR, primarily through a possible interaction with the known G proteins in *M. oryzae*. The outcomes for such studies will be presented in Chapter V. If PLG1 has a key role in the *M. oryzae* disease cycle, PLG1 or the extracellular stimulus it perceives may serve as a target for fungicide development or genetic modification which may provide durable control of rice blast disease in the years to come.

CHAPTER II

PLG1 IS A PREDCITED PTH11-LIKE GPCR

Introduction

The genome sequence of the rice pathogenic strain of *M. oryzae* 70-15 was completed in 2005 (Dean et al., 2005). Analysis of the *M. oryzae* genome sequence revealed genes encoding a diverse set of secreted proteins, an expanded family of G-protein-coupled receptors (GPCRs), new virulence-associated genes and enzymes associated with secondary metabolism (Dean et al., 2005). Of particular interest among these *in silico* identified *M oryzae* genes are the GPCRs.

GPCRs constitute a large family of receptors encoded by genes present in diverse eukaryotic species. GPCRs transduce signals from the extracellular environment to the cellular machinery that controls metabolism, growth and development (Van Dijck, 2009). GPCRs are characterized by seven transmembrane (7-TM) α-helices whose extracellular amino termini interact with a ligand, and whose intracellular carboxyl termini interact with heterotrimeric G proteins (Kulkarni et al., 2005). A G protein is a trimer of α, β and γ subunits (Gα, Gβ, and Gγ, respectively) and is rendered inactive when the Gα subunit is bound to GDP and is active when the Gα subunit is bound to GTP. A GPCR is activated when a specific ligand binds to its amino terminus. This results in a conformational change in the receptor which activates the G protein by

facilitating GDP-GTP exchange. This exchange leads to the release of the Gβγ dimer. The GTP-bound Gα and the released Gβγ dimer are then able to independently control the activity of downstream signaling pathways (Liu et al., 2007c; Kumamoto, 2008).

To successfully infect a plant host, *M. oryzae* must overcome the plant's innate immune system and direct various plant host processes to favor its growth (Dean et al., 2005). Since interaction of *M. oryzae* with plants requires contact sensing, it is likely that GPCRs are important in fungal perception of environmental and plant-surface signals. Kulkarni et al. identified 76 GPCR-like proteins in the *M. oryzae* proteome, which represent the largest number of receptor-like proteins reported in fungi. The amino acid sequences of previously characterized GPCRs from the GPCR database (GPCRD) were used as query sequences in a protein BLAST search (BLASTP) against the predicted *M. oryzae* proteome, with an E-value limit of 1×10^{-9} (Kulkarni et al., 2005). One of the characterized receptors which plays a role in *M. oryzae* pathogenicity is PTH11. *PTH11* encodes a plasma-membrane receptor that responds to the presence of hydrophobic surfaces. *PTH11* mutants are non-pathogenic because of defects in appressorium differentiation. On inductive surfaces, Δ*pth11* mutants still form appressoria but at a significantly lower frequency compared to wild type. DeZwann et al. concluded that *PTH11* is not crucial for appressorium morphogenesis but is most likely involved in plant host surface recognition and/or response (DeZwaan et al., 1999). With the relevance of PTH11 as surface receptor, Kulkarni et al. then used the PTH11 sequence as a query sequence in an independent BLASTP search against the *M. oryzae* proteome.

Out of the 76 GPCR-like receptors predicted in the proteome, 61 of them were found to be similar to PTH11. These proteins were classified under the PTH11 class of cell receptors in *M. oryzae*.

The identification of the PTH11-like GPCRs in *M. oryzae* represents an important finding as these new putative receptors may have functions in established signaling pathways, or novel pathways that may be involved in fungal development and pathogenicity. This chapter describes the sequence comparison between PTH11 and PLG1 at the nucleotide and the amino acid levels. It is useful to identify predicted protein domains in PTH11 and PLG1 to provide initial considerations about how their expression patterns, localization and potential roles in the cell compare with each other. Moreover, I will also present the transcript analysis for PLG1 after exposure and incubation of the wild type spores on an inductive surface at different time points.

Materials and Methods

Fungal Strain, Media and Culture Conditions

The wild type rice pathogenic *M. oryzae* strain 70-15 from the Fungal Genetics Stock Center (Kansas City, Missouri) was cultured at 25^{o}C under fluorescent light on TNKYE (1% glucose, 0.2% $NaNO_3$, 2% KH_2PO_4, 1% $MgSO_4$, 1% $CaCl_2$, 0.1% $FeSO_4$, 0.1% micronutrients, 0.2% yeast extract agar plates. Long-term storage of *M. oryzae* was done

by growing the fungus on sterile filter discs, desiccating these for 48 h, and storing them at –20^{o}C.

Bioinformatics Analysis

Nucleotide and amino acid sequences were obtained for PLG1 and PTH11 from the *Magnaporthe oryzae* database found on the Broad Institute website (http:/www.broadinstitute.org/annotation/genome/magnaporthe_grisea/MultiHome.html) using gene identifiers *MGG03584.6* and *MGG05871.6*, respectively. Protein sequences were aligned using ClustalW2 and the shading was generated with BoxShade 71. In order to identify PLG1 transmembrane domains, several applications were used namely TMHMM 2.0 (http://www.cbs.dtu.dk/services/TMHMM) (Krogh et al., 2001), SOSUI 11 (http://bp.nuap.nagoya-u.ac.jp/sosui/) (Hirokawa et al., 1998), TMpred (http://www.ch.embnet.org/software/TMPRED_form.html) (Hofmann, 1993) and DAS (http://www.sbc.su.se/~miklos/DAS/) (Cserzo et al., 1997). To identify functional domains, applications such as InterPro (http://www.ebi.ac.uk/interpro/) (Mitchell et al., 2015) and PROSITE (http://prosite.expasy.org/scanprosite/) (de Castro et al., 2006) were used.

RNA Extraction

Conidia were initially harvested from 15-day-old TNKYE cultures, with 5 mL sterile deionized water per plate, using a glass spreader. Another 5 mL of water is added to the plate to collect the remaining conidia. The suspension is filtered once through three layers of Miracloth (Calbiochem), and all the collected spores are finally resuspended in 50 mL of water, ensuring a conidia concentration of 1×10^5 spores/mL or more, to get a high RNA yield. Using a multichannel pipettor, 15 µl drops of the conidial suspension were inoculated on Teflon (CS Hyde) laid on a Whatman 3MM chromatography paper (Fisher Scientific), which were both autoclaved and cut to fit inside a 500 cm^2 lidded tray. The plating tray (Genetix), originally designed for construction of plant bacterial artificial chromosome libraries were modified as humidity chambers for fungal development on Teflon. The trays were filled with water, then overlaid with sterile Teflon on chromatography paper, prior to conidia inoculation. Trays were placed in the 25^{o}C incubator and the germlings were collected with a cell scraper (Fisher Scientific) at these time points: 4 hours post exposure (hpe), 6 hpe, 12 hpe, 15 hpe, 24 hpe and 36 hpe (Liu et al., 2008).

For the 0 h time point, collected spores were immediately subjected to RNA extraction. The germlings for the later time points were collected in a 50 mL conical tube placed on ice, and the suspension is centrifuged (IEC) at 3400 rpm and 4^{o}C for 10 min. The supernatant is removed and the pellet is transferred into a 2-mL microfuge tube with an

amount of sterile and baked acid-washed glass beads (Sigma Aldrich) reaching the 0.2 mL mark. For a 2 mL RNA extraction buffer preparation, 0.02 mL 1 M Tris-HCl, pH 7.5 (0.01 M), 0.04 mL 0.5 EDTA (0.01 M), 0.05 mL 20% SDS (0.5%), 200 µL acidic phenol, pH 4.5 and 1.69 mL nuclease free H_2O have been added together (Sambrook and Russell, 2006). Five hundred microliters of the RNA extraction buffer were added to the microfuge tube containing the cell pellet and was subjected to bead-beating for 1 min, followed by centrifugation at 8, 150 rpm and 4^oC for 10 min. The supernatant was extracted twice with 500 µL of acidic phenol, pH 4.5, vortexing the mixture for 5 secs and centrifuging at 14,000 rpm and 4^oC for 5 min for every treatment. The resulting supernatant was transferred to a microfuge tube containing 500 µL of chloroform:isoamyl alcohol mixture (24:1), vortexed for 5 secs and centrifuged at 14,000 rpm and 4^oC for 5 min. Finally, the supernatant was added to 1 mL of 100% ethanol with 10 µL of 3 M sodium acetate, pH 5.2, allowing the precipitation to take place overnight at -20^oC. The mixture was centrifuged at 14,000 rpm and 4^oC for 15 min. The resulting RNA pellet was resuspended in 1 mL 70% ethanol and centrifuged at 14,000 rpm and 4^oC for 10 min. The extracted RNA was kept on ice and air-dried for 10 min, and was resuspended in 25 µL nuclease-free H_2O.

DNA contamination was removed with Turbo DNA-Free (Ambion), following the manufacturer's instructions. The RNA concentration was quantified with the NanoDrop spectrophotometer and its quality was assessed with the Agilent 2100 Bioanalyzer following the recommended settings.

cDNA synthesis and Quantitative RT-PCR analysis

cDNA was synthesized from 1 µg RNA using the TaqMan® reverse transcription reagents (Life Technologies), following the recommended RT reaction mix preparation and thermal cycling parameters for the RT reactions. The quantitative RT-PCR (qRT-PCR) was performed using the SYBR Green real-time PCR Master Mix (Life Technologies) on the Applied Biosystems® 7500 Real-Time PCR System. Primer pairs were designed using Primer Express Software v2.0. Three technical replicates for the qRT-PCR experiments were done for each of at least two independent biological replicates for every sample. Cycling conditions were 1 min at 95°C, followed by 40 cycles of 30 sec at 95°C, 20 sec at 55°C, 20 sec at 72°C and plate read at an optimal temperature. The elongation factor gene, *EF1α* (*MGG03641*) and the isoleucine-valine biosynthetic gene *ILV5* (*MGG01808*) were used as internal controls, and the $2^{-\Delta\Delta Ct}$ method was used to calculate relative expression levels (Livak and Schmittgen, 2001). Primer sequences for the qRT-PCR are listed in Appendix A.

Results

Nucleotide and Amino Acid Sequence Comparison between PLG1 and PTH11

The coding region of *PLG1* is 1645-bp and is interrupted by five introns, while *PTH11* has a 2715-nt long coding region and is interrupted by six introns. The translated

sequences have 397 amino acids and 632 amino acids, for PLG1 and PTH11, respectively. Using ClustalW2, a pairwise alignment between PTH11 and PLG1 was performed and BoxShade v.3.21 was used to highlight conserved or similar sequences (Figure 3). The black shading denotes amino acid identity and gray shading denotes similarity. The maroon shading indicates gaps between the aligned sequences.

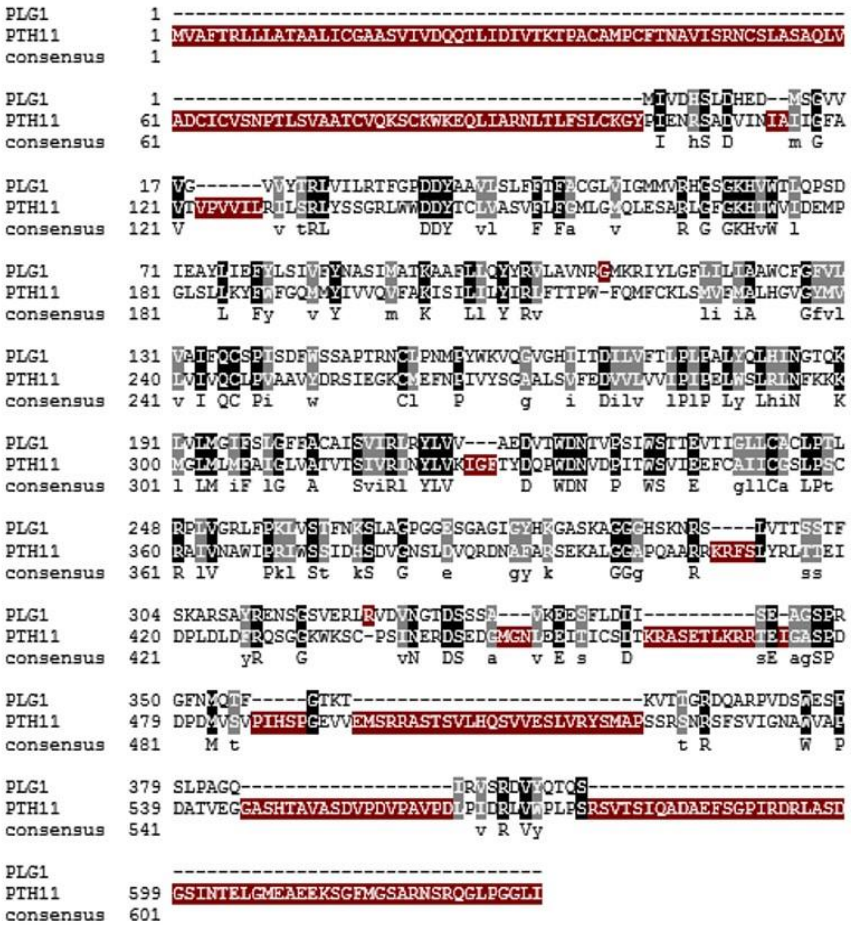

Figure 3. ClustalW2 Pairwise Alignment between PLG1 and PTH11.

The amino acid sequences of PLG1 and PTH11 were retrieved from the *M. oryzae* database found in the Broad Institute website, and were analyzed for similarity using ClustalW2 and BoxShade v.3.21.

A protein BLAST analysis was also done for the two proteins and it showed that PLG1 is 25% identical and 44% similar to PTH11 for over 250 amino acids. As seen in Figure 3, the first 50 amino acids in PTH11 do not match any from PLG1 based on the best pairwise alignment possible. This PTH11 amino-terminal domain is predicted to contain the extracellular EGF-like cysteine rich CFEM domain, followed by the seven transmembrane regions. Such domain is not found in PLG1, but it was identified in 12 other PTH11-like receptors described previously (Kulkarni, 2005). Most of the conserved and similar amino acid residues between PLG1 and PTH11 are seen in the regions spanning the membrane.

Hydropathy Analysis of PLG1

To identify the transmembrane domains in PLG1, protein topology prediction software such as TMHMM 2.0, SOSUI 1.11, TMpred and DAS were applied. All algorithms clearly identified transmembrane regions in PLG1, but differed in the number of the predicted helices spanning the membranes. TMHMM 2.0 and TMpred identified 6 strong transmembrane helices in which both the N-terminal and C-terminal domains appeared to be intracellular (Figure 4A and Figure 4D). On the other hand, SOSUI and DAS predicted 7 transmembrane helices with an extracellular N-terminal domain and an intracellular C-terminal domain (Figure 4B and Figure 4C). Looking closely at the SOSUI output, 9 amino acids and 138 amino acids are predicted to be in the extracellular N-terminal region and cytosolic C-terminal region, respectively. Further analysis of the

two termini using InterPro (http://www.ebi.ac.uk/interpro/) (Mitchell et al., 2015) and PROSITE (http://prosite.expasy.org/scanprosite/) (de Castro et al., 2006) did not reveal any additional functional domain or a canonical signal peptide sequence for PLG1.

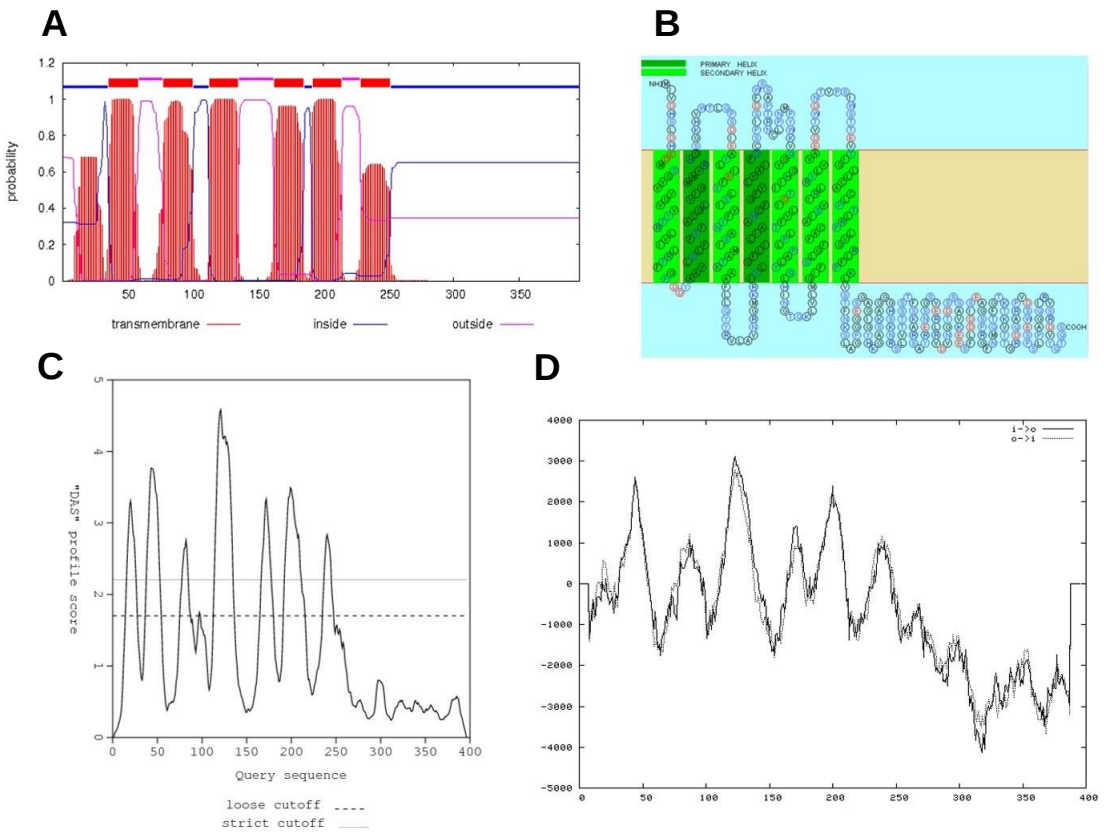

Figure 4. Proposed Models of PLG1 Transmembrane Topology.

Six strong transmembrane helices with intracellular N-terminal and C-terminal domains were predicted using **(A)** TMHMM 2.0 and **(D)** TMpred. On the other hand, the prediction programs SOSUI 1.11 **(B)** and DAS **(C)** identifies 7 transmembrane helices with an extracellular N-terminal domain and cytosolic C-terminal domain.

PLG1 is Expressed During Disease-Related Morphogenesis

To gain insights into the expression patterns of *PLG1* during infection-related morphogenesis, qRT-PCR was performed to monitor *PLG1* transcript abundance at different time points. Conidia were allowed to develop on Teflon, a hydrophobic surface that induces germination and appressorium formation. RNA was extracted at time zero, i.e. from conidia immediately after isolation from the culture plates, and then at later time points, i.e. from conidia germinated on Teflon at 4 hpe, 6 hpe, 12 hpe, 24 hpe, and 36 hpe. The quality of the RNA was verified prior to cDNA synthesis.

Using the $2^{-\Delta\Delta Ct}$ method, *PLG1* expression was calculated relative to the transcript levels of the constitutively expressed fungal genes *EF1α* and *ILV5*. *EF1α* and *ILV5* both show stable transcript levels during fungal development and hence are commonly chosen as reference genes for qRT-PCR experiments (Gogvadze et al., 2007). *EF1α* encodes an isoform of the alpha subunit of the elongation factor-1 protein and delivers aminoacyl tRNAs to the ribosome enzymatically (Hasegawa et al., 2010). *ILV5* on the other hand, encodes aceto-hydroxy-isomero-reductase which is involved in the isoleucine-valine biosynthetic pathways (Holmberg and Petersen, 1988). *PLG1* gene expression at time zero was normalized to 1. The calculated $2^{-\Delta\Delta Ct}$ values for the later time points were then compared to that of time zero to generate the expression profile. A no-RNA template control consisting of nuclease-free water for cDNA synthesis, was also run for the qRT-PCR experiments. On average, the Ct value for the negative control was

around 39. Hence, any resulting qRT-PCR Ct value that was close to the baseline set at 39, indicates absence of any transcript converted to cDNA that will serve as template for whichever primer pair was used. Figure 5A and Figure 5B, show the fold changes in *PLG1* expression relative to *EF1α* and *ILV5*, respectively. The plots show that the expression patterns relative to both reference genes are similar, in which *PLG1* is maximally expressed at 24 hpe. In detail, upon comparison of the actual plotted $2^{-\Delta\Delta Ct}$ values for different time points resulting from *EF1α* normalization, *PLG1* transcripts were detected in very trace amounts (0.5% of maximum expression) as early as 4 hpe. At 12 hpe, *PLG1* transcript levels have increased to 12% of maximum expression, and peaking at 24 hpe. It is then followed by a decrease at 36 hpe (5% of maximum) to 48 hpe (0.8% of maximum).

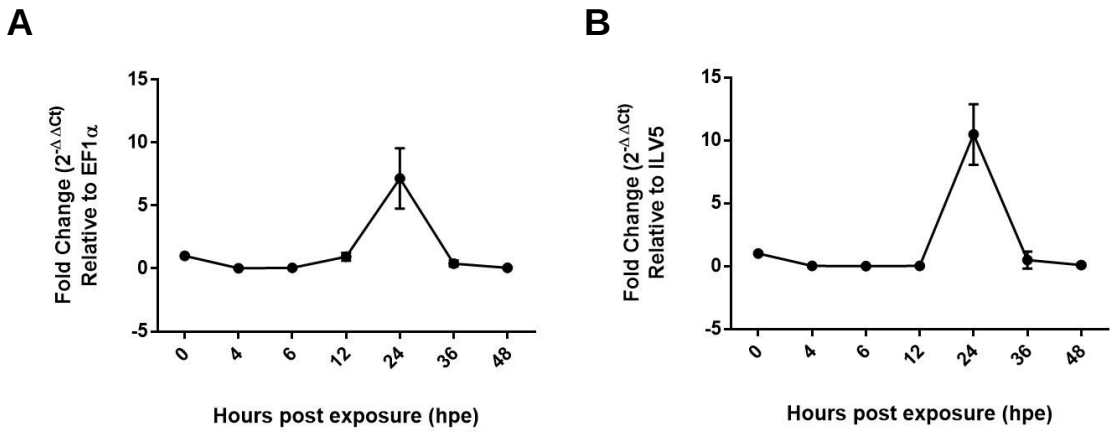

Figure 5. Kinetics of PLG1 Gene Expression on Teflon membrane.

Total RNA was extracted from germlings growing on Teflon membranes at different time points. qRT-PCR was performed using gene-specific primers for *PLG1*. The transcript abundance relative to the internal controls **(A)** *EF1α* and **(B)** *ILV5* are shown. Relative gene expression is normalized to 1 at 0 hpe. These results were obtained from three and two independent biological replicates for *EF1α* and ILV5 normalization, respectively. Standard deviations are indicated by the error bars.

Discussion

GPCRs belong to a large family of proteins in eukaryotes, and they have the vital function of relaying signals in cells so that an organism can initiate an appropriate response. While a wealth of information is available for GPCR structure-function relationship in animal systems, less information exist for fungi. Most of the GPCRs characterized in fungi have been shown to be important for processes involved in growth, mating and survival. For their biological significance, the identification of additional GPCRs in fungi had been active in the recent years through bioinformatics approaches (Affeldt et al., 2014).

M. oryzae has evolved to be a powerful model system for plant-pathogen interactions because of the genetic programs involved in its infection cycle. Specifically, its ability to switch from vegetative growth to a pathogenic state upon recognition of appropriate cues is already a subject of numerous studies. Such surface sensing capability may be due to the presence of receptors, presumably GPCRs. Therefore, the identification of the GPCRs or GPCR-like proteins in *M. oryzae* by Kulkarni et al. (2005), paved the way for dissecting the putative GPCRs in detail. Just as animal GPCRs are major targets for therapeutic intervention, the predicted fungal GPCRs can possibly become targets as well for controlling rice blast disease. One of the GPCR-like proteins of the PTH11 class that was identified in the screen was PLG1 (MGG03584.6). ClustalW2 pairwise alignment of PLG1 and PTH11 revealed sequence conservation in the membrane-

spanning regions, but not in the N-terminal and C-terminal regions. This was consistent with the results of Kulkarni et al. (2005) and previous observations that sequence similarity is usually limited to the transmembrane regions in GPCRs, even within related classes. Moreover, PLG1 does not possess the EGF-like CFEM domain in its N-terminal region unlike PTH11. The CFEM domain contains eight cysteine residues and was characterized to be fungal-specific through *in silico* annotation. Through the PSI-BLAST application, no animal, plant or prokaryotic proteomes were found to contain such a domain (Kulkarni et al., 2003). EGF refers to epidermal growth factor receptor which is a transmembrane glycoprotein belonging to a certain family of tyrosine kinase receptors and it has been thought to serve as signaling mediator for entry of obligate intracellular pathogens in mammalian cells (Herbst, 2004; Eierhoff et al., 2010). While such findings make PTH11 appear like a better candidate as a pathogenicity determinant than PLG1, it is still worthwhile to do further studies on PLG1 to gain insights into how PTH11 and PTH11-like receptors lacking the CFEM domain compare with respect to function. Pursuing PLG1 function may also provide a better understanding as to how *M. oryzae* evolved to have more GPCR-like proteins in comparison with other ascomycetes.

Classical GPCRs possess seven transmembrane domains. The secondary structure of PLG1 was examined using robust transmembrane domain prediction applications. Interestingly, TMHMM 2.0 and TMpred predicted six strong transmembrane helices, while SOSUI and DAS predicted seven. On the other hand, previous studies have shown that PTH11 was predicted to have nine transmembrane domains by TMpred and

eight transmembrane domains by SOSUI, yet it was proposed to have a possible signaling role that was GPCR-like in nature (DeZwaan et al., 1999). These inconsistencies in topology prediction are most likely due to differences in the algorithms and cutoffs set by the programs, in distinguishing a transmembrane domain from what is not. Moreover, as discussed in Chapter I, some GPCRs do not seem to have 7-TM domains which may be due to annotation or sequence errors (Li et al., 2004). Thus, any conclusion drawn for PLG1 and PTH11 GPCR prediction studies must be supported with further genetic or biochemical experiments testing for their GPCR properties.

To monitor the expression of *PLG1* across time points corresponding to infection-related fungal development on an inductive surface, a qRT-PCR assay was performed. This surface is Teflon, which is hydrophobic and so, it mimics the surface of plant leaves. *EF1α* served as the internal control. The expression analysis for both genes indicate their involvement in infection-related morphogenesis. The transcripts were present at very low levels in the germinating spores, around 4 hpe, but showed increasing transcript levels in the germinated spores, specifically at time points spanning the initiation of appressorium formation and maturation (12 hpe to 24 hpe). *PLG1* had its highest expression at 24 hpe. Since it was of interest to find out how PLG1 expression will change when the spores are inoculated on actual plant material instead, RNA extraction was attempted from barley leaves inoculated with the wild type 70-15 spores for 24 h. A good amount of high quality RNA was obtained from such samples, based on

Bioanalyzer results, however qRT-PCR experiments were not successful in detecting *PLG1* at 24 hpi on leaves. Even though a high concentration of RNA was obtained from the inoculated leaves, most of it is plant RNA. This is a common problem when looking at relatively early time points in plant infection, because it is difficult to enrich the fungal biomass using conventional spray or drop infection assays at such time frame (Kankanala, 2007).

In recent years, most of the *M. oryzae* appressorium-specific gene expression data were generated from spores inoculated on artificial appressorium-inducing substrates (Gowda et al., 2006; Oh et al., 2008; Soanes et al., 2012). For example, a set of genes, called the appressorium consensus genes was established, after looking at genome-wide expression changes during wild type 70-15 spore germination and appressorium formation (~9 hpe) on hydrophobic and hydrophilic GelBond surfaces, in response to cAMP (Oh et al., 2008). In an earlier attempt to identify the expressed genes encoded in the fungal genome, the *M. oryzae* mycelium and appressorium transcriptomes from wild type 70-15 were analyzed using massively parallel signature sequencing (MPSS), robust-long serial analysis of gene expression (RL-SAGE) and oligoarray methods. RNA samples were collected from spores inoculated on plastic (Falcon) petri plates for 24 h (Gowda et al., 2010). More recently, a genome-wide transcriptome profiling was done for *M. oryzae* Guy11 during appressorium formation using next generation sequencing (NGS) technologies such as RNA-Seq and High-Throughput SuperSAGE. RNA was extracted from germlings exposed to 1,16-hexadecanediol on plastic coverslips at 4 h, 6, 8, 14 and

16 h. These resulted in transcript profiles for 10,591 genes which comprise 96% of the total predicted genes in *M. oryzae*. Thus far, it gave the most complete coverage of the transcriptome in *M. oryzae* published studies (Soanes et al., 2002). Interestingly, after reviewing the three published papers that were just discussed, *PLG1* did not come up as a transcript of particular interest from their studies. For example, it was not classified as a member of the appressorium consensus genes. Although according to the *M. oryzae* Community Database (MGOS; http://www.mgosdb.org/), and after inspection of actual experimental conditions and data sets from the Geo Profiles database (http://www.ncbi.nlm.nih.gov/geoprofiles/), *PLG1* transcript was detected in the experiments performed by Gowda et al. As inferred from expression pattern (IEP), it was assigned with GO:0044408 for growth or development of symbiont on or near host (Gowda et al., 2006; Meng et al., 2009). Furthermore, the other reasons why *PLG1* was not significantly enriched in their experiments may include the kind of surface on which the spores were allowed to germinate, the wild type strain that was used, light and temperature conditions, and the exact time at which the germlings were collected for RNA extraction.

The use of MPSS and RL-SAGE proved to be useful technologies for transcript mining, although results revealed that the transcripts detected in both methods were overlapping but not identical (Gowda et al., 2004). RL-SAGE technique is an improvement of the SAGE method, which is done by having short-tags that correspond to a unique transcript. The frequency at which the tag appears correlates with mRNA abundance

and results give a snapshot of the mRNA population in a certain sample (Velculescu et al., 2000; Gowda et al., 2004). MPSS on the other hand, is also a tag-based technique where cDNAs are cloned on microbeads, digested by the enzymes such as Sau3A or DpnIII, and sequenced to give 17-20 bp tag readouts. Since the technique ensures that only one type of sequence is on a microbead, a transcript with more than one copy will be captured on different microbeads, allowing for quantification of transcript abundance (Brenner et al., 2000). The discrepancy mentioned earlier has been proposed to be due to different anchoring enzymes in the library construction. Thus despite being both powerful methods, they still had limitations (Gowda et al., 2004).

Moreover, some surprising results were obtained even for known genes that were shown to be associated with appressorium differentiation. In the study by Oh et al., during appressorium induction on the artificial hydrophobic substrate, *PTH11* and *MPG1* were significantly downregulated. Remarkably, they were more highly expressed in germinating spores on a hydrophilic surface than in developing appressoria (Oh et al., 2008). They explained that the products of *PTH11* and *MPG1* expression might be required at the onset of the morphological changes, but once the signal is detected and intracellular signaling pathways are in play, both proteins are no longer needed. This explanation is consistent with the possible roles of both PTH11 and MPG1 (Oh et al., 2008).

In Chapter I, it was discussed that the basis of *PLG1* functional analysis is the identification of a bZIP transcription factor, BIP1 which was found to regulate *PLG1* expression, in addition to three more PTH11-like GPCRs. The promoter sequences, which were limited to approximately 1-kb upstream from the start codon of the 44 downregulated genes were tested for conserved *cis* regulatory elements using the Weeder algorithm v.1.3 (Pavesi et al., 2004; Tag et al., in preparation). A core motif consisting of the consensus GCN4-like sequence TGACTC was identified in the promoters of the 44 genes, while a longer sequence, ATGACTCG was present in 77% of the promoters. Moreover, the promoters of the PTH11-like downregulated genes appeared to contain multiple GCN4-like binding motifs. Through EMSA experiments, the specific binding of BIP1 to the promoter elements of the three genes, including *PLG1*, was confirmed (Tag et al., in preparation).

BIP1 expression was also analyzed by isolating RNA from spores, mycelia and 24 h old appressoria of the wild type P1.2. To determine the kinetics of *BIP1* expression, RNA was collected from infected barley leaves drop-inoculated with wild type Guy11 spores. *BIP1* was found to be maximally expressed at 17 hpi (Tag et al., in preparation). Since *PLG1* is highly expressed at 24 hpe, it suggests that *BIP1*, which is expressed prior to 24 hpe may be responsible for binding to the *PLG1* promoter to activate its transcription. By 24 hpe, *PLG1* transcripts are enriched and detectable via qRT-PCR. Interestingly, despite the use of different conditions: RNA extracted from leaves inoculated with wild type Guy11 spores for BIP1 studies, and RNA extracted from wild type 70-15 spores

inoculated on Teflon for PLG1 studies, the expression patterns for both genes appear reasonable.

Overall, the results of this chapter set the foundation for the functional analysis of *PLG1*. Knowing that it is highly expressed at 24 hpe, future experiments will be done spanning the time point at which its transcript levels peak. Furthermore, one should be cautious in drawing conclusions from GPCR prediction software, or any prediction software for that matter. The use of multiple software for analysis is important for comparison of results and to establish reliability of data. Lastly, transcriptomic analysis proved to be a valuable tool for looking at *M. oryzae* gene expression under a certain set of conditions. It would be really interesting to know how the current and developing NGS strategies will improve detection of transcripts, perhaps those expressed in trace amounts. Results from such studies may have a great impact on how the expressed genes are annotated.

CHAPTER III

A NOVEL RECEPTOR-ENCODING GENE, *PLG1*, IS REQUIRED FOR RICE BLAST PATHOGENICITY

Introduction

The GPCRs are the major and most diverse family of membrane receptors found in eukaryotes. Their ability to bind endogenous and exogenous ligands triggers a signaling cascade inside the cell, allowing the organism to initiate an appropriate response. Thus, GPCRs play significant roles in various cellular functions, as there are a wide variety of signaling molecules that multicellular organisms are exposed to. Just in humans for example, a recent phylogenetic analysis identified over 800 GPCR-encoding genes, and each GPCR is specific to a particular ligand (Fredriksson et al., 2003). Despite the importance of such cell receptors, only a few of them are well-characterized in filamentous fungi. Most of these identified GPCRs were shown to be important for fungal growth and survival. With the availability of genome and proteome sequences for most filamentous fungi, it has become easier to perform bioinformatics studies and to search the genome for potential cell surface receptors of the GPCR type.

As discussed earlier, homologs of known GPCRs and a novel class of PTH11-like membrane receptors specific to the ascomycetes were identified in *M. oryzae* (Kulkarni et al., 2005). These PTH11-related receptors were highly represented in *M. oryzae*,

suggesting their possible roles in pathogenicity. As a result of the BIP1 transcription factor studies (Tag et al., in preparation), four genes that were previously described to encode PTH11-like receptors were shown to be downregulated in the *BIP1* deletion mutant. This work is focused on one of the downregulated genes, *MGG03584.6*, designated as *PLG1*.

A bi-directional BLASTP analysis of PLG1 against the *N. crassa* proteome identified NCU00700.1 as the hit with the highest sequence similarity with PLG1, and thus the two were classified as orthologs (Kulkarni et al., 2005). A search on NCU00700.1 did not reveal any characterization study for which results for the functional analysis of PLG1 may be compared with. In recent years, two studies implicated PLG1 in a possible fungal defense response function (Mathioni et al., 2013) and a possible signaling role (Xu et al., 2014).

Mathioni et al. looked at the transcriptional profile of *M. oryzae* upon its interaction with a bacterial antagonist *Lysobacter enzymogenes* (Mathioni et al., 2013). *M. oryzae* has been shown in the past to colonize not only the aerial parts of the plants, but also the root system (Sesma and Osbourn, 2004). When *M. oryzae* gets through the rhizosphere, it can potentially interact with other soil dwellers and must have mechanisms to protect itself from biotic stresses. *L. enzymogenes* is a soil-inhabiting bacterium that has antagonistic activities towards organisms such as fungi, oomycetes, nematodes, and other bacteria, and thus can be possibly used as a biocontrol agent for plant diseases.

Using an RNA-seq transcriptional profiling method to look at the genome transcriptional changes in *M. oryzae* when challenged with either a pathogenic (C3) or a non-pathogenic (DCA) strain of *L. enzymogenes*, they detected *PLG1* as a gene that was downregulated in the C3-challenged fungus, but upregulated in the DCA-challenged one. This differential expression hinted at the possibility of *PLG1* having a role in fungal defense response. They did not perform any further test involving PLG1, but rather with the previously characterized PTH11 receptor with which PLG1 shares sequence similarity (Mathioni et al., 2013).

More recently, *PLG1* has been reported in a paper which revealed that the rice endophyte *Harpophora oryzae* evolved from its pathogenic ancestor *M. oryzae*. *H. oryzae* is a fungus which can promote rice growth and biomass accumulation, and can protect rice roots from invasion by *M. oryzae*, which makes it a biocontrol agent candidate. In order to identify the genes that were associated with the shift of *H. oryzae* from a pathogenic to an endosymbiotic nature, they performed a genome-wide expression profiling study using RNA-seq on rice roots which were exposed to either *H. oryzae* or *M. oryzae*, and subsequent transcript verification with qRT-PCR. Although the overall genomic structure of the two fungi were similar, outcomes of the transcriptional profiling studies revealed major differences in the infection patterns, host defense response stimulation, signal transduction and nutritional preferences. Out of the 61 PTH11-like receptor-encoding genes that were previously described in *M. oryzae* (Kulkarni et al., 2005), only 15 of them have orthologs in *H. oryzae*. PLG1, and another

BIP1-regulated gene *MGG06535* were among those which were reported to be present in both fungi. In addition, they also had detectable transcripts at 3 dpi in rice roots that were challenged with either *H. oryzae* or *M. oryzae.* PTH11 itself is present in both fungi and showed the highest transcript level among the receptors (Xu et al., 2014). They also performed a comparative genomic analysis with other ascomycetes which are soil-borne root pathogens, such as *Gaeumannomyces graminis* and *Magnaporthe poae*. Interestingly, among the 15 orthologs, only PLG1 was absent in both *G. graminis* and *M. poae*. This suggests that PLG1 may not play a role in the infection strategy found in roots, or that there is a different gene which plays a similar function to *PLG1* in the typical root pathogens.

The two studies mentioned above mainly implicated *PLG1* in some possible functions based on transcriptional profiling evidence. Here, I report the characterization of *PLG1* by targeting it for deletion and examining the resulting phenotypes from the loss of *PLG1* in the *M. oryzae* genome.

Materials and Methods

Fungal Strains, Media and Culture Conditions

The wild type rice pathogenic *Magnaporthe oryzae* strain 70-15 from the Fungal Genetics Stock Center (Kansas City, Missouri) was used throughout this work. The

wild type 70-15 and mutant Δ*plg1* strains were cultured at 25ºC under fluorescent light on TNKYE (1% glucose, 0.2% $NaNO_3$, 2% KH_2PO_4, 1% $MgSO_4$, 1% $CaCl_2$, 0.1% $FeSO_4$, 0.1% micronutrients, 0.2% yeast extract) alone and TNKYE supplemented with 250 μg/mL hygromycin B (*Phyto*Technology Laboratories) agar plates, respectively. Long-term storage of *M. oryzae* was done by growing the fungus on sterile filter discs, desiccating these for 48 h, and storing them at –20ºC.

Generation and Transformation of Fungal Protoplasts

Protoplasts were generated and transformed following the procedure described previously (Leung et al., 1990). Protoplasts were prepared from fungus grown on TNKYE medium at 25ºC for 18 h. Resulting mycelia were harvested and washed with a modified enzyme buffer (20% sucrose, 20 mM trisodium citrate, 50 mM EDTA, pH 8.0) containing 40 mg/mL Novozyme 234 (Interspex Products). Protoplasts were subsequently washed and stored in STC (20% sucrose, 25 mM Tris-HCl, pH 7.5, 25 mM $CaCl_2$). Approximately 3 μg of transforming DNA was dissolved in STC and added to 200 μL of protoplast suspension. The protoplast mixture was incubated at 25ºC for 15 min before addition of PEG 3550 buffer (PEG 3550 in 25 mM $CaCl_2$, 25 mM Tris-HCl, pH 7.5). After incubation of the mixture at 25ºC for 20 min, complete medium (0.5% sucrose, 0.6% yeast extract, 0.6% casein hydrolysate) was added. The mixture was incubated overnight in a shaker at 26ºC. Regeneration agar (CM, 2 M sorbitol, 2% agar) was added to the incubated mixture and distributed in sterile plates maintained at 25ºC.

The plates were overlaid the next day with minimal media (MM, 1% sucrose, 0.1% $Ca(NO_3)_2$, 0.02% KH_2PO_4, 0.025% $MgSO_4$, 0.015% NaCl) with 1.5% agar and 250 μg/mL hygromycin B. The plates were incubated at 25°C for about 5 days.

Construction of PLG1 Gene Replacement Mutant

To generate the *PLG1* gene replacement mutant, the split-marker deletion method was applied (Catlett et al., 2003). Fragments corresponding to 1.43-kb upstream (*UFR*) and 28-kb downstream (*DFR*) of *PLG1* were amplified from the 70-15 genomic DNA with primers P1/P2 and P3/P4 (Appendix A), respectively using *ExTaq* polymerase (TaKaRa Bio Inc.). A 1.38-kb hygromycin B phosphotransferase gene (*HYG*), under the control of the *trp* promoter was amplified using primers M13F and M13R (Appendix A) from plasmid pBP15. The *PLG1* gene replacement constructs, *UFR-HYG* and *DFR-HYG* were generated with primers P1/YG and P4/HY (Appendix A), respectively. The DNA templates used to generate *UFR-HYG* were the *UFR* and *HYG* fragments, while *DFR* and *HYG* fragments served as templates to generate *DFR-HYG*. PCR-completed reaction mixtures were ran on 1% agarose gels with 1x Tris-borate running buffer, and the desired fragments were extracted and purified from the gel using the Qiagen Gel Extraction Kit. The purified DNA fragments were individually cloned into the pGEM-T vector (Promega) and transformed into DH10B™ electrocompetent *E.coli* cells (Life Technologies). Individual white colonies which grew on LB-carbenicillin agar plates, supplemented with X-gal and IPTG were picked and grown overnight at 37°C on LB

medium containing 200 μg/mL carbenicillin. Plasmid was extracted from each sample, following the instructions that came with the Qiagen DNA Plasmid Extraction Kit. Each resulting plasmid was submitted for sequencing of the desired insert. After confirmation of the correct sequences, 2.5 μg each of the *UFR-HYG* and *DFR-HYG* DNA fragments were used to transform *M.* oryzae protoplasts. The transformants in which only the two overlapping marker fragments have successfully recombined will grow on the medium containing hygromycin B. Hygromycin B-resistant transformants were picked for secondary screening, single-spore isolation and further testing.

DNA Isolation and Analysis

Genomic DNA from wild type 70-15 and Δ*plg1* mutant strains was extracted from mycelia using phenol-chloroform extraction as described by Sweigard et al. (1990). A DNA template concentration of 200 ng/μL was used for PCR using various primer combinations (Appendix A), to initially check for *PLG1* deletion and *HYG* integration. Twenty μg of wild type and mutant genomic DNA was digested with XhoI, gel blotted onto Hybond-N+ membrane (Ausubel et al., 1992) and hybridized to the 1.64-kb *PLG1* target gene or 1.38-kb *hph*. The membrane was exposed to a phosphor imaging screen overnight at room temperature and was scanned using the Typhoon 9410 Variable Mode Imager under the Storage Phosphor imaging mode.

Pathogenicity and Penetration Assays

Pathogenicity assays were carried out using barley (*Hordeum vulgare L.*) Golden Promise cultivar and rice (*Oryza sativa*) Nipponbare cultivar. Barley seedlings were cultivated at 15ºC with 60% humidity for 5 weeks. Rice seedlings were grown at 27ºC with 85% humidity for 3-4 weeks. Conidia were harvested from 15-day-old cultures, resuspended in 0.4% gelatin-water medium, filtered once through three layers of Miracloth (Calbiochem), and diluted to a concentration of 1 x 10^4 conidia/mL. For the intact detached leaf assay, 10 µL droplets of the conidial suspension were inoculated on 3 cm long segments of barley and rice leaves placed on 1% water agar plates containing 2 mg/L kinetin (Gibco Laboratories). The plates were incubated at 25ºC with a 12 h photoperiod. Disease symptoms on leaves were recorded 7 days post inoculation (dpi). For the infection assay of wounded leaves, barley leaves were stripped of the waxy layer by rubbing the leaf surface with a sterile emery board thrice and spot-inoculated with conidial suspension as described earlier. For the spray inoculation procedure, conidial suspension with a concentration of 1×10^5 conidia/mL was spray-inoculated on 4 week-old rice and 3 week-old barley plants. Plants were placed in biohazard bags for 24 h to maintain high humidity and then transferred to their respective controlled environment chambers for 7 days.

At least three independent experiments were performed for the detached leaf, wounded leaf and spray inoculation assays. Lesions were analyzed using the Image J software

(http://rsb.info.nih.gov/ij/), and disease was scored as described previously (Valent and Chumley, 1991).

In Vitro and In Vivo Appressorium Formation Assays

Appressorium formation was assayed *in vitro* on Teflon membrane (CS Hyde Company) by inoculating 20 μL droplets of the conidial suspension onto the membranes and incubating them in a humidity chamber (Sigma-Aldrich). Germling differentiation and appressorium formation were monitored at 0, 2, 4, 8, 10, 12 and 24 hours post exposure (hpe) by counting 100 germlings in six independent experiments using an Olympus IX70 inverted fluorescence microscope. For *in planta* assessment of appressorial penetration within a 48-hour period, onion epidermal cells were inoculated as described by Xu et al. (1997) Appressorial penetration in rice was studied as described (Koga and Nakayachi, 2004) using detached leaf sheaths of 3-4-week old rice plants. Leaf sheaths of the sixth leaves of rice plants were peeled off with leaf blades and roots. The leaf sheath was laid horizontally on a support in a large petri dish with a moistened filter paper bottom. Approximately 250 μL of the conidial suspension was introduced into the leaf sheath with a $23G_1$ needle and a 1-mL syringe. Tissue sections from the leaf sheath were prepared as described (Kankanala et al., 2007) and viewed under the microscope immediately after preparation. On the other hand, appressorial penetration in barley leaves were examined by clearing of the plant pigments from diseased leaves. The infected leaves for each isolate were fixed with 1 mL lactophenol (1:1:1:1 volume ratio

of lactic acid, glycerol, phenol and water) in a 2 mL microfuge tube for 16 h. The leaves were then decolorized twice within 2 h with a 1:1 volume ratio of lactophenol and 95% ethanol solution at 95 ºC. Fungal hyphae in the leaves were stained with Cotton blue (0.01% aniline blue in a 1:1:1 volume ratio of ethanol, lactic acid and phenol) for at least 24 h at 25°C (Oh and Lee, 2000).

Complementation Assay

For the complementation assay, the *PLG1* gene containing a 2-kb upstream fragment and a 2-kb downstream fragment was amplified from the 70-15 genomic DNA with primers 5'-UPFAR/3'-DOWNFAR (Appendix A), and cloned into the 4.9-kb-sized pBARGEM7-2 via the XhoI restriction site. The resulting construct pBARGEM7-2-PLG1 was linearized with BamHI and 5 µg of the linearized DNA was transformed into the Δ*plg1* mutant following the transformation procedure described earlier. Transformants were selected on complex medium (1.7 g/L yeast nitrogen base without amino acids, 2 g/L asparagine, 1 g/L NH_4NO_3 and 10 g/L glucose adjusted to pH 6.0 with Na_2HPO_4) supplemented with 500 µg/mL glufosinate ammonium (GoldBio). Colonies which grew on the medium after 7 days were picked and were verified by PCR and Southern blot.

Results

Construction of a Δplg1 Knockout Mutant

The coding region of *PLG1* is 1645-bp long and is interrupted by five introns. The translated sequence encodes 397 amino acids predicted to have seven transmembrane regions. To determine the role of *PLG1*, a split-marker deletion method (Catlett et al., 2003) was applied to inactivate *PLG1*. This method requires two rounds of PCR reactions. In the first round, the upstream flanking region (*UFR*) and the downstream flanking region (*DFR*) of PLG1, along with the selectable marker, *HYG* are amplified with primers P1/P2, P3/P4 and M13F/M13R (Figure 6A, Appendix A), respectively. The 5' extensions for the P2 and P3 primers are complementary to the M13F and M13 primer sequences, respectively. This allows fusion of the flanks and the marker sequences. In the second round of PCR, two constructs namely 5' and 3' are generated though PCR splicing by overlap extension (Catlett et al., 2003) (Figure 6B). The 5' construct is generated by using primers P1/YG (Appendix A) with *UFR* and *HYG* as templates, while the 3' construct is produced by using primers HY/P4 (Appendix A) with *DFR* and *HYG* as templates. The two resulting constructs are used for protoplast transformation.

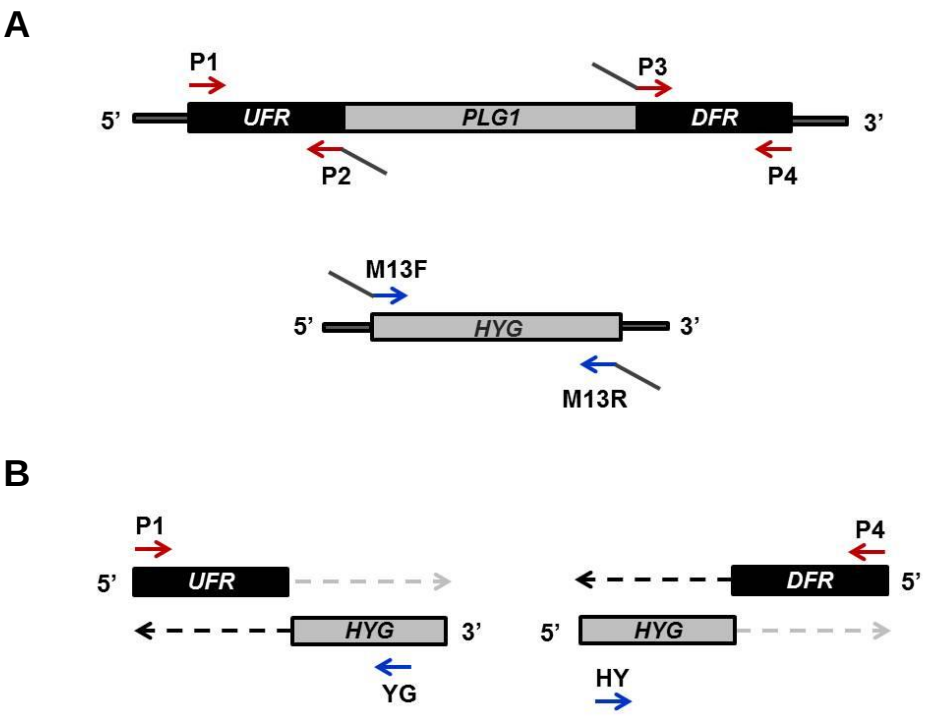

Figure 6. Strategy for Creating a Targeted Deletion Using the Split-Marker Deletion Method.

(A) The first round of PCR amplifies thee fragments: *UFR*, *HYG* and *DFR* using primer sets P1 and P2, M13F and M13R, and P3 and P4, respectively.
(B) The second round of PCR generates two constructs which are used for the fungal transformation: *UFR-HYG* and *DFR-HYG*. The *UFR-HYG* and *DFR-HYG* fragments were amplified using P1 and YG, and HY and P4 primer sets, respectively.

A hygromycin-resistant transformant is obtained when homologous recombination between the overlapping regions of the *HYG* gene and between the flanking regions and their genome counterparts take place. The split-marker method was modified so that there is a 763-bp overlap between the *HYG* regions instead of just 445-bp (Beasley et al.,

2006). These additional bases were expected to increase the probability of recombination and consequently increase the transformation efficiency. Twenty two hygromycin-resistant transformants, labeled 1-1, 1-2, 1-3, 3, 4, 5, 3-1, 3-2, 3-3, 3-4, 3-5, 4-1, 5-1, 6-1, 6-2, 6-3, 7-1, 7-2, 7-3, 7-4, 8-1 and 8-2 were obtained from the initial selection. PCR and Southern analyses were used to validate successful gene replacement. For Southern blots, XhoI was used to digest wild type 70-15 and mutant Δ*plg1* genomic DNA, and probes 1 and 2 (Figure 7A) were generated to detect target (*PLG1*) and replacement (*HYG*) genes. Twelve out of the 22 transformants did not show *PLG1* (Figure 7B). After probing with *HYG*, only transformant, 7-2, was determined to have a single copy of *HYG* with the expected DNA size. Three single-spore isolates were obtained for 7-2 and the DNA gel blot is shown on Figure 7C. The 4.3-kb band hybridized to probe 1 in 70-15 was not seen in Δ*plg1* transformants, while the 4.0-kb band hybridized to probe 2 in Δ*plg1* but was absent in 70-15. Two more independent fungal transformations were done to create the Δ*plg1* mutant and a total of four transformants, designated as 9-1, 2a, 5a and 8a were shown by PCR to lack the *PLG1* gene, but contain the *HYG* gene. Since all five deletion mutants were indistinguishable in phenotype with respect to *in vitro* appressorium formation and pathogenicity assays, only mutant 7-2 was used for further analyses. These results suggest that the PLG1 locus can be targeted for deletion and that PLG1 is not essential for viability as the mutants grow well on the selective growth medium. However, despite the use of the split-marker method for generating the deletion mutants, the recombination rate at the

intended locus is still low as shown by the number of recovered transformants with the desired replacement.

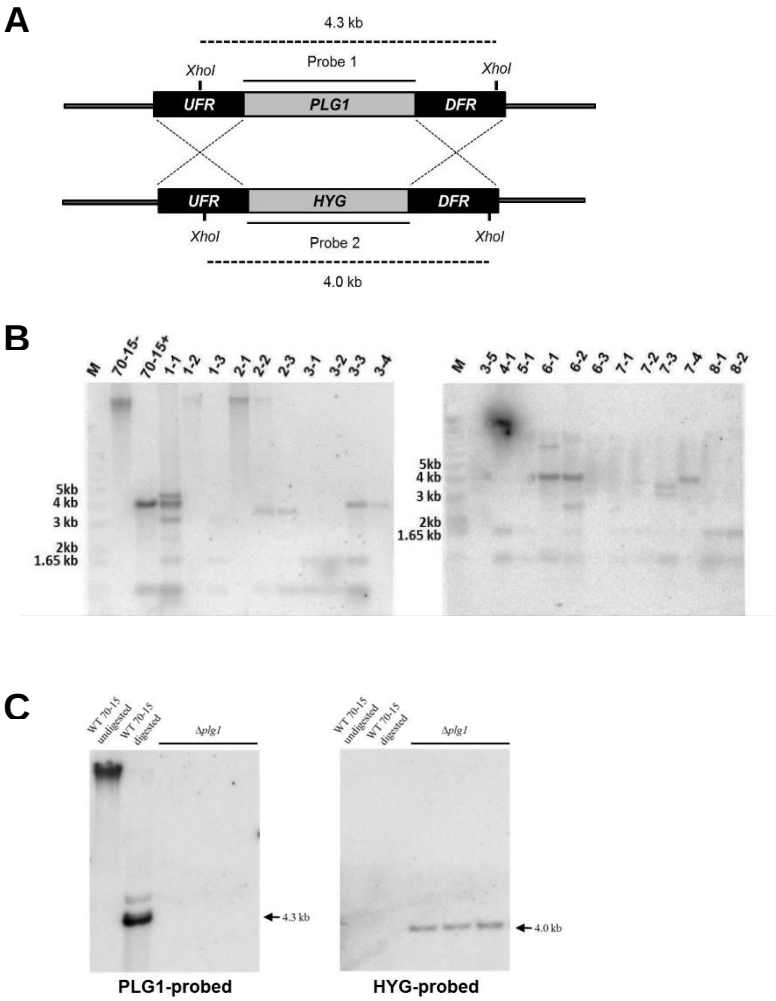

Figure 7. Development of a PLG1 Gene Replacement Mutant, Δ*plg1*.

(A) A *plg1* deletion mutant was generated via the split-marker deletion method. Probe 1 and probe 2 are PCR fragments amplified from the 70-15 genomic DNA and pBP15 respectively.
(B) Genomic DNA from the wild type strain 70-15 and twenty-two putative Δ*plg1* mutants was digested with XhoI, separated on agarose gels and probed with Probe 1.
(C) Blots of the XhoI-digested genomic DNAs of 70-15 and the Δ*plg1* mutant were hybridized with *PLG1*-specific (**left**) or hygromycin-specific (**right**) probes.

Δplg1 Is Non-Pathogenic on Drop-Inoculated Detached Barley Leaves

To investigate the function of *PLG1* during the infection cycle of *M. oryzae*, a pathogenicity assay was performed by inoculating detached barley leaves with wild type and Δ*plg1* conidial suspensions. After 7 dpi, barley leaves treated with the 70-15 conidial suspension showed lesions on inoculation sites while those inoculated with Δ*plg1* conidia did not exhibit gray lesions with reddish brown margins, characteristic of invasive growth (Figure 8). Lesion areas were measured using Image J software, and the average areas are reported in Table 1. The measured lesion areas served to quantify the extent of pathogenicity. A greater lesion area suggests that the isolate was able to colonize a cell and was able to invade adjacent cells. On average, the lesion areas measured for the wild type 70-15 and Δ*plg1* strains were 0.14 ± 0.014 cm^2 and 0.015 ± 0.008 cm^2, respectively. These results indicate that either Δ*plg1* isolate does not readily form the infection structures required to breach the leaf surface or that it breaches the leaf surface but is defective in colonizing one cell and its surrounding cells.

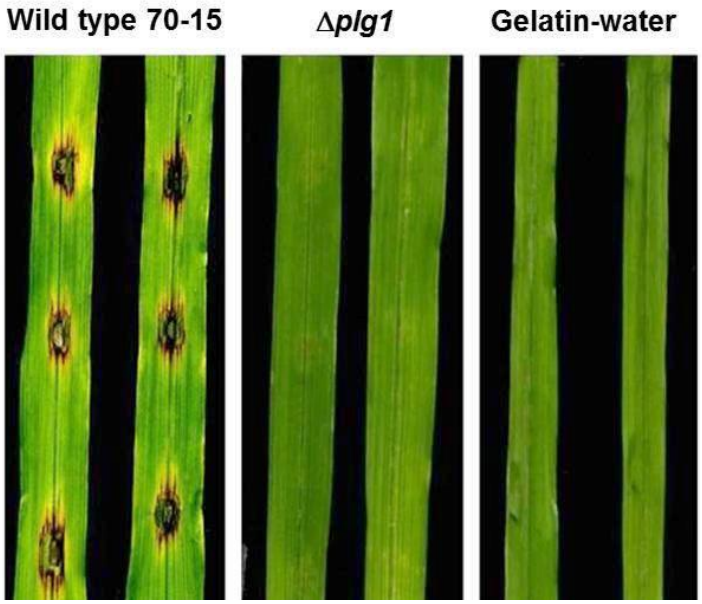

Figure 8. Deletion of PLG1 Leads to Reduced Pathogenicity on Barley.

Three 10 µL droplets of 1 x 10^4 conidia/mL suspension were inoculated on detached barley leaves. For the negative control, leaves were inoculated with three 10 µL droplets of 0.4% gelatin-water medium. At least three independent experiments were performed for the detached leaf assay.

Table 1. Physical Dimensions of Lesion Areas on Detached Barley Leaves Inoculated with the Wild type 70-15 or Δ*plg1* Strain

Strain	**Lesion Area (cm^2)**
Wild type 70-15	0.14 ± 0.014
Δ*plg1* isolate 7-2	0.015 ± 0.008

Each detached barley leaf was inoculated with thee 10 µL droplets of conidial suspension and incubated for 7 days. Thirty leaves for each isolate were evaluated for lesion sizes using the Image J software.

Δ*plg1 Mutant Forms Appressoria Inefficiently*

To address the possibility that the Δ*plg1* mutant is non-pathogenic because it does not readily form the infection structures required to breach the leaf surface, an *in vitro* appressorium formation assay was performed. Infection-related morphogenesis assay was done on an inductive surface such as Teflon to further compare wild type and mutant strains. A striking difference between the 70-15 and Δ*plg1* strains was observed at about 10 hpe. At that time point, most 70-15 conidia have already developed appressoria while most Δ*plg1* conidia exhibited extension of the germ tubes and apical swelling. By 24 hpe, most of the appressoria in the 70-15 conidia were already melanized, while most Δ*plg1* conidia still exhibited germ tube extension. The Δ*plg1* germ tubes also showed multiple apical swelling at 24 hpe (Figure 9). The defect is not a mere delay in the formation of mature appressoria, because even as late as 48 h, the Δ*plg1* mutant formed only about 10% of melanized appressoria (Figure 10). These observations suggest that Δ*plg1* mutant is not defective in spore germination and differentiation, but in the completion of appressorium morphogenesis, leading to functional appressoria. Although necrotic lesions were not observed on leaves treated with mutant inoculum, small brown pinprick spots were observed on the inoculation sites (Figure 8). This suggests that the infrequent appressoria that the Δ*plg1* mutant formed may still be functional and can penetrate some cells.

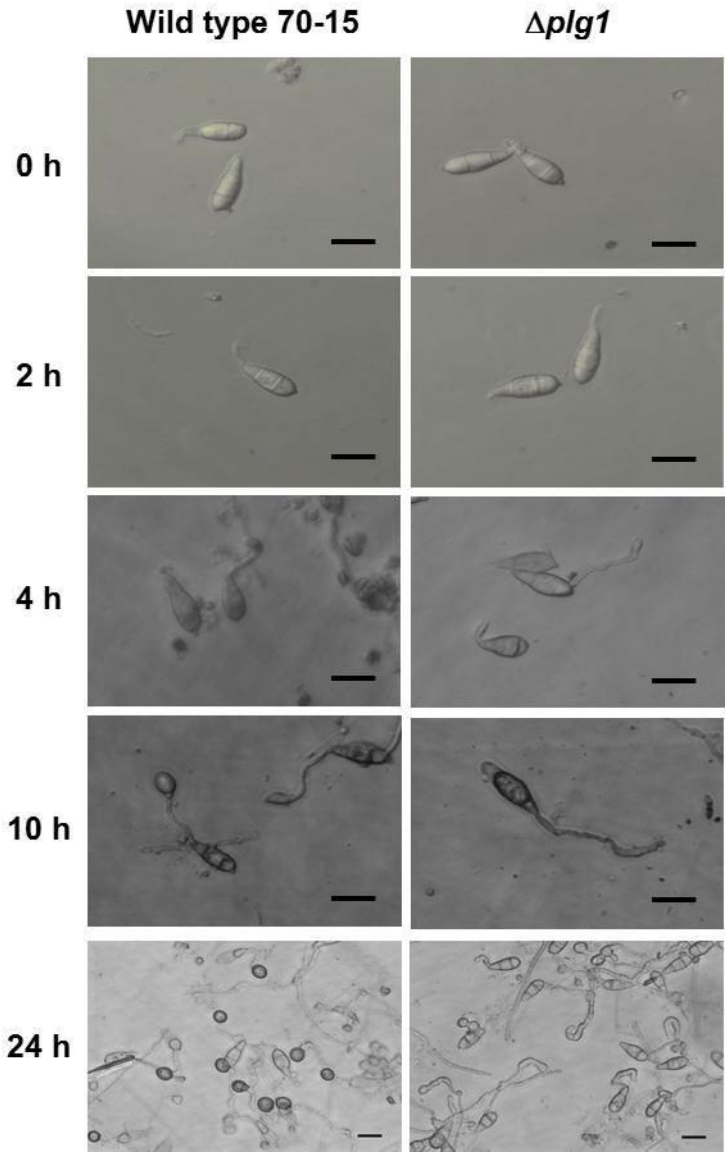

Figure 9. Kinetics of Appressorium Formation in 70-15 and Δ*plg1* Strains.

Teflon membranes inoculated with 70-15 and Δ*plg1* isolates from 0h to 10h were viewed under the microscope at 40x magnification. (bars = 20 µm)

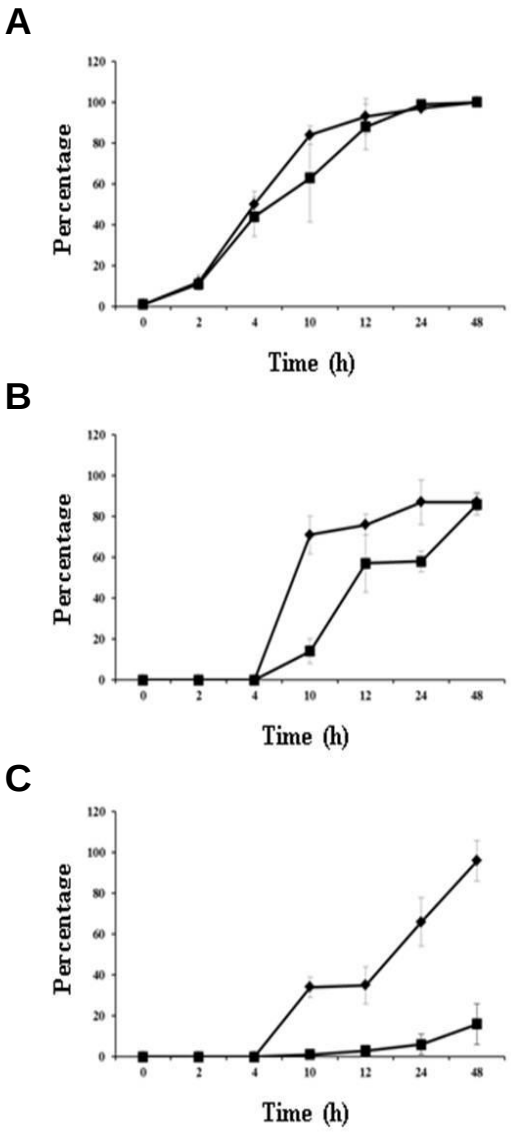

Figure 10. Quantitative Assessment of Appressorium Formation Kinetics in 70-15 and Δ*plg1* Strains.

Germination **(A)**, hooking **(B)** and appressorium formation **(C)** of 70-15 (♦) and Δ*plg1* (■) on Teflon membrane were verified microscopically. Each data point is an average from six Teflon membranes inoculated with either 70-15 or Δ*plg1* conidial suspension, evaluating 100 conidia per membrane. Standard deviations are indicated.

Elongated germ tubes can be distinguished from the infection hyphae because they appear to be just at the surface of the cells rather than within the cells. In most cases, they also appear thinner in comparison to the infection hyphae which are bulbous in appearance. The infected barley leaves were cleared of pigments and were examined under the microscope. While 70-15-infected leaves showed appressoria and bulbous invasive hyphae within cells, Δ*plg1*-infected ones mostly showed conidia with extended germ tubes on the surface of the cells. For the Δ*plg1*-infected leaves, there were a few instances where mature appressoria were observed, particularly on the areas where the brown pinprick spots were seen but there was no ramification of infectious hyphae within several adjacent cells similar to 70-15. Drop-inoculation infection assay on detached rice leaves were tried but were not successful because rice leaves were thinner and that caused the conidial drops to slide on the side too often. Instead of rice leaves, leaf sheaths were inoculated and examined under the microscope. The tissue sections were optically clear, hence there was no need for chemical clearing. Similar results were obtained in comparison with the barley leaf cells, showing that the inability of Δ*plg1* strain to infect is not host-specific (Figure 11A and Figure 11B).

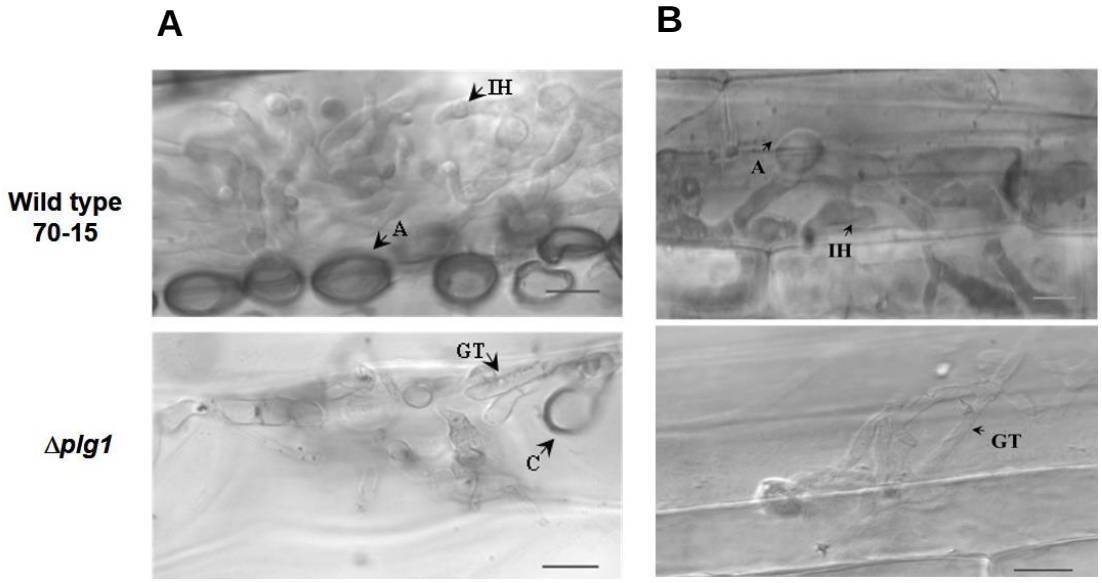

Figure 11. Visualization of Appressorium Formation and Cell Penetration of 70-15 and Δplg1 Strains in Barley Leaves and Rice Leaf Sheaths.

(A) The barley leaves from the pathogenicity assay at 7 dpi were cleared of pigments. The inoculation sites where lesions and/or brown spots were seen were viewed at a magnification of 100x.
(B) Rice leaf sheaths were excised 5 dpi for viewing under a 100x objective. (IH = infection hypha, A = appressorium, C = conidium, GT = germ tube; bars = 5 µm)

Appressorium Formation and Pathogenicity Are Partially Restored in the Complemented Δplg1/PLG1 Strain

Several attempts were carried out to generate the *PLG1*-complemented strain using two transformation vectors, pBARGEM7-2 and pCB1532, carrying the bar and sulfonylurea resistance genes, respectively. The transforming vector construct was also varied, using either a circular or linearized construct. Attempts to transform using the circular

construct for both vectors were not successful. A few transformants grew on the selective medium, but after a PCR screen, none of them had the desired *PLG1*gene insert. The stringency of the selection was also modified by varying the concentrations of the selective agents, namely glufosinate ammonium for the pBARGEM7-2 construct and chlorimuron ethyl for the pCB1532 construct, to see if more transformants with the desired integration will be recovered. When none of the attempts with the circular constructs was fruitful, the vectors were linearized. This gave rise to transformants which grew on the selective medium and were then PCR-verified to contain the *PLG1* gene. For one independent transformation with either vector, the pCB1532-PLG1 construct generated transformants labeled 21B and 25B, while the pBARGEM7-2-PLG1 construct resulted in transformants labeled 1C and 2C. Transformants 1C and 2C showed the expected 1.65-kb *PLG1* gene upon PCR using primers 5'-PLG1/3'-PLG1 (Appendix A). These are the primers spanning the 1st 20 bases and the last 20 bases of the *PLG1* open reading frame (ORF). Interestingly, transformants 21B and 25B did not give a PCR product for *PLG1* when amplified using outer primers 5'-PLG1/3'-PLG1, but an expected 1-kb product was observed when inner primers 5'-innerPLG1/3'-innerPLG1 (Appendix A) were used for amplification. There is a possibility that some bases required for annealing with one or two of the outer primers were lost in 21B and 25B during the reintroduction of PLG1 in the genome, so no PCR product was obtained using the outer PCR primers. For this reason, the pBARGEM7-2-PLG1 construct 1C and 2C were used for further testing. The resulting PCR products using 1C and 2C as templates were cut from the gel and were sequenced. Sequencing results showed

alignment with *PLG1*, indicating that *PLG1* has integrated back into the genome. When isolates 1C and 2C were subjected to Southern analysis after a restriction digest with XhoI, each showed two well-defined bands when probed with PLG1. In Figure 12A, wild type 70-15 shows two bands with approximate sizes of 4-kb and 5-kb. The complemented strains, 1C and 2C however, show one band at around 5-kb, and a band at around 10-kb. The 10-kb band is clearly absent in 70-15. This indicates ectopic integration of *PLG1* in the genome.

The complemented strain, 1C, which will be referred to as Δ*plg1*/*PLG1* from here onwards, was tested for its ability to form appressorium on Teflon at 24 hpe. Quantification of the appressoria at 24 hpe for at least three independent experiments revealed that Δ*plg1*/*PLG1* formed more melanized appressoria than the Δ*plg1* mutant strain, but less than that of 70-15 (Figure 12C). This increase in the number of functional melanized appressoria in Δ*plg1*/*PLG1* compared to Δ*plg1* was supported by the infection assay on barley leaves at 7 dpi (Figure 12D). The lesions caused by Δ*plg1*/*PLG1* appeared less severe than those caused by 70-15, but it caused more visible lesions compared to Δ*plg1*. This suggests that the pathogenicity was restored, albeit not to wild type levels in the Δ*plg1*/*PLG1* strain.

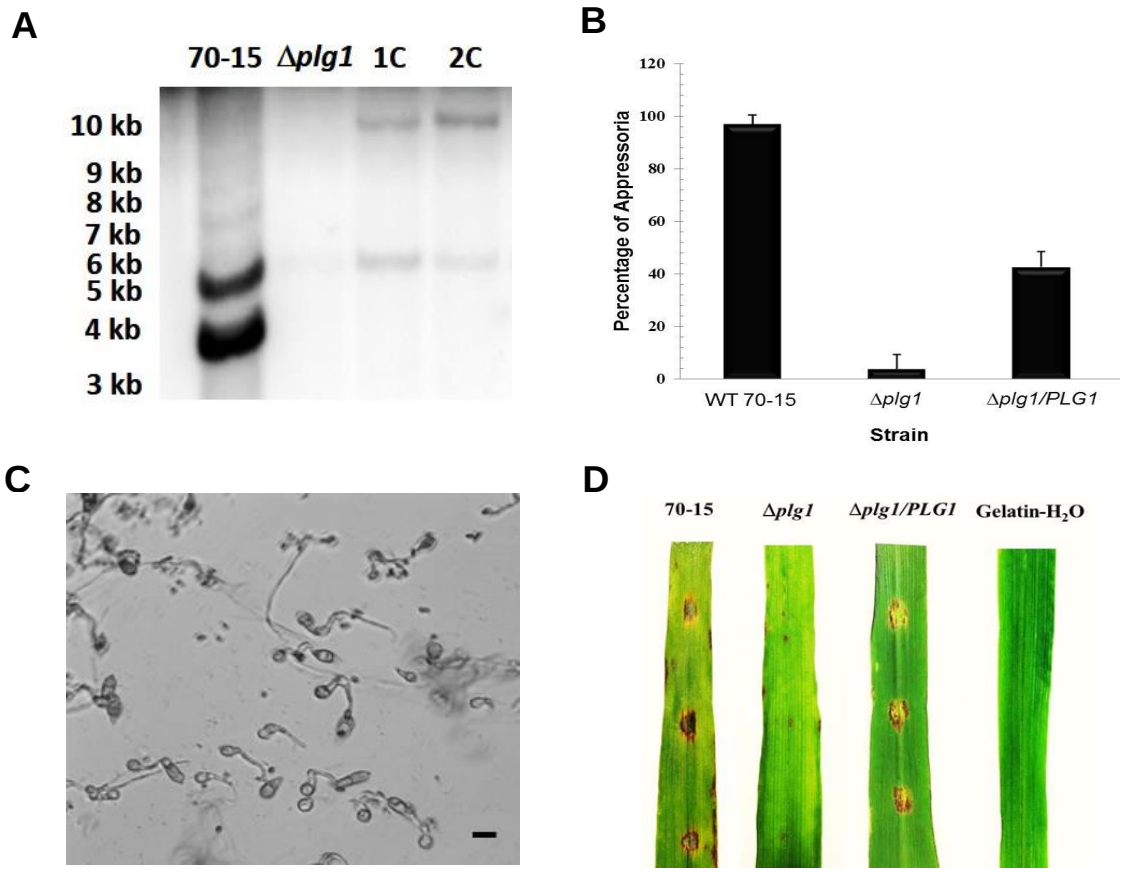

Figure 12. Appressorium Formation and Pathogenicity Are Partially Restored in the PLG1-Complemented Strain.

(A) Southern analysis of 70-15, Δ*plg1* and complemented strains 1C and 2C using the *PLG1* probe.
(B) Visualization of appressorium formation in the Δ*plg1*/*PLG1* strain 1C. Conidia were inoculated on Teflon and were monitored microscopically at 24 hpe under a 20x magnification. (bar = 20 µm)
(C) Quantitative assessment of appressorium formation in 70-15, Δ*plg1* and Δ*plg1*/*PLG1* strains. Conidia were inoculated on Teflon and were monitored microscopically at 24 hpe. Each bar is an average from three Teflon membranes, evaluating 100 conidia per membrane. Standard deviations are indicated.
(D) Barley leaves were inoculated with either wild type 70-15, Δ*plg1* mutant, Δ*plg1*/*PLG1* spores or gelatin-water as negative control and were examined at 7 dpi. At least three independent experiments were performed for the detached leaf assay.

To verify that the lesions caused by Δ*plg1*/*PLG1* are indeed due to infection hyphae ramifying the plant cells, cleared barley leaves were once again examined microscopically at 7 dpi (Figure 13). Results show that Δ*plg1*/*PLG1* can form functional appressoria *in planta* as the cells under the inoculation sites were filled with infection hyphae. This resulted from appressoria which were capable of breaching the surface of an intact, unwounded leaf. Thus, the lesions caused by the Δ*plg1*/*PLG1* strain on barley were due to cells harboring the infection hyphae.

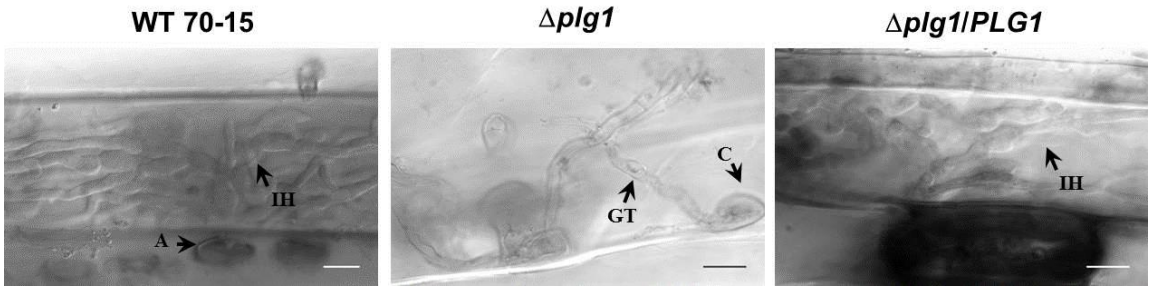

Figure 13. Δ*plg1*/*PLG1* Strain Develops Functional Appressoria and Infection Hyphae.

Barley leaves were inoculated with either wild type 70-15, Δ*plg1* or Δ*plg1/PLG1* spores. Leaves were cleared of pigments at 7 dpi and were examined microscopically. (bars = 5 µm)

Δplg1 Mutant Is Non-Pathogenic on Spray-Inoculated Rice and Barley Plants

Thus far, the infection assay described was carried out by inoculating conidial suspensions on barley leaves which were cut from 3-week old plants. It is known that plants have defense strategies against invading pathogens. In order to assess the

response of whole live plants upon being challenged with the 70-15, Δ*plg1* and Δ*plg1*/*PLG1* strains, spray inoculation assays were performed on 4 week-old rice and 3 week-old barley plants. The results shown in Figure 14 support the outcomes of the drop-inoculation detached leaf assay. It appears however that the lesions caused by Δ*plg1*/*PLG1* look significantly less serious than those caused by 70-15. On barley, there are lesser points of infection and on rice, the infection appears chlorotic and less spreading. This is consistent with the previous finding that Δ*plg1*/*PLG1* forms less functional appressoria compared to 70-15. However, it is also possible that the whole plants put up their defenses upon interaction with the fungal spores and that particular condition posed an additional challenge for Δ*plg1*/*PLG1* to cause infection, whereas the fully virulent 70-15 can easily overcome such plant defense.

Figure 14. Appressorium Formation and Pathogenicity Are Partially Restored in the *PLG1*-complemented strain.

Rice leaves **(A)** and barley leaves **(B)** were excised after 7 days from whole live plants, after spray inoculation with wild type 70-15, Δ*plg1* mutant and complemented Δ*plg1*/*PLG1* spores, to a final concentration of 1 x 10^5 spores/mL. Gelatin-water served as negative control. At least three independent experiments were performed for the spray inoculation assay.

Δplg1 Mutant Is Pathogenic on Wounded Leaves

Detached and intact leaf infection assays showed that the Δ*plg1* mutant is defective in forming a high number of melanized appressoria necessary to breach the leaf surface, and eventually cause macroscopic necrotic lesions to develop. Those outcomes led us to ask whether the defect in the Δ*plg1* mutant is just limited to the pre-infection stage, or if it affected invasive growth as well. This was addressed by performing wounding experiments on the leaves. Barley leaves were abraded with an emery board and were inoculated with the various strains. Abrading the leaves removes the surface cuticle and

thus, bypasses the need for the penetration peg arising from the appressorium. Clearly, as shown in Figure 15A, wounding the barley leaf enabled the Δ*plg1* mutant to cause brown necrotic lesions, whereas the unwounded leaf inoculated with the same strain did not show necrotic lesions, as expected based on the results of previous detached leaf infection assays. The unwounded leaves inoculated with either 70-15 and Δ*plg1*/*PLG1* strains showed lesions on the inoculation sites, and abrading the leaves caused even more extensive disease symptoms. These results confirm the ability of the 70-15, Δ*plg1*, and Δ*plg1*/*PLG1* strains to colonize the plant cells, once they are given direct access to the cells by stripping off the upper epidermal layer of the leaves. To examine fungal invasion on the sites of inoculation, the leaves were cleared of pigments and viewed under the microscope. Figure 15B shows the infection hyphae produced by the Δ*plg1* mutant in one of the barley leaf cells under the inoculation site. Overall, these results indicate that PLG1 is not required for invasive growth once the fungus bypasses the pre-infection stage.

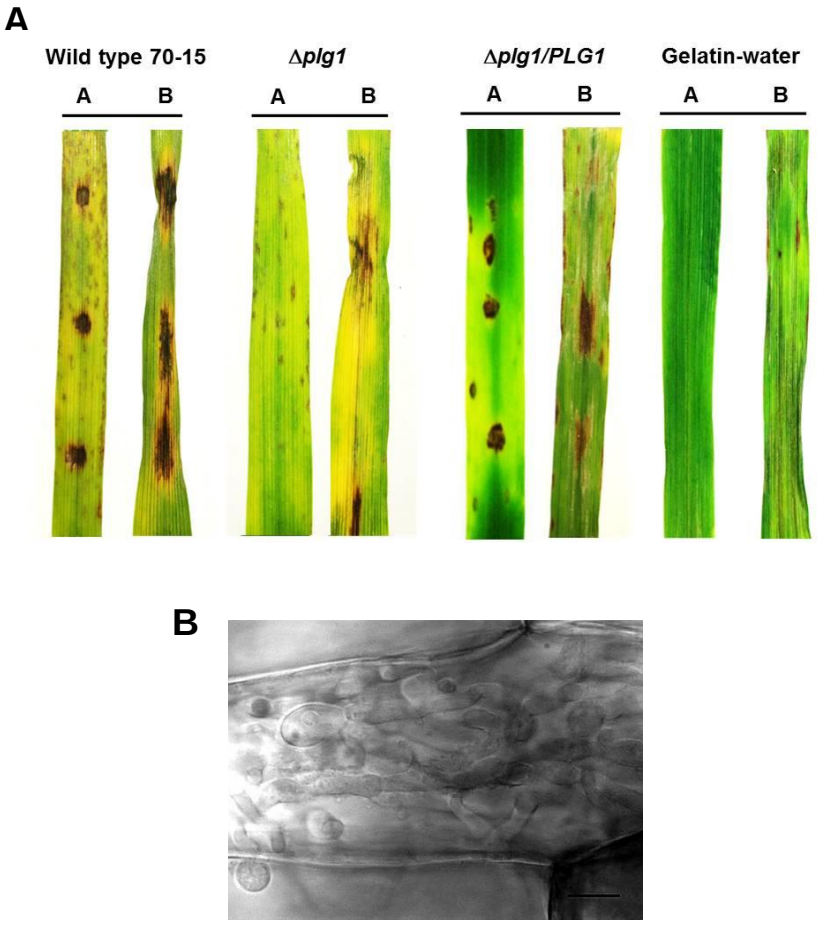

Figure 15. Δ*plg1* Mutants Are Pathogenic on Wounded Leaves.

(A) Barley leaves infected with 0.4% gelatin-water, wild type 70-15 and Δ*plg1* mutant strains were observed at 7 dpi. A = unwounded leaf and B = abraded leaf.
(B) Infected barley leaves which were cleared of plant pigments were observed at 7 dpi at a magnification of 100x. (bar = 5 µm)

PLG1 Is Not Required for Vegetative Growth and Conidiogenesis

PLG1 was shown to be necessary for pathogenic development. To investigate its role in vegetative growth, the wild type 70-15, Δ*plg1* mutant and complemented strain Δ*plg1/PLG1* were grown on solidified glucose, salts and yeast extract (TNKYE), V8 vegetable juice (V8), oatmeal (OA) and complete media (CM). In radial growth assays on the four types of media, the Δ*plg1* mutant was similar to 70-15 in terms of growth rate and pigmentation (Figure 16A). Colony diameters were measured at 10 dpi from the inoculated TNKYE plates, and the spores were then extracted and quantified for each strain. As shown in Figure 16B and Figure 16C, there are no significant differences among the colony diameters and conidia counts, respectively, for the three strains. These indicate that *PLG1* is dispensable for vegetative growth and conidia formation in *M. oryzae*.

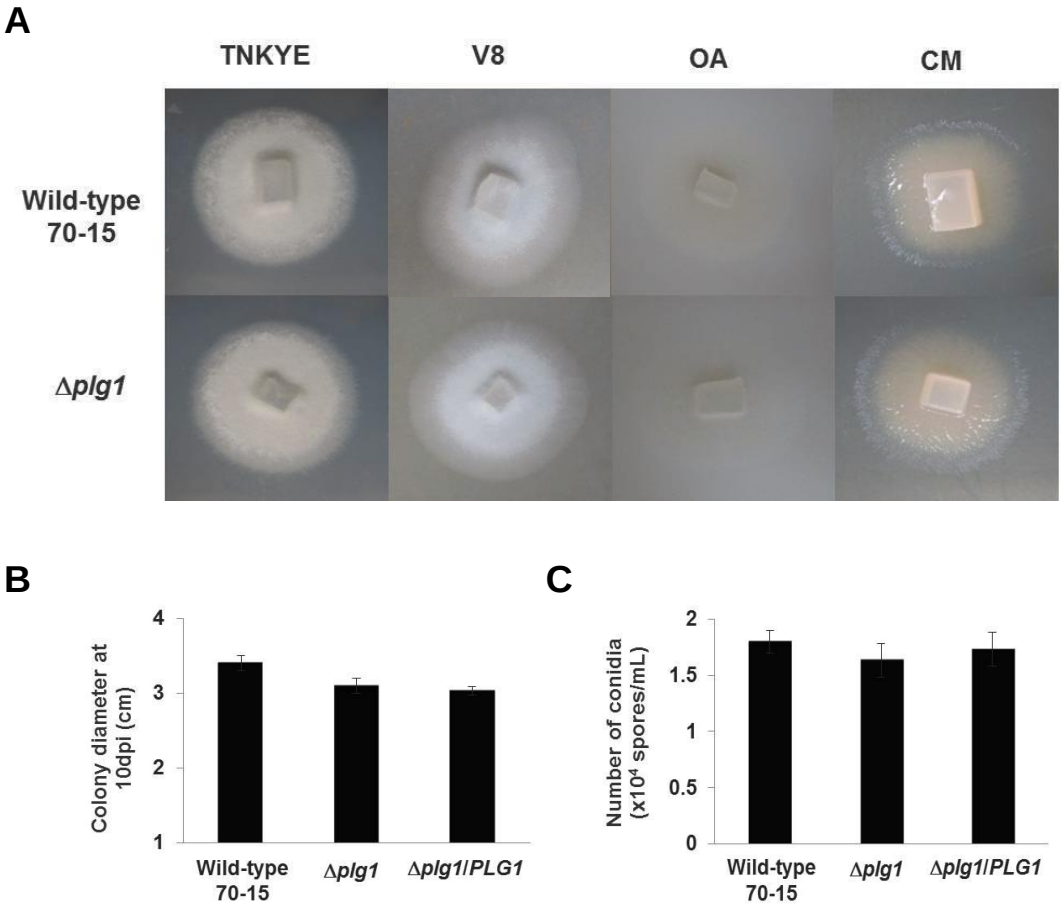

Figure 16. Deletion of *PLG1* Does Not Affect Vegetative Growth and Conidia Formation

(A) Mycelial growth of wild type 70-15 and Δ*plg1*mutant strains on glucose, salts and yeast extract (TNKYE), V8 vegetable juice (V8), oatmeal (OA) and complete (CM) agar media at 10 dpi.
(B) Colony diameters of wild type 70-15, mutant Δ*plg1*, and complemented Δ*plg1*/*PLG1* strains at 10 dpi on TNKYE media. Standard deviations are indicated for three independent experiments for each strain.
(C) Amount of conidia isolated for wild type 70-15, mutant Δ*plg1*, and complemented Δ*plg1*/*PLG1* strains on TNKYE media, at 10 dpi. Standard deviations are indicated for three independent experiments for each strain.

Discussion

Surface recognition is a crucial step in the appressorium-mediated infection process of *M. oryzae*. Although the signaling pathways and downstream components involved in appressorium formation and penetration have been characterized, there is much to be discovered about the upstream sensors initiating such pathways. There are a variety of signals that are present on the surface of plants; and the presence of a significant number of GPCR-like proteins in *M. oryzae* hints at the possibility of those proteins acting as upstream sensors in the phytopathogenic fungi.

I described how the deletion of *PLG1*, a gene predicted to encode a PTH11-like GPCR, led to a non-pathogenic mutant. It is a pathogenicity determinant because it mainly affected the pathogenic lifestyle of the fungus, but not its vegetative growth and the ability to form conidia. The Δ*plg1* mutant showed significantly reduced pathogenicity on both rice and barley, suggesting that the defect is not host-specific. Germ tube formation, hooking and apical swelling are processes which are known to constitute the early recognition phase of fungal development on inductive surfaces. At this stage, the fungus monitors the conditions of the substrate, and after perception of appropriate physical and chemical cues, it commits to further infection through appressorium differentiation and maturation. The Δ*plg1* mutant did not appear to be defective in the aforementioned features of the critical substrate sensing phase as it showed germ tube extension, hooking and apical swelling on Teflon, at time points similar to wild type 70-

15. Its development on an inductive surface is reminiscent of the development of the wild type strain on a non-inductive surface. The Δ*plg1* mutant exhibited further germ tube extension across the surface, often with multiple swellings at the germ tube tip, observed even as late as 48 h. Rather, the non-pathogenicity of the *PLG1*-deficient strain appears to be due to a defect in the completion of appressorium morphogenesis. On Teflon, the Δ*plg1* mutant still formed appressoria, but only at 10% of the wild type frequency. Moreover, detached barley leaves which were inoculated with Δ*plg1* mutant conidia showed small, brown disease spots on the sites of inoculation. When these sites were viewed under the microscope, infectious hyphae were seen inside the cells, indicating that the infrequent appressoria which formed are still functional. As opposed to the wild type inoculated leaves, where almost every cell under the inoculation site were filled with infectious hyphae, only a small number of cells were found with the infectious hyphae caused by the Δ*plg1* mutant strain. Taken together, the results indicate that the ability to undergo the early stages of appressorium differentiation is not incapacitated in the Δ*plg1* mutant, but the defect is most likely in the ability to complete appressorium maturation in response to surface signals. It can be hypothesized that as a putative receptor, PLG1 functions in sensing substrate cues after germ tube hooking and apical swelling; and that this detection process is ultimately important in forming the mature appressoria. Additionally, the observation that multiple swellings are found in most of the Δ*plg1* germ tube tips, alludes to the scenario in which the fungus attempts to sense a certain cue repeatedly but fails because of the absence of the relevant surface receptor.

The failure of Δ*plg1* mutant to cause infection appears confined to the surface recognition stage because it still exhibited plant cell colonization leading to necrotic lesions when the leaves were wounded. The wound sites created by abrading the leaves with an emery board allowed for invasive growth of the fungus via direct entry of the mycelia through the wound site. This process is independent of the use of appressorium. Hence, the Δ*plg1* mutant which was incapable of forming a significant number of functional appressoria was still able to colonize the wounded leaves because *PLG1* is most likely not required for penetration or invasive growth.

A complementation assay was performed to ensure that the pathogenicity defect was due to the loss of *PLG1*. The ability to form functional appressoria which translated to the level of pathogenicity on infected barley and rice, was only partially restored in the Δ*plg1*/*PLG1* strain. The integration of *PLG1* at an ectopic locus can explain why wild type levels of appressorium formation and pathogenicity were not achieved. There is a possibility that all required promoter elements were not present, leading to a variation in expression strength or that an unintended gene disruption took place. Upon examination of the regions surrounding *PLG1*, there is no immediate predicted ORF upstream (about 0.7 Mbp away from *PLG1*). However, there are two ORFs downstream of *PLG1*. One is a predicted cystathionine gamma synthase-encoding gene and the other, a predicted RING-14 zinc finger-encoding gene, which are 3-kb and 7-kb away from *PLG1*, respectively. Cystathionine gamma synthase is an enzyme which catalyzes the first specific step in L-methionine biosynthesis by the reaction of O(4)-succinyl-L-

homoserine and L-cysteine to produce L-cystathionine and succinate (Clifton et al., 2011). The RING-14 zinc finger protein on the other hand is predicted to play a key role in the ubiquitination pathway, where it is believed to act as an E3 ubiquitin ligase (Nakamura, 2011). Thus far, there are no reported characterization studies for the two genes in *M. oryzae* and their roles in pathogenicity. An accidental disruption of either ORFs or both, may have caused the incomplete restoration of appressorium formation and pathogenicity in *M. oryzae*.

The timing of *PLG1* qRT-PCR-based expression as discussed in Chapter II appears to correlate with the phenotypes exhibited by the Δ*plg1* mutant both on Teflon and on plants. The induction of *PLG1* expression was found at 12 hpe on Teflon, and steadily increased from 15 hpe to 24 hpe. Generally in *M. oryzae* wild type strains, most of the incipient appressoria have formed at around 12 h, and are melanized by 24 h. Since the Δ*plg1* mutant still forms occasional functional appressoria by 24h, it can be thought that the loss of *PLG1* is most likely not important at the very early stages of substrate recognition since it's expression was insignificant at those time points. However, when the germ tube starts to develop mature appressoria between 12 h and 24 h, it is when PLG1 comes into play. Its absence causes defects in the completion of appressoria for most germlings inoculated *in vitro*. Two hypotheses come into mind from such results. First is the possibility that PLG1 acts by itself as a receptor of topographic signals such as hydrophobicity, hardness or ridges that may be present on the artificial membrane. Second is the probability that PLG1 might be interacting with another protein. At the initial stages of substrate

recognition, that protein causes the *M. oryzae* to respond, thereby facilitating the germination and hooking stages. However, during the later stages, it requires PLG1 to complete appressorium differentiation. It may directly interact with PLG1, or it may have downstream effectors which trigger the activity of PLG1.

It can be recalled that *BIP1* was found to regulate *PLG1* expression monitored at 24 h and that indicates that *PLG1* is under the control of the *BIP1* transcription factor. The question now is, why is the Δ*plg1* mutant showing a developmental defect at a time point prior to its maximum expression? *BIP1* is maximally expressed at 17 hpi, but it already had significant expression as early as 8 h (Tag et al., in preparation) . Perhaps, the level of *BIP1* transcript at 8 h is sufficient to control the expression of *PLG1* whose earliest expression is seen at 12 hpe. Moreover, it is a good experiment to compare *BIP1* and *PLG1* expression from the same wild type strain, both on leaves and on artificial substrates. It may lead to additional insights into how *PLG1* may be regulated on different surfaces. Interestingly however, Δ*bip1* and Δ*plg1* mutants do not share the same phenotype. The Δ*bip1* mutants formed a significant number of fully melanized appressoria, but are unable to penetrate either intact or wounded host leaves. The Δ*plg1* mutant looked like it has a more severe phenotype, as evidenced by the infrequent appressoria it formed. There is a possibility that *PLG1* is controlled by transcription factors, other than BIP1, considering that the Δ*bip1* and Δ*plg1* were constructed under different, although related wild type backgrounds.

It is interesting to note that at this level of analysis, *PLG1* shares a similar phenotype with *PTH11*. *PTH11* was previously characterized in the *M. oryzae* strain 4091-5-8 and the *pth11* deletion mutant is also non-pathogenic on barley because they form appressoria only at 10 – 15% of wild type frequency (DeZwaan et al., 1999). In the same study, the authors described the plasticity of PTH11 function among different *M. oryzae* strains. They discovered that *PTH11* was important for appressorium differentiation and pathogenicity in strains 6043 and Guy11, but not in 4224-7-8 and CP987. In contrast, *PLG1* was studied in the *M. oryzae* 70-15 genetic background. Unfortunately, there are no reported PTH11 deletion mutants yet in the 70-15 background for us to directly compare the Δ*plg1* mutant phenotypes with. When the *PTH11* ORF was PCR-amplified using the Δ*plg1* genomic DNA as template, a product with the expected size was obtained, suggesting that *PTH11* is intact in the Δ*plg1* strain (data not shown). There lies the question however if *PLG1* may function in place of *PTH11* in the 70-15 background, given that they share the same phenotype at the level of appressorium formation and pathogenicity; and no *pth11* mutants have been described in the 70-15 background so far. To further explore this idea, PLG1 was tested for its cell surface receptor properties and its possible roles in the signaling pathways involved in appressorium formation. The results for these are highlighted in the next chapter. Since such studies were also previously performed for PTH11, the outcomes may once again provide another layer of comparison for PLG1 and PTH11.

CHAPTER IV

SIGNALING PATHWAYS INVOLVED IN PLG1 FUNCTION

Introduction

The ability of a fungal phytopathogen to cause infection relies on its successful entry into the plant host. The fungal structure playing the major role in the direct penetration of the host is the appressorium (Saunders, 2015). In *M. oryzae*, the formation of appressorium is an elaborate process, which can be divided into two stages, initiation and maturation (Vidhyasekaran, 2007). The initiation phase involves the hooking stage, in which the germ tube tips swell and get flattened against the leaf surface. Both chemical and physical topographic signals are known to trigger appressorium morphogenesis (Emmett and Parbery, 1975). The plant surface has a complex mixture of very hydrophobic components, typically long-chain aliphatic compounds which are collectively called waxes (Kolattukudy et al., 1987). Knowing that such surface is favorable for the development of foliar fungal pathogens, studies emerged in which different artificial hydrophobic substrates, mimicking plant surfaces were tested for development of infection structures. Yong-Hwan and Dean have examined *M. oryzae* spores on materials with varying levels of hydrophobicity. They reported that surface hydrophobicity is indeed essential to generate a high level of appressoria (Yong-Hwan and Dean, 1994). The cutin monomer 1,16-hexadecanediol (HDD), which has a backbone of 16 carbons and terminal hydroxyl groups was also implicated in

appressorium formation, even at nanomolar amounts. This chemical is thought to be one of the hydrolytic products when fungal cutinases degrade the plant cuticle layer. Experiments have shown that modifying the chain length or the presence and positioning of the hydroxyl groups greatly affect the activity of HDD, which results in the reduction of appressoria in germlings exposed to HDD (Gilbert et al., 1996). More recently, it was reported that primary alcohols such as 1-octacosanol (C28) and 1-triacontanol (C30), which comprise the leaf waxes in grasses, also serve as chemical cues for appressorium formation (Liu et al., 2011a). Exogenous addition of chemicals like secondary messengers in eukaryotic signaling pathways, or their analogs was also shown to induce appressorium development. Specifically, the extracellular addition of secondary messengers such as cAMP or its analog 8-bromo-cAMP and diacylglycerol (DAG) led to appressorium formation of germlings even on non-inductive hydrophilic surfaces (Lee and Dean, 1993; Thines et al., 1997). These studies thus implicated the cAMP signaling pathway involving protein kinase A (PKA) and adenylate cyclase (MAC1) (Xu and Hamer, 1996; Choi and Dean, 1997); and the protein kinase C (PKC) signaling pathway where DAG acts as a secondary messenger.

The physical contact of fungal germ tubes with a hard surface was also identified as a requirement for appressorium differentiation. Liu et al. isolated the *RGS1* mutant in a screen for transformants which formed normal levels of appressoria, even on a non-inductive surface (Liu et al., 2007a). They compared the development of the *rgs1*Δ deletion mutant and wild type strains on artificial surfaces with various physicochemical

properties. Results showed that neither a combined hydrophobic and soft surface nor a combined hydrophilic and soft surface can induce appressorium formation. These also implied that surface hydrophobicity alone did not appear to be sufficient for inducing appressorium formation (Liu et al., 2007a). A study in which light appeared to increase the number of appressoria by approximately more than 50% compared to germlings grown in the dark, was also reported (Jelitto et al., 1994).

Once the hooking stage has been established, the appressorium proceeds to maturation. To produce functional appressoria, the germlings undergo several series of developmental processes in this particular order: completion of mitosis, nuclear migration and conidial autophagy. The apex of the germ tube, described as a hook at this point, differentiates into a dome-shaped structure. As the appressorium matures, the cell wall lying against the host surface is specialized and lacks chitin. Chitin, a β-(1,4)-linked homopolymer of *N*-acetylglucosamine, is the essential carbohydrate component of the cell walls and septa of all pathogenic fungi. The chitin-less layer is much thinner compared to the other areas of the appressorial wall, and it becomes even thinner at the fungus-host interface, as the appressorium completes development of its cell wall. The appressorium has reached its maturation once a homogenous melanin layer, approximately 100 nm thick has been deposited in between the appressorial plasma membrane and wall. Melanin is found around the appressorium, except in the wall-less site described earlier. This site then becomes the appressorium pore, which is surrounded by an “O ring”, which ensures that the appressorium is sealed tightly onto the host

surface (Kankanala et al., 2007). Under a compound light microscope, the mature appressorium appears as black, round structure because of melanin. In *M. oryzae*, this pigment belongs to a class of fungal melanins produced by pentaketide biosynthesis, where the melanin product is a polymer of 1,8-dihydroxynaphthalene (DHN). Deposition of the DHN melanin on the appressorial wall is important to allow the buildup of hydrostatic pressure in the appressorium. This mechanical pressure then becomes the driving force for the penetration component (Forrest, 1990).

The level of cellular turgor that the appressorium develops was estimated to be as much as 8 MPa, the highest measured turgor pressures for any cell (Howard et al., 1991). Glycerol accumulates in the appressorium at concentrations above 3.0 M, and is believed to generate the counteracting osmotic pressure when surrounding water is drawn into the cell. Since the appressorium is sealed off by the melanin layer, glycerol cannot move out of the appressorium, and thus results in turgor generation (de Jong et al., 1997). The importance of this feature was examined in melanin-deficient mutants, which did not generate appressorial turgor, and thus were non-pathogenic on the plant host (Forrest, 1990).

Appressoria which form on the leaf surface do not require nutrients to be functional. This suggests that all the necessary requirements for development and infection are found in the spore itself. Studies about the genetic control and biochemical mechanism for turgor generation indicated that both carbohydrate and lipid reserves in the cell are

sources of glycerol synthesis in *M. oryzae.* Specifically, glycerol is produced from the most abundant carbohydrate source in the appressoria which is glycogen, via a NADH-dependent activity of glycerol-3-phosphate dehydrogenase (GPD) and the NADPH-dependent reduction of dihydroxyacetone and glyceraldehyde by glycerol dehydrogenase (GD). These were discovered by assaying the glycerol-generating enzymes from crude appressorial extracts, using enzymatic reaction test kits. Although GPD and GD were implicated in glycerol production, their activities did not appear to be highly induced to produce the level of glycerol found in the appressoria. An alternative source of glycerol, the lipid triacylglycerol, thus was tested by assaying the protein extracts from the developing appressoria for triacylglycerol lipase activity. This activity was found to be rapidly induced at the beginning of appressorium formation, all the way to turgor generation (Thines et al., 2000). If glycogen and triacylglycerol were being used up to generate glycerol, one can hypothesize that the amount of these sources might decrease over time as the appressorium matures. Such idea was validated by staining glycogen and lipid bodies with I_2 in KI and Nile Red, respectively, and monitoring cellular distribution of the stained components during spore germination and appressorium formation. Results showed that both components disappeared over time. Rapid glycogen degradation was observed for the wild type strain during conidial germination, followed by accumulation in the young appressoria, and dissolution before turgor generation. Under the light microscope, the I_2 in KI-stained components appeared brown in color, and by the end of appressorium maturation, no significant glycogen staining was observed in the wild type appressoria. A similar case was observed for the

lipid droplets, which fluoresced in the presence of Nile Red. They were abundant in the wild type conidia, but disappear and move into the incipient appressorium where they coalesced and were taken up into large vacuoles, followed by rapid lipid degradation during appressorium maturation (Thines et al., 2000). Although an appressorium may generate glycerol from various sources, its functionality is ultimately determined by the amount of glycerol it has produced and the level of turgor pressure that amount translates into. Cytorrhysis or appressorium collapse assays were initially performed to estimate the turgor pressure generated by the *M. oryzae* appressorium. Such assays eventually became useful for analyzing mutant strains which appear to have mature appressoria, but were still defective in plant penetration. The assay is done by allowing appressoria to develop, then adding increasing amounts of glycerol to the drops to give a final concentration between 1 and 5 M glycerol. The idea is that when the extracellular concentration of glycerol exceeds the intracellular glycerol concentration, the appressorium collapses due to the loss of water through osmosis (de Jong et al., 1997). When appressoria collapse, their shape changes from round into something that resembles a "fortune cookie". A concentration of 3 M glycerol was found to be sufficient to collapse around 50% of the mature appressoria. This suggests that the average glycerol concentration in the appressoria lies within the 2 M to 4 M range (Dixon et al., 1999). Therefore, a low number of collapsed appressoria, upon treatment with 2 M to 4 M glycerol, suggests that most appressoria have not reached the optimum level of glycerol for that specific strain.

If PLG1 as a receptor is hypothesized to act upstream of any intracellular signaling pathway, then presumably it may also affect transcript levels of the downstream genes involved in each pathway. As discussed earlier, the known signaling pathways in filamentous fungi include the cAMP/protein kinase A (PKA), DAG/protein kinase C (PKC) pathways, and the MAPK pathway, with the PMK1 MAP kinase as the downstream kinase. Hence, the transcript levels of the genes encoding the following can be examined in both wild type 70-15 and Δ*plg1*mutant backgrounds: a) catalytic subunit of protein kinase A, cPKA (MGG06368), b) the singleton *M. grisea* sequence that encodes the archetypal fungal PKC (MGG08689), and c) the MAP kinase, PMK1 (MGG09565) (Mitchell and Dean, 1995; Xu and Hamer, 1996; Zhang et al., 2001; Skamnioti and Gurr, 2007).

The previous chapter described the generation of the *PLG1* deletion mutant, Δ*plg1* that was shown to be non-pathogenic because of its failure to form a good number of mature appressoria to cause infection. In this chapter, the localization of PLG1 is described through the generation of a GFP-tagged PLG1 strain. This will serve as a confirmatory test for the results described in Chapter II, in which qRT-PCR analysis detected most *PLG1* transcripts, at time points where appressoria develop and mature; and where protein topology prediction software predicted a membrane localization for PLG1. More importantly, the placement of *PLG1* in the established signaling pathways in *M. oryzae* will also be described as a result of the exogenous addition of secondary messengers on both hydrophobic and hydrophilic surfaces.

Materials and Methods

Construction of an N-terminal GFP-Tagged PLG1

An N-terminal *GFP*-tagged *PLG1* was created by first amplifying *GFP* from the *Neurospora* expression vector pCCG*::*N-GFP (obtained from Dr. Deborah Bell-Pedersen, TAMU Department of Biology) using primers 5'-GFP_Inframe_EcoRI and 3'-GFP_Inframe_EcoRI to generate *GFP* with EcoRI restrictions sites; and *PLG1* with its 2-kb upstream and downstream flanking regions from the wild type 70-15 genomic DNA with primers 5'-UPFAR/3'-DOWNFAR (Appendix A). The *2-kbUP-PLG1-2kbDOWN* fragment was cloned into pGEM-T (Promega), and the EcoRI sites were introduced in between the 2-kb upstream flank and the *PLG1* ORF with the use of the QuikChange® Site Directed Mutagenesis Kit (Stratagene) with primers 5'-SDMEcoRI and 3'-SDMEcoRI (Appendix A), following manufacturer's instructions. The *GFP* and the pGEM-T plasmid harboring *2-kbUP-PLG1-2kbDOWN* were then cut with EcoRI. The linearized plasmid was treated with calf intestinal phosphatase (NEB) and was ligated to the EcoRI-cut *GFP* fragment using T4 DNA ligase (Promega). The resulting ligation mixture was transformed into Electromax DH10B competent cells (Invitrogen) and white colonies were picked to screen for both *PLG1* and *GFP*. The positive clones were then sequenced for an in-frame insertion of *GFP* in between the 2-kb upstream flanking region and *PLG1*. After sequence confirmation, the *2-kbUP-GFP-PLG1-2kbDOWN* fragment was cut out of pGEM-T with ApaI and SpeI. This was then cloned

into the 5.2-kb pCB1532 plasmid, carrying the sulfonylurea resistance gene. After confirmation of the correct insertion, 3 µg of the plasmid was transformed into Δ*plg1* mutant protoplasts. Transformants were selected on complex medium (1.7 g/L yeast nitrogen base without amino acids, 2 g/L asparagine, 1 g/L NH_4NO_3 and 10 g/L glucose adjusted to pH 6.0 with Na_2HPO_4) supplemented with 100 µg/mL chlorimuron ethyl (Chem Service). Colonies which grew on the medium after 7 days were picked and were verified by PCR. For visualization of fluorescence, conidia were resuspended in water with 1,16-hexadecanediol to promote appressorium differentiation on Teflon and viewed with the Olympus IX70 inverted fluorescence microscope.

cAMP, Diacylglycerol and 1,16-Hexadecanediol Treatments

70-15 and Δ*plg1* conidia were collected from 15-day old TNKYE cultures with sterile deioinized water, filtered once through three layers of Miracloth (Calbiochem) and diluted to a concentration of 1×10^3 conidia/mL. Twenty microliter drops of conidia were inoculated on plastic strips of Teflon (CS Hyde), and the hydrophobic and hydrophilic sides GelBond (FMC BioProducts), without any treatment or with the addition of appressorium formation inducers 8-Bromo-cAMP (Santa Cruz Biotechnology), added to a final concentration of 10 mM from a 50 mM aqueous stock, the diacylglycerol 1,2-dioctanoyl-*sn*-glycerol (Calbiochem), added to a final concentration of 20 µg/mL from a 10 mg/mL DMSO stock, and the plant cutin monomer 1,16-hexadecanediol (Sigma Aldrich), added to a final concentration of 2 µg/mL from a

0.5 mg/mL DMSO stock. The plastic strips were placed on microscope slides and incubated in humidity chambers (Sigma-Aldrich) at 25ºC. They were examined microscopically for appressorium formation at 24 hpe.

Cytological Analysis with Glycogen and Nile Red Staining

70-15 and Δ*plg1* conidia were collected from 15-day old TNKYE cultures as described previously. Twenty microliter drops of conidia were inoculated on plastic strips of Teflon (CS Hyde) or cover slips (VWR) with or without treatments of the appressorium formation inducers described earlier. The Teflon strips for the glycogen staining and the cover slips for Nile Red staining were supported with microscope slides and kept inside humidity chambers for 0 h, 4 h, 12 h and 24 h (for glycogen staining) and 0 h, 4 h and 24 h (for Nile Red staining) at 25ºC. The presence for glycogen was determined by staining the 20 conidial drops with 10 µL of the glycogen staining solution consisting of 60 mg/mL KI (brand) and 10 mg/mL I_2 (brand) in distilled water, and allowing the reactions to proceed for 10 min (Thines et al., 2000). The presence of lipid in vacuoles were visualized with a Nile Red staining solution consisting of 50 mM Tris/maleate buffer, pH 7.5, 20 mg/mL polyvinylpyrrolidone (approximate M.W. 40,000; Sigma) and 2.5 µg/mL Nile Red (Sigma) (Thines et al., 2000). Three microliters of the Nile Red staining solution was mixed with the 20 µL conidial drops and incubated for 10 min. Yellowish-brown glycogen deposits and fluorescing lipid droplets were observed for the

glycogen staining and Nile Red staining, respectively, when analyzed with the Olympus IX70 inverted fluorescence microscope.

Cytorrhysis Assay

70-15 and Δ*plg1* conidia were collected from 15-day old TNKYE cultures as described previously. Twenty microliter drops of conidia were inoculated on plastic strips of Teflon (CS Hyde) with or without treatments of the same concentrations of 8-Bromo-cAMP, diacylglycerol 1,2-dioctanoyl-*sn*-glycerol and 1,16-hexadecanediol as described earlier. The Teflon strips were supported with microscope slides and kept inside humidity chambers for 24 h at 25ºC. After the 24 h period, the liquid surrounding the spores were removed with a micropipettor and was replaced with 20 µL of 1 M glycerol, 3 M glycerol or 5 M glycerol to monitor appressorium collapse microscopically.

qRT-PCR Analysis of Genes Involved in the M. oryzae Signaling Pathways

Wild type 70-15 and Δ*plg1* RNA were collected from spores and germlings on Teflon at 24 hpe. RNA extraction, cDNA synthesis and qRT-PCR were carried out as described previously in Chapter II. The expression of downstream genes *CPKA* (*MGG06368*), *PKC* (*MGG08689*), and *PMK1* (*MGG09565*) were monitored at 0 hpe and 24 hpe under the wild type 70-15 and mutant Δ*plg1* backgrounds. Three technical replicates for the qRT-PCR experiments were done for each of four independent biological replicates per

sample. *EF1α* gene was used as internal control, and the $2^{-\Delta\Delta Ct}$ method was used to calculate relative expression levels. The 24 hpe expression level was further normalized against 0 hpe, thus setting all 0 hpe transcript levels to 1 for both wild type 70-15 and Δ*plg1* strains (Livak and Schmittgen, 2001). Statistics were performed with GraphPad Prism v.6, in which the significance of changes in gene expression of the signaling genes between wild type 70-15 and Δ*plg1* strains was defined by (P) < 0.05 with a two-tailed Student's t-test.

Results

PLG1 Localizes to the Appressorial Plasma Membrane at 24 hpe

In Chapter II, the predicted secondary structure of PLG1 using different transmembrane topology prediction programs was discussed. To see whether PLG1 localizes to the plasma membrane, a GFP-PLG1 fusion protein was constructed under the control of the native *PLG1* promoter. The *GFP* fragment was amplified from the *Neurospora* expression vector *pCCG::*N-GFP and was fused in frame between the 2-kb upstream flanking sequence of *PLG1* and the *PLG1* ORF. This creates an N-terminal GFP-tagged *PLG1*, which is presumed to be under the control of the native *PLG1* promoter within the 2-kb upstream flank. In one transformation experiment, out of six transformants which grew on the selective medium containing chlorimuron ethyl, only one transformant was found to be positive for the presence of *PLG1* and *GFP* after PCR

validation. This transformant was labeled as A2-1, and will be referred to as GFP-PLG1 from here onwards. When GFP-PLG1 conidia were incubated on Teflon, they formed appressoria and caused pathogenicity similar to the levels found for the complemented strain Δ*plg1*/*PLG1*. To monitor fluorescence, the conidia were resuspended in water with 1,16-hexadecanediol to further promote appressorium differentiation (DeZwaan et al., 1999). The untransformed wild type 70-15 strain served as a negative control for monitoring GFP signals. Fluorescence was monitored during germ tube formation (4 hpe on Teflon) and during the onset of appressorium formation (10 hpe), but no GFP signal was detected for either 70-15 or GFP-PLG1. The exposure was then increased for capturing any signal. Some signals were detected on the conidia, but they were similar both for GFP-PLG1 and 70-15 which does not carry any GFP construct. When the spores were incubated further until 24 h, GFP signals differing between GFP-PLG1 and 70-15 were finally observed. The GFP signal appeared to be enriched at the appressorial plasma membrane in the GFP-PLG1 strain. In some spores that were just developing the appressoria, weak GFP signals were observed outlining the germ tubes and the incipient appressoria. No signal can be detected at a similar region or any region in the 70-15 germlings (Figure 17).

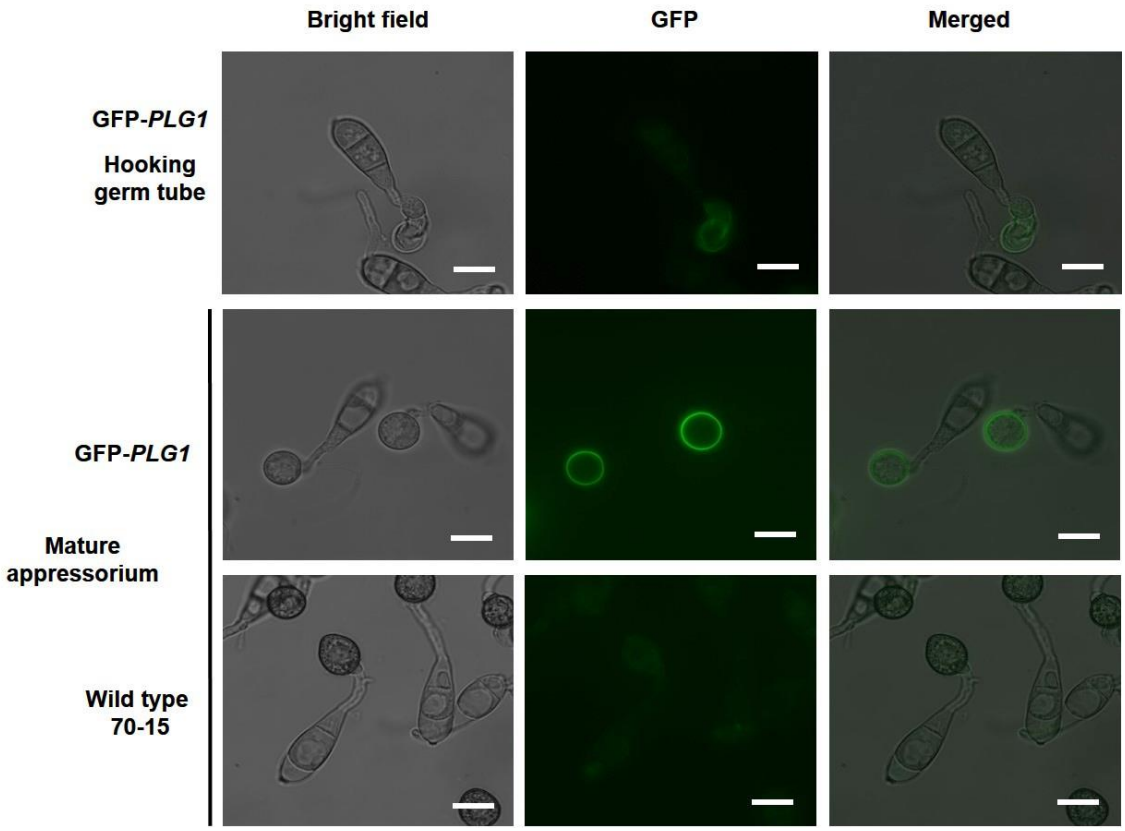

Figure 17. Imaging of GFP-PLG1 on Teflon at 24 hpe.

Wild type 70-15 and *GFP-PLG1* conidia were resuspended in water containing 2 µg/mL 1,16-hexadecanediol and inoculated on Teflon for 24 h. (bars = 10 µm)

1,16-Hexadecanediol Induces Appressorium Formation to Wild Type Levels in the Δplg1 mutant on an Inductive Surface

The cutin monomer 1,16-hexadecanediol (HDD) was shown to be the most effective aliphatic alcohol that induces *M. oryzae* appressorium formation on non-inductive surfaces (Gilbert et al., 1996). Since it is a leaf wax component, one can think of it as an external signal that receptors can respond to. In order to evaluate the response of the Δ*plg1* mutant in the presence of HDD, spores were incubated on Teflon for 24 h with 2 µg/mL HDD. In the absence of HDD, the Δ*plg1* mutant formed 5% appressoria, and this percentage increased to 97% upon addition of HDD. All appressorial-like structures with similar diameters, regardless of the level of melanization were included in the quantification. The appressorium which the HDD-treated Δ*plg1* spores formed appeared normal in terms of morphology, and no extensive germ tube hooking was observed prior to appressorium formation (Figure 18B). However, the level of melanization appeared less intense in the resulting Δ*plg1* appressorium compared to wild type. Wild type 70-15 formed 95% and 99% appressoria in the absence and presence of HDD, respectively. In both wild type 70-15 and Δ*plg1* mutant strains, there appeared to be an increase in the induction of appressorium formation on an inductive surface (Figure 18A and Figure 18B). Taken together, these indicate that PLG1 may not be required in actually recognizing HDD as a surface signal, and that it may not be mediating the signaling pathways that HDD activates downstream leading to appressorium differentiation.

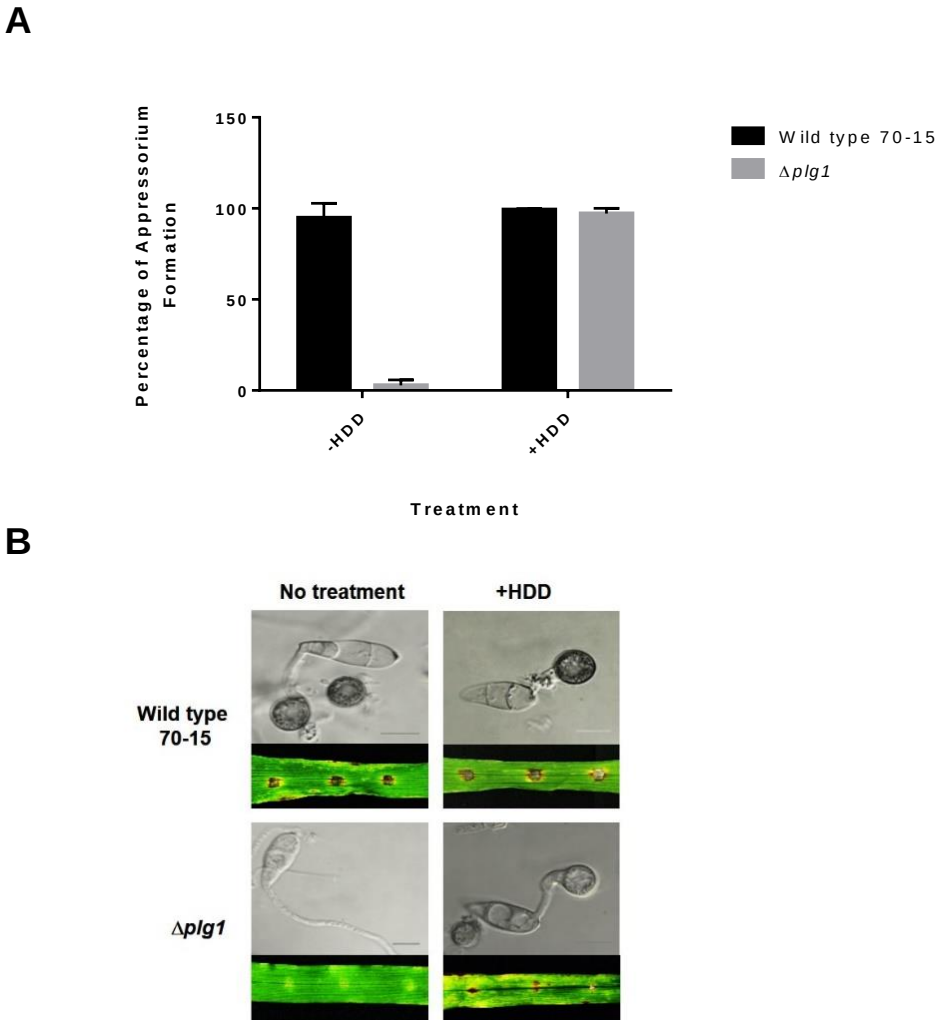

Figure 18. Effect of 1,16-Hexadecanediol Treatment on Wild Type 70-15 and Δ*plg1* Mutant Spores.

(A) Wild type 70-15 and Δ*plg1* conidia were resuspended in water containing 2 µg/mL 1,16-hexadecanediol and inoculated on Teflon. Appressoria were quantified microscopically after a 24 h incubation. Reported values are averages of at least three biological replicates, looking at 100 conidia per replicate. Standard deviations are indicated.
(B) Wild type 70-15 and Δ*plg1* conidia were resuspended in water containing 2 µg/mL 1,16-hexadecanediol and inoculated on Teflon for 24 h (upper panels) or drop-inoculated on barley leaves (lower panels). The differentiated spores were viewed at 100x and barley infection was evaluated at 7 dpi. (bars = 10 µm)

Despite the apparent dispensability of *PLG1* in HDD recognition, the increase in the appressorium formation in the Δ*plg1* mutant was remarkable so a pathogenicity assay

was carried out to test whether the appressoria that formed in the presence of HDD were functional. Using the drop inoculation method on barley leaves and disease evaluation at 7 dpi, it can be seen in Figure 18B that while brown spots are seen at the sites where Δ*plg1* spores with HDD were inoculated, spreading lesions of wild type levels were not observed on the leaf surface. The Δ*plg1* spores without HDD are non-pathogenic, while wild type 70-15 spores with or without HDD cause extensive lesions on barley leaves. These results indicate that although there was a significant increase in the number of normal-looking appressoria in the HDD-treated Δ*plg1* spores, not all of them rescued the pathogenicity defect of the mutant. Most likely, this is due to below optimum appressorial turgor pressure in the HDD-treated Δ*plg1* spores.

Δplg1 Mutant Responds to Either cAMP or DAG on an In Vitro Inductive Surface but Not on a Non-inductive Surface

cAMP and its more water-soluble analog 8-Br-cAMP, in addition to DAG are chemicals that can be added exogenously at optimal concentrations, to drive appressorium in *M. oryzae* wild type spores that are inoculated on a non-inductive (hydrophilic) surfaces. To test whether the Δ*plg1* spores will respond in a manner similar to the wild type, they were treated with either 10 mM 8-Br-cAMP, or 20 µg/mL of the diacylglycerol 1,2-dioctanoyl-*sn*-glycerol or a combination of both for 24 h prior to microscopic examination. Untreated spores were monitored as well for comparison. In Chapter III, it was described that the Δ*plg1* mutant formed appressoria at only 10% of wild type

frequency on Teflon, an inductive (hydrophobic) surface. This defect was rescued in the Δ*plg1* mutant upon addition of cAMP, DAG and both cAMP and DAG over a 24 h time period, giving the following respective appressorium formation frequencies: 39.5%, 45.9% and 58.6% (Figure 19A). Once again, all appressorial-like structures with similar diameters, regardless of the level of melanization were included in the quantification. Figure 19B shows the morphology of the wild type and Δ*plg1* appressoria under various treatments on Teflon. Results were taken at 24 hpe, and images were examined at 100x magnification to clearly see possible differences in appressorium morphology. Wild type spores still gave high levels of melanized appressoria under all treatments, and it can be seen that the appressorium formation in the treated Δ*plg1* mutant still did not reach wild type levels (Figure 19A). However, the rescue of appressorium differentiation on the hydrophobic surface is indicative of *PLG1*, most likely lying upstream of both the cAMP and DAG pathways, to generate the described responses upon addition of the two inducers.

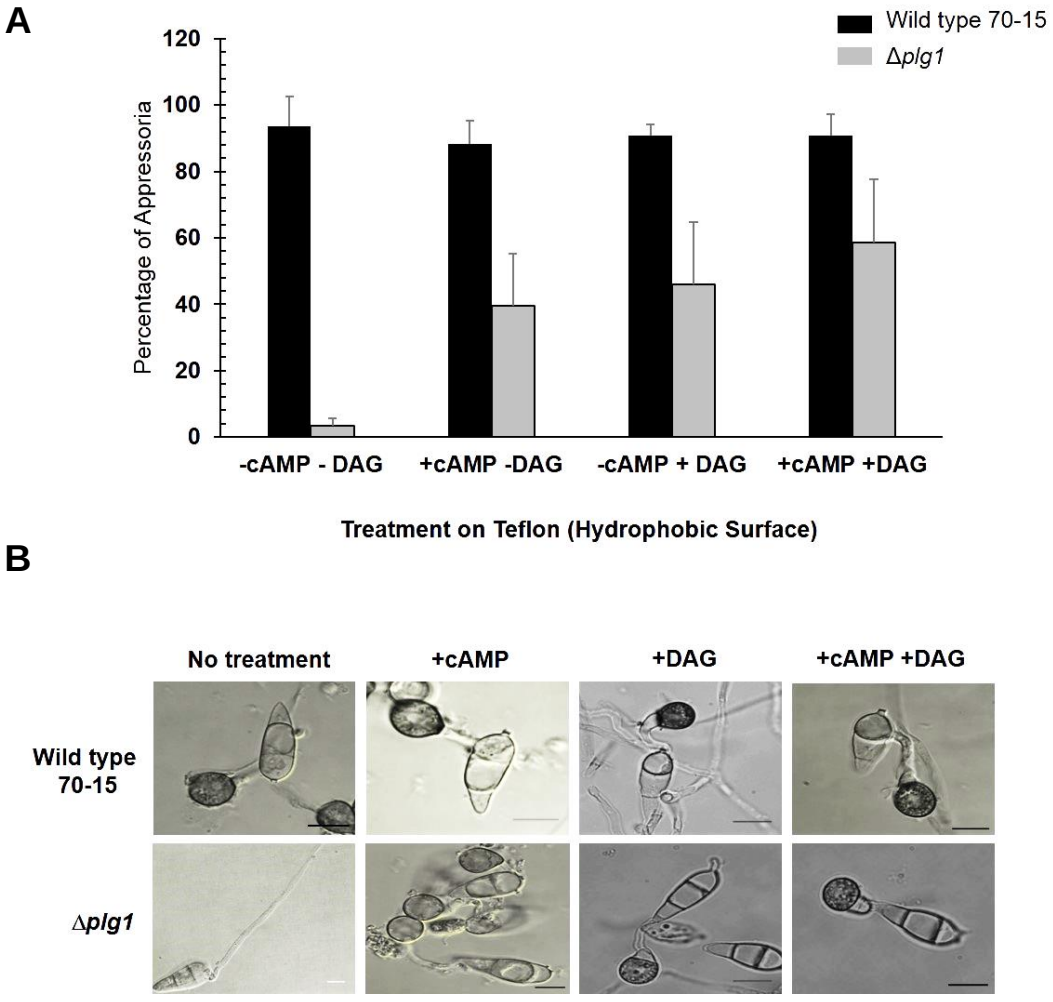

Figure 19. Δ*plg1* Appressorium Formation is Enhanced by cAMP and DAG on a Hydrophobic Surface.

(A) Appressorium formation of 70-15 and Δ*plg1* on Teflon membrane in the absence or presence of 10 mM 8-Br-cAMP and/or 20 µg/ml DAG was verified microscopically at 24 hpe. Each bar is an average from three biological replicates, where at least 100 conidia are evaluated per replicate. Standard deviations are indicated.
(B) Appressorium formation of 70-15 and Δ*plg1* on Teflon membrane in the absence or presence of 10 mM 8-Br-cAMP and/or 20 µg/ml DAG was monitored at 24 hpe and observed at 100x. (bars = 10 µm)

As introduced earlier, the need for a hydrophobic surface in forming appressoria is bypassed by the addition of either cAMP or DAG in wild type spores. Likewise, the response of the Δ*plg1* mutant in the presence of the inducers was tested on a hydrophilic surface. For this purpose, the hydrophilic side of GelBond was used, employing similar treatments and incubation times as described for Teflon earlier. In Figure 20, it can be seen that the untreated wild type spores did not develop a significant number of appressoria (4%), but addition of cAMP alone, DAG alone, and both cAMP and DAG led to appressorium formation frequencies 55%, 39% and 58%, respectively. Surprisingly, when the same treatments were done for the Δ*plg1* mutant, almost no appressoria was observed upon addition of either cAMP or DAG, but appressoria were observed at 17% frequency when both inducers were present. These observations were intriguing because they suggest a possible synergistic activity of cAMP and DAG or a feedback mechanism between the two pathways, when surfaces are non-inductive for appressoria formation. Accordingly, the response appears to be mediated by PLG1. Such outcomes still put PLG1 upstream the cAMP and DAG signaling pathways, but there appears to be a surface requirement for obtaining a high level of appressorium formation when only cAMP or DAG is available.

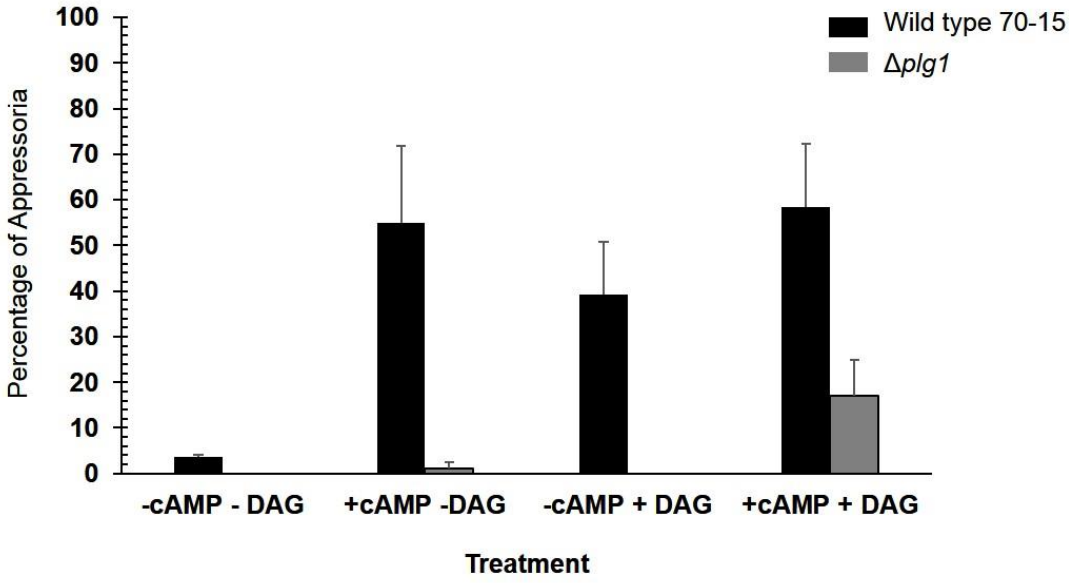

Figure 20. Δ*plg1* Appressorium Formation on a Hydrophilic Surface is Observed Only Upon Treatment with Both cAMP and DAG.

Appressorium formation of 70-15 and Δ*plg1* on the hydrophilic side of GelBond, in the absence or presence of 10 mM 8-Br-cAMP and/or 20 µg/ml DAG was verified microscopically at 24 hpe. Each bar is an average from three biological replicates, where at least 100 conidia are evaluated per replicate. Standard deviations are indicated.

In Figure 21, it is shown how most of the spores appear after cAMP and DAG treatments on a hydrophilic surface at 24 hpe. Images were taken at 20x magnification for an increased field of view. Without any treatment, both wild type and Δ*plg1* spores exhibited vegetative growth, i.e. continuous elongation of germ tubes on a surface that is non-inductive for appressorium formation. Upon addition of cAMP, DAG and both inducers, wild type showed appressorium formation. There are still wild type spores that exhibited germ tube elongation, but there is an obvious response of appressorium formation.

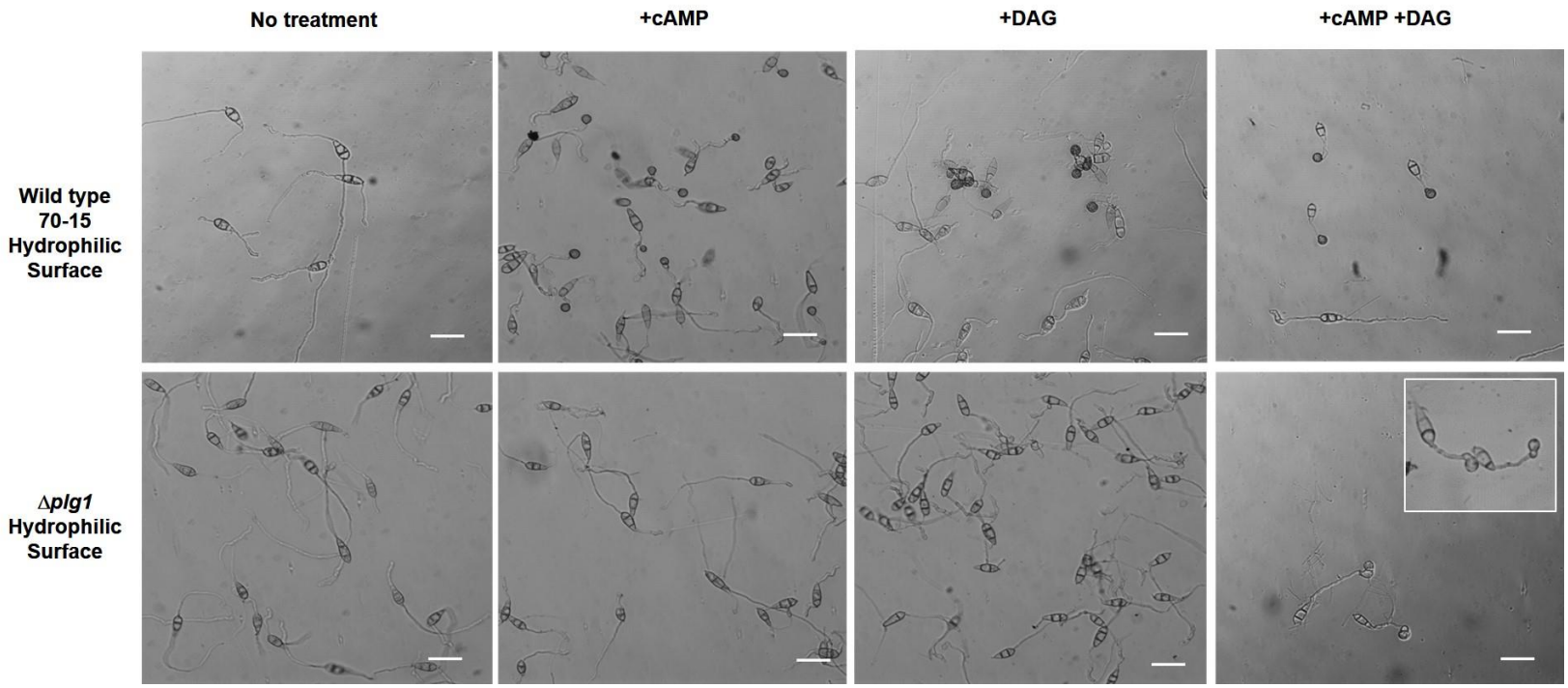

Figure 21. Microscopic Examination of Wild Type and Δplg1 Appressorium Formation on a Hydrophilic Surface.

Appressorium formation of 70-15 and Δ*plg1* on the hydrophilic side of GelBond, in the absence or presence of 10 mM 8-Br-cAMP and/or 20 µg/ml DAG was verified microscopically at 24 hpe. The inset in the cAMP- and DAG-treated Δ*plg1* shows the resulting appressoria taken at a higher magnification. (bars = 20 µm)

Interestingly, it is only upon treatment with both cAMP and DAG that the Δ*plg1* spores showed apparent germ tube tip swelling, hooking and appressorium formation. As seen in Figure 21 for the cAMP- and DAG-treated Δ*plg1* mutant, it did not take too much germ tube elongation before the incipient appressoria were observed. The inset shows the appressoria they formed, taken at a higher magnification. Upon closer inspection, these appressoria did not appear completely melanized similar to the wild type spores treated with both cAMP and DAG.

Δplg1 Mutant Pathogenicity Defect is Rescued by Diacylglycerol but Not cAMP

It can be recalled that the Δ*plg1* mutant formed appressoria, between 40% to 60% in the presence of cAMP and DAG on a hydrophobic surface. Since the leaf surface shares the same hydrophobic property, the cAMP and DAG-treated spores were tested on detached barley leaves to see whether the appressoria they formed were functional. In the absence of any treatment, wild type 70-15 is pathogenic, while the Δ*plg1* mutant is not. This is consistent with the results of the infection assays presented in Chapter III. As shown in Figure 22, in the presence of either cAMP or DAG, or both, wild type 70-15 remains pathogenic on the leaves, showing necrotic and spreading lesions on the sites of inoculation. Surprisingly, the cAMP-treated Δ*plg1* spores did not appear to be pathogenic on the barley leaves, showing small brown spots which were typical of the Δ*plg1* mutant phenotype. On the other hand, the spores which were treated with DAG and, DAG combined with cAMP, showed more evident disease symptoms. There is no

significant difference between the levels of pathogenicity exhibited by the two types of treatment, suggesting that it is most likely the DAG treatment that is contributing to the disease symptom. It can be observed however, that the severity of infection still does not reach wild type levels, in the sense that the lesion margins did not appear to be spreading. The infection seemed to be confined to the actual inoculation sites. Perhaps, if left longer, more extensive necrosis will be observed. However, at longer incubation times, the leaves exhibit yellowing, which might obscure the results, especially at the inoculation sites.

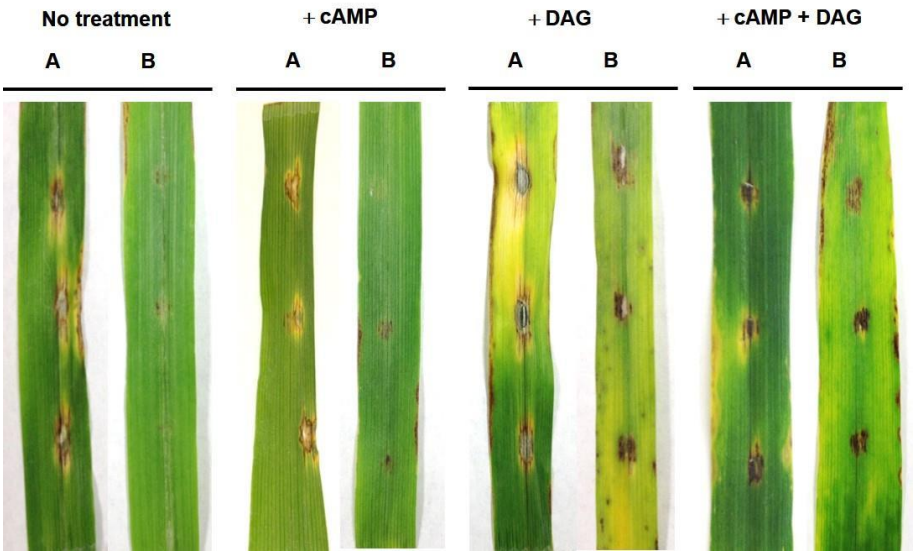

Figure 22. Effects on Pathogenicity of cAMP and DAG Treatments on Wild Type 70-15 and Δ*plg1* Mutant Strains

Detached and intact barley leaves inoculated with wild type 70-15 **(A)** and Δ*plg1* mutant **(B)** treated with 10 mM 8-Br-cAMP and/or 20 µg/ml DAG were examined at 7 dpi. At least three biological replicates were performed for the different conditions, and showed similar results.

Δplg1 Mutant Treated with cAMP Alone Exhibited Reduced Appressorial Turgor Pressure Than Δplg1 Mutant Treated with DAG Alone or cAMP with DAG

It was already shown earlier that on Teflon, the Δ*plg1* mutant responds to cAMP and/or DAG treatments resulting in appressoria. When infection assays were performed to check for the functionality of the appressoria in the treated Δ*plg1* mutant spores, they revealed that only Δ*plg1* mutant spores treated with both cAMP and DAG, and DAG alone showed disease symptoms. As introduced in this chapter, there are some instances where although a certain strain produces normal-looking appressoria, the appressoria can still be defective in infection. This is primarily due to the required turgor pressure not being met, thereby reducing the disease symptoms that the particular strain can cause (Thines et al., 2000). Thus, to explain the reduced disease symptom in the Δ*plg1* mutant treated with cAMP alone, cytorrhysis or appressorium collapse assays were performed. The experiment is straightforward, where spores are allowed to develop under the various treatments, and at 24 hpe, varying concentrations of glycerol (1 M, 3 M and 5 M) were added to the developed spores. Glycerol accumulates in the appressoria and is responsible for the appressorial turgor pressure. The rationale behind the experiment is that when the extracellular concentration of glycerol exceeds the intracellular glycerol concentration, the appressorium collapses due to the loss of water through osmosis (de Jong et al., 1997). In effect, a low number of collapsed appressoria for a particular strain, suggests that the appressoria have not reached the optimum level of glycerol in the appressoria, which on average is 3 M (de Jong et al., 1997). The results of this

particular assay are shown in Figure 23. Note that the percentage of collapsed appressoria for each treatment was the dependent variable. This was obtained by counting the number of collapsed appressoria which resemble the shape of a "fortune cookie" and dividing by the total number of appressoria (collapsed and non-collapsed) counted for each treatment.

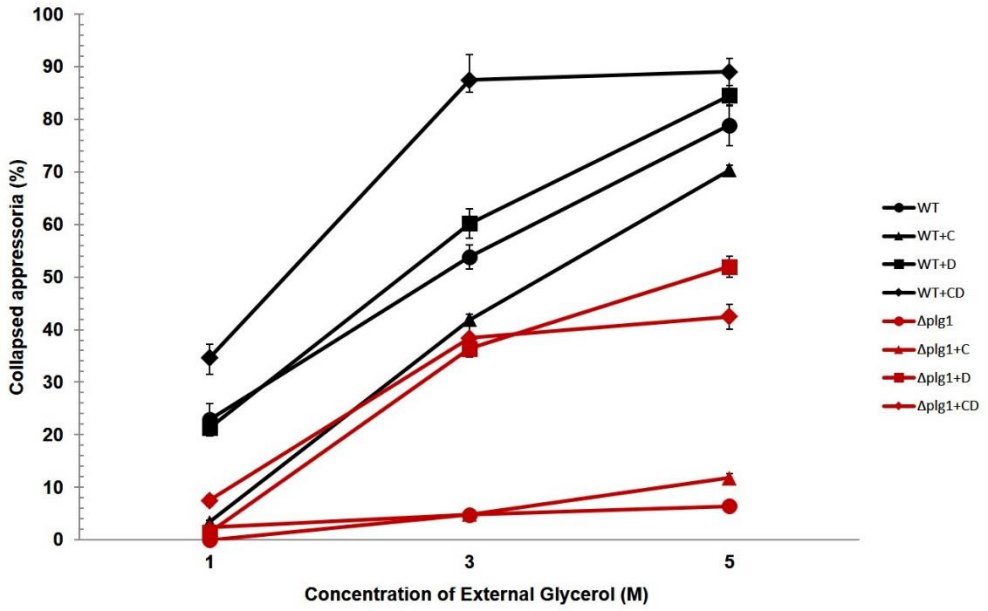

Figure 23. Quantitative Analysis of the Collapsed Appressoria in the Wild Type 70-15 and Δ*plg1* Mutant Strains Treated with cAMP and DAG.

Appressoria were allowed to form in various treatments with 10 mM 8-Br-cAMP and/or 20 µg/ml DAG for 24 h on Teflon, and were treated with 1 M, 3 M and 5 M glycerol prior to microscopic examination. Each data point shows an average of the percentage of collapsed appressoria for at least three biological replicates. All black lines and red lines correspond to the untreated and treated wild type 70-15 and Δ*plg1* mutant, respectively. For both strains, different conditions were tested: untreated (●), cAMP alone (▲), DAG alone (■) and both cAMP and DAG (◆).

In Figure 23, all black lines correspond to the wild type 70-15 response, while red lines correspond to the Δ*plg1* mutant response, under various conditions. The glycerol concentrations tested were 1 M, 3 M, 5 M, following experiments based on literature. These concentrations were also chosen because they span the estimated average glycerol concentration inside the mature appressorium. For both strains, different conditions were tested: untreated (●), cAMP alone (▲), DAG alone (■) and both cAMP and DAG (◆). Looking at each individual line, it can be seen that as the external glycerol concentration increased, the percentage of collapsed appressoria also increased. Steeper slopes are observed for the treated wild type compared to the Δ*plg1* mutant. These indicate that the wild type appressoria were more sensitive to increasing glycerol concentrations because the optimum glycerol content in the appressoria had been met. These may also indicate that there is no defect in glycogen and lipid mobilization across development. It has been proposed that glycogen and triacylglycerol were being used up for the biosynthesis of glycerol (Thines et al., 2000). So if there is no defect in the biosynthetic pathways leading to glycerol production, then its appressorial concentration should be optimum. The conditions showing low percentages of collapsed appressoria were the untreated Δ*plg1* spores and the cAMP-treated Δ*plg1* spores. Treatment with DAG, and cAMP combined with DAG, resulted in more collapsed appressoria for the Δ*plg1* spores, but still less than all wild type conditions. These most likely explain why the cAMP-treated Δ*plg1* spores did not show significant disease symptoms on barley. They indicate that glycogen and/or lipid mobilization is either defective or delayed even after cAMP treatment. An alternative explanation for the results is the level of

melanization in the treated Δ*plg1* spores. Previous studies have shown that melanized appressoria tend to be plasmolyzed by higher external solute concentrations, and they collapse during plasmolysis due to cytorrhysis. On the other hand, non-melanized appressoria do not undergo cellular collapse (Howard and Ferrari, 1989). This is because melanin acts as a seal, preventing solute efflux which gives rise to the high osmotic potential found within the melanized appressoria. Thus, the cAMP-treated Δ*plg1* spores could also be diminished of the melanin layers that are usually present in the wild type. Experimentally, this can be tested through the ultrastructure analysis of the appressoria via electron microscopy (Wilson and Talbot, 2009) or by looking at defects in melanin biosynthesis (Forrest, 1990). However, these were not done to confirm whether the cAMP-treated Δ*plg1* appressoria are differentially melanized compared to wild type.

cAMP- and DAG- Treated Δplg1 Mutant Showed Delay in Glycogen Mobilization on Teflon

Since the appressorium collapse assay showed that the Δ*plg1* mutant in general, regardless of any treatment, showed lower percentage of collapsed appressoria than wild type, the mobilization of glycogen was monitored in the developing spores. Glycogen is thought to be a precursor for glycerol which accumulates in the appressoria. It is detected in the spores by I_2 in KI treatment, where glycogen is stained brown as result of iodine-glycogen complex formation. It is expected that glycogen will be detected in the

spores, germ tubes and in the appressoria at early time points, but should decrease rapidly as the cell completes appressorium maturation. Thus, the staining should not be as intense, or absent at all in spores that have mature appressoria, if there is no glycogen mobilization defect (Thines et al., 2000). In Figure 24, images from each treatment are presented. These images are representative of the stained appearance of the developed spores that are frequently seen for each treatment at that particular time point. At early time points, 0 hpe and 4 hpe on Teflon, both wild type 70-15 and Δ*plg1* germlings showed intense staining on the spores. This staining should slowly go away by 12 h from the conidia, and staining could be observed in the germ tubes and eventually only in the appressoria. At the onset of melanization, glycogen would have been rapidly degraded, and no staining will be observed. At 12 h it can be seen that some staining is still observed in the conidia, on the germ tubes, but more intensely in the appressoria for both wild type and Δ*plg1* mutant. Comparing wild type and Δ*plg1* mutant, however, a more intense or darker brown staining is seen in the appressoria for the wild type, indicating that the level of glycogen could be higher because of more efficient mobilization. At 24 hpe, almost all of the wild type conidia and germ tubes are free of any stain. Some appressoria may still have staining, as the case for the untreated wild type in Figure 24. Expectedly, once melanization took place, no brown staining was observed and instead a gray or black color is seen for the appressorium, for example in wild type treated with cAMP alone in Figure 24. A sample of a situation in which less brown staining is observed, suggesting that glycogen is being degraded and melanin forming at the same time, is seen in wild type treated with DAG alone in Figure 24.

Some brown patches are seen at the center, but the region closer to the appressorial membrane and cell wall, starts to show melanin (gray to black) deposition. As a comparison, at 24 h, majority of the untreated Δ*plg1* just showed germ tube elongation, and staining from the conidia, germ tube, and all the way to the appressoria which seemed to develop at the tip.

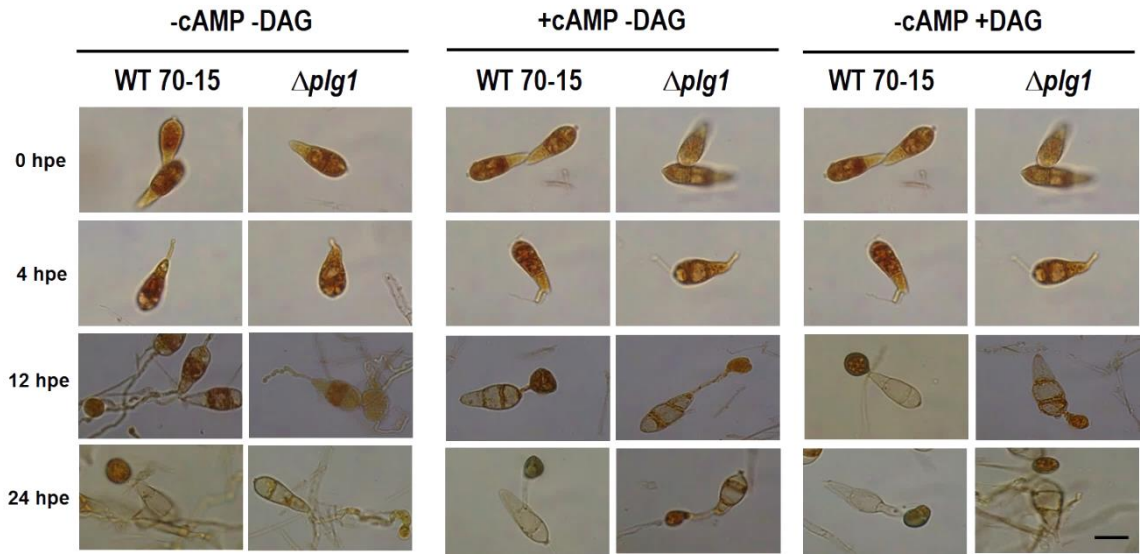

Figure 24. Cellular Distribution of Glycogen in the cAMP and/or DAG-Treated Wild Type 70-15 and Δ*plg1* Mutant.

Conidia from 70-15 and Δ*plg1* were allowed to develop on Teflon membrane in the absence (-cAMP -DAG) or presence of 10 mM 8-Br-cAMP and/or 20 µg/ml DAG (+cAMP -DAG or –cAMP +DAG). After the indicated time points (0 hpe, 4 hpe, 12 hpe and 24 hpe), 10 µL of the I_2 in KI staining solution was added to each 20 µL droplet of conidial suspension and samples were incubated for 10 min. Yellowish brown glycogen deposits were verified microscopically at each developmental stage. (bar = 10 µm)

Also at 24 h, both cAMP- and DAG-treated Δ*plg1* spores showed residual staining on the conidia and germ tubes, although stronger stain is observed in the appressoria. This

differed from wild type, because most of the spores were already clear and germ tubes were free of the stain at 24 hpe. Between the Δ*plg1* mutant treated with cAMP alone and DAG alone, however, it is difficult to distinguish any significant difference in the staining for the different structures. It can be recalled that in the appressorium collapse assays, DAG-treated Δ*plg1* mutant showed a higher number of collapsed appressoria compared to the cAMP-treated ones, indicating achieving sufficient appressorial turgor pressure to cause disease symptoms on barley. The glycogen mobilization in the cAMP-treated Δ*plg1* spores did not seem to be different from the DAG-treated ones, hence it might not be the cause of the reduced turgor pressure in cAMP-treated Δ*plg1* appressoria. The number of stained spores, germ tubes and appressoria were quantified at 24 hpe, and are reported in Table 2.

Table 2. Cellular Distribution of Glycogen in Developing Spores Under cAMP or/and DAG treatments at 24 hpe

	Spores with glycogen (%)		Germ Tubes with Glycogen (%)		Appressoria with Glycogen (%)	
	70-15	Δ*plg1*	70-15	Δ*plg1*	70-15	Δ*plg1*
Untreated	10.71 ± 1.00	85.43 ± 6.08	17.86 ± 0.58	75.50 ± 2.65	32.14 ± 2.00	5.96 ± 1.00
with cAMP	12.50 ± 0.58	60.66 ± 8.33	25.00 ± 0.58	60.00 ± 5.29	56.25 ± 2.00	96.67 ± 11.14
with DAG	13.33 ± 1.15	33.78 ± 3.51	26.67 ± 0.58	72.13 ± 10.41	66.67 ± 0.59	98.36 ± 6.08

Conidia were allowed to germinate on Teflon and form appressoria. After 24 hpe, the samples were stained for the presence of glycogen. The average ± standard deviation is for three biological replicates, observing at least 30 conidia per replicate.

Note that the values reported are the structures showing an amount of staining at 24 hpe. For the quantification involving the appressoria, recall that once the appressoria have developed melanin, one does not observe significant amount of yellowish brown deposits anymore, and so the percentage counted for staining is much lower. That is especially true for the wild type treated with cAMP and DAG (second to the last column in Table 2). The percentage of stained appressoria for the cAMP and DAG-treated Δ*plg1* is reported to be higher than wild type. This is because some of the wild-type appressoria are already fully melanized, and glycogen are degraded and presumably converted to glycerol already. Overall, those results indicate that there could be a delay in glycogen mobilization in the Δ*plg1*mutant for any treatment, compared to wild type.

Lipid Mobilization is Not Severely Impaired in cAMP- and DAG-treated Δplg1 Mutant on Teflon

Similar to glycogen, the mobilization of lipid droplets, composed of triacylglycerol, in the developing spores may also be monitored. The stain that is typically used is Nile Red, and fluorescence is observed for lipid droplets stained with Nile Red (Thines et al., 2000). At 0 hpe, lipid droplets are abundant in both wild type and Δ*plg1*mutant, for all treatments. At 4 hpe, lipid droplets were seen translocated into the germ tubes and into the nascent appressoria. At this time point, less fluorescence is observed in the conidia for all wild type and Δ*plg1*mutant treatments, except for the untreated Δ*plg1*mutant. At 24 hpe, it can be seen in Figure 25 that the untreated Δ*plg1*mutant still exhibit staining

all over the conidia and germ tubes, whereas in the other samples, fluorescence appeared to be concentrated in the appressoria. At this time point, it looks like there is no significant delay in the treated Δ*plg1*mutant versus the treated or untreated wild type spores, most of the signal is seen in the appressoria for most of them. Upon closer inspection however, smaller fluorescent spots are observed within the wild type appressoria for all treatments, whereas the fluorescent signal is more diffused all over the appressoria in the treated Δ*plg1*mutant. Presumably these are indicative of lipid droplets being degraded faster in the wild type, leading to lesser components stained by Nile Red.

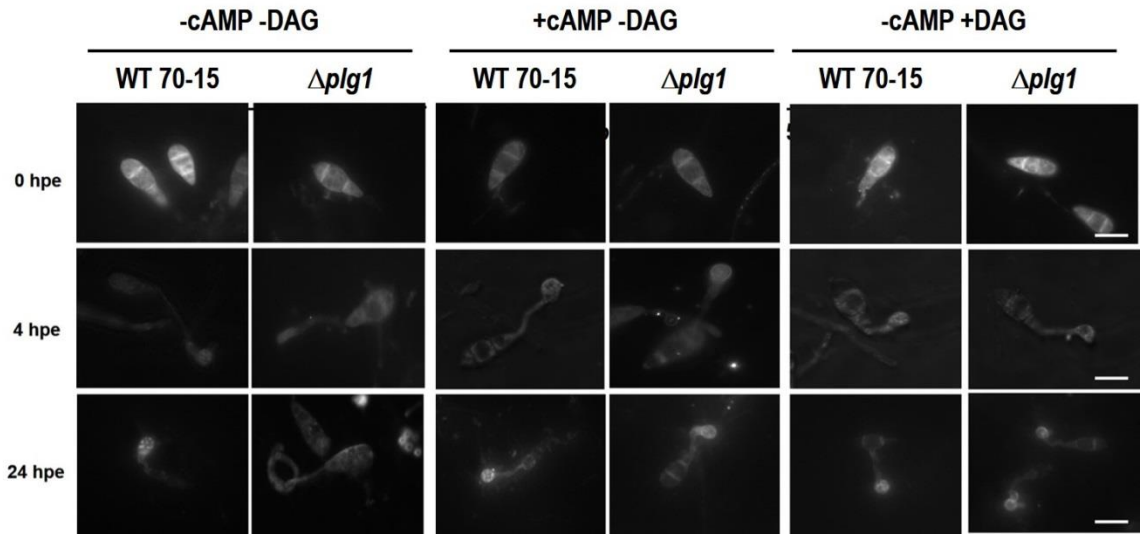

Figure 25. Cellular Distribution of Lipid Droplets in the cAMP and/or DAG-Treated Wild Type 70-15 and Δ*plg1* Mutant.

Conidia from 70-15 and Δ*plg1* were allowed to develop on Teflon membrane in the absence (-cAMP -DAG) or presence of 10 mM 8-Br-cAMP and/or 20 µg/ml DAG (+cAMP -DAG or –cAMP +DAG). After the indicated time points (0 hpe, 4 hpe, and 24 hpe), 3 µL of the Nile Red staining solution was added to each 20 µL droplet of conidial suspension and samples were incubated for 10 min. Fluorescence was verified microscopically at each developmental stage. (bars for 0 h and 24 h = 20 µm, bar for 4 h = 10 µm)

Taken together, the results suggest that there is no significant delay in lipid mobilization in the treated wild type and Δ*plg1* mutant since fluorescence was mainly seen in the appressoria at the final time point that was tested. This is not true for the untreated Δ*plg1* mutant however, since lipid droplets are still detected all throughout the developmental stages at 24 hpe.

Expression of the PKC-Encoding Gene is Significantly Downregulated in the Δplg1 Mutant at 24 hpe on Teflon

It was shown earlier that addition of either cAMP and DAG recovers appressorium formation in the Δ*plg1* mutant on Teflon. Moreover, DAG treatment rescues the pathogenicity defect of the Δ*plg1* mutant. Overall, these indicate that PLG1 may be involved in the regulation of the cAMP- and DAG-mediated pathways. To further demonstrate a functional connection, the expression of three genes, namely *cPKA*, *PKC*, and *PMK1* were examined under the wild type and Δ*plg1* mutant backgrounds. Briefly, undifferentiated (at 0 hpe) and differentiated spores on Teflon (at 24 hpe), were isolated for RNA extraction. The $2^{-\Delta\Delta Ct}$ method was used to calculate relative expression levels, using *EF1α* gene was used as internal control. Since this was the type of method used for data analysis, the 24 hpe expression data were normalized against the 0 hpe expression data, separately for the wild type and Δ*plg1* mutant. This sets the 0 hpe transcript level to 1, and bars are not shown for these information in Figure 26. In Figure 26, the relative expression of the downstream signaling genes at 24 hpe, under

wild type and Δ*plg1* mutant conditions, are presented. Although it is obvious from the graph that there are differences between the gene expression of the signaling genes, under the two backgrounds, it is absolutely necessary to determine whether the differences are significant or not. For this purpose, a two-tailed Student's t-test was performed according to the method employed in the GraphPad Prism v.6 software. Statistical significance was defined by (P) < 0.05, for the four independent biological replicates. As seen in Figure 26, black bars and gray bars represent expression of the genes under the wild type 70-15 and Δ*plg1*mutant backgrounds, respectively. After the statistical significance was analyzed using the Holm-Sidak method (Holm, 1979), at a 95% confidence interval, results showed that only the *PKC* differential expression was significant, with $p = 0.009$, which is less than 0.05. The p values for *CPKA* and *PMK1* differential expression was determined to be 0.04 and 0.7 respectively. Interestingly the p value for the *CPKA* differential expression was less than 0.05, but most likely, the software applied a more stringent criterion for it to classify the change in *CPKA* expression as not significant. However, these results suggest that *PKC* expression, which is likely under the control of the DAG pathway, is significantly downregulated when *PLG1* is absent.

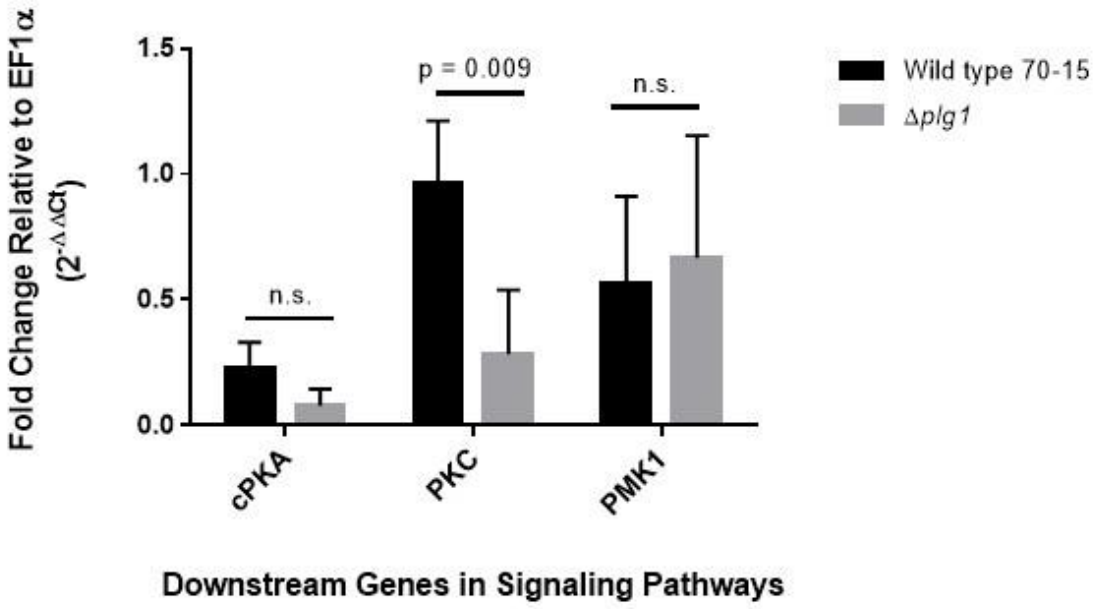

Figure 26. Transcript Analysis of Signal Transduction Genes in Germlings Differentiated on Teflon.

Total RNA was extracted from undifferentiated spores (0 hpe) and germlings growing on Teflon membrane at 24 hpe. Transcript levels of the genes *CPKA*, *PKC* and *PMK1* were quantified through qRT-PCR, relative to the internal control gene *EF1α*. Using the $2^{-\Delta\Delta Ct}$ method, the expression at 24 hpe was further normalized against the 0 hpe expression, separately for the wild type and Δ*plg1* mutant strains. Presented here are the $2^{-\Delta\Delta Ct}$ values at 24 hpe after normalization. Four independent biological replicates were analyzed and standard deviations are indicated by the error bars. Statistical significance is defined by $p < 0.05$ after a Student's t-test performed with GraphPad Prism v.6. The *p* value is indicated for *PKC*, while n.s. above *CPKA* and *PMK1* indicates "not significant" for the statistical parameters that were set.

Discussion

In Chapter III, the pathogenicity defect of the Δ*plg1* mutant on both barley and rice was described to be due to the inability of the mutant to complete appressorium differentiation for a significant number of developing spores. It is known that appressorium differentiation in *M. oryzae* is an elaborate process resulting from various

intracellular signaling pathways which include those mediated by cAMP and diacylglycerol (Lee and Dean, 1993; Gilbert et al., 1996; Choi and Dean, 1997). Given the phenotypes observed for the Δ*plg1* mutant, it was hypothesized that as a predicted transmembrane protein, PLG1 acts as a plasma membrane receptor which responds to signals that drive one or multiple pathways in *M. oryzae*. The coordinated input from the pathways mediated by PLG1 is most likely leading to appressorium differentiation, and hence the absence of PLG1, causes defects in the said developmental phase.

To confirm the membrane localization of PLG1, a GFP N-terminal fusion strategy was employed. The Δ*plg1* mutant was transformed with the GFP-tagged PLG1 construct under the control of the native promoter. This resulted in spores which formed appressoria on Teflon, similar to the levels formed in the Δ*plg1*/*PLG1* complemented strains. Pathogenicity assay on barley also showed disease symptom at the sites of inoculation, albeit at lower levels compared to wild type. These indicate that PLG1 is being expressed at some level, and leads to partial recovery of appressorium formation and pathogenicity. When viewed microscopically, no GFP signals were detected at early time points, such as 4 h. Weak GFP signals were observed outlining the incipient appressoria during the hooking stage and stronger GFP signals were observed on the appressorial plasma membrane at 24 hpe. These results suggest that the *GFP-PLG1* construct was functional and the observation of the GFP signals was also consistent with the expression studies reported in Chapter II, where *PLG1* was shown to be highly expressed at 24 hpe on Teflon. Initially, the possibility that the N-terminal GFP fusion

construct might not be functional has been considered. It has long been known that signal sequences on proteins for membrane localization, which are usually found at the N-terminal, are cleaved after the precursor proteins have crossed the membrane (Alberts et al., 2013). However, some signal sequences may be found within the polypeptide chain rather than the N-terminus. Such signals are never cleaved, and they serve to retain the protein in the membrane (Alberts et al., 2013). Perhaps, such is the case for the *GFP-PLG1* construct, hence GFP signals are still observed. Moreover, N-terminal GFP tagging has been shown to be successful in reported *M. oryzae* experiments (Dagdas et al., 2012; Ramanujam et al., 2013). When the constructs used in the referenced papers were targeted to the appressorial plasma membrane, the GFP membrane localization was similar to what was observed with the N-terminal *GFP*-tagged *PLG1*.

To assess the upstream signaling function of PLG1, appressorium formation inducers such as 1,16-hexadecanediol (HDD), 8-Br-cAMP (cAMP) and the diacylglycerol 1,2-dioctanoyl-*sn*-glycerol (DAG). HDD is a cutin monomer which is a component of leaf waxes, so it can be thought of as an external stimulus for appressorium formation. When the Δ*plg1* mutant was treated with HDD, a significant increase in appressorium formation was seen. If we think of HDD as a signal or stimulus, the results indicate that PLG1 is not required for its detection because appressorium formation was seen even in the absence of PLG1. Perhaps, another receptor is detecting HDD, and this leads to the enhanced activation of signaling pathways driving appressorium formation. One

receptor which comes to mind is PTH11, since treatment of Δ*pth11* mutant with HDD did not result in appressorium formation. With respect to receptor properties, this is one aspect where PLG1 and PTH11 differed. Alternatively, it can also be thought that HDD crosses the membrane, bypasses the need for PLG1, and triggers the downstream pathways for appressorium formation. For HDD to eventually cross the membrane and act as a potential secondary messenger does not seem to be the case since HDD is poorly water soluble and may not be found in the cytoplasm. However, it has been reported that the cutin monomers could penetrate model membranes to some extent and exhibit some level of solubility in the phospholipid matrix. This penetration leads to membrane perturbation as a result of the hydrophobic mismatch between the membrane thickness and the monomer string length (Douliez, 2004). Perhaps, when HDD encounters the fungal cell wall and membrane, it initiates some mechanical perturbation, which can serve as the signal for appressorium formation. To date, how cutin monomers act as signals or messengers in plant-pathogen interactions is still not clearly understood (Schweizer et al., 1996; Heredia, 2003; Douliez, 2004).

In the presence of exogenous cAMP and/or DAG, the Δ*plg1* mutant formed a significantly higher number of appressoria compared to the untreated Δ*plg1* spores on Teflon. Still, Δ*plg1* did not reach wild-type levels with respect to appressorium formation. However, suppression of the Δ*plg1* defect by cAMP and DAG treatment suggests a bypass of the necessary signal recognition phase. This indicates that PLG1 functions upstream of both cAMP-mediated and DAG-mediated signaling pathways,

which is consistent with its localization and proposed role as a receptor. Since appressorium formation was observed, the functionality of the appressoria was tested by doing detached barley inoculation assays.

Although cAMP and DAG rescued appressorium formation in the Δ*plg1* mutant, the ability to form any appressoria is not sufficient for pathogenicity. This is the case when the appressoria have not reached the optimal turgor pressure due to a reduced glycerol content, or when the appressoria has melanization defects (de Jong et al., 1997; Farman, 2002). The most straightforward way to address these is by performing appressorium collapse or cytorrhysis assays. Cytorrhysis, which usually follows plasmolysis, is the complete collapse of the organism's cell wall. It occurs when the external solute concentration is higher compared to the intracellular solute concentration, and the organism has a prolonged exposure to such condition. Upon testing the wild type 70-15 and Δ*plg1* spores in the absence or presence of cAMP and/or DAG, results showed that both the untreated Δ*plg1* spores and the cAMP-treated Δ*plg1* spores had the lowest number of collapsed appressoria, indicating a low number of spores with the optimum appressorial turgor pressure. This most likely explained why even though cAMP rescued appressorium formation in the Δ*plg1* mutant on Teflon, the cAMP-treated spores were still non-pathogenic on barley leaves. Addition of DAG however, rescued both appressorium formation on Teflon and the pathogenicity defect on barley. Although the lesions were not as extensive as the wild type-induced lesions, disease symptoms on barley were evident on the sites of inoculation. Addition of both DAG and cAMP also

resulted in appressorium formation, but the level of pathogenicity is similar to that of DAG treatment alone. Clearly, both cAMP and DAG have signaling roles that are mediated by PLG1, but results indicate that cAMP treatment alone is insufficient for pathogenicity of the Δ*plg1* mutant. These outcomes are noteworthy because they are opposite to what were discovered for PTH11. As introduced earlier, either cAMP or DAG restored the appressorium formation in the Δ*pth11* mutant, but only cAMP restored the pathogenicity on barley leaves. Could there be a possible interaction between PTH11 and PLG1 which leads to the activation of pathways mediated by cAMP and DAG? It is a possibility, but further evidence is required to establish their functional connection.

Interestingly, when the surface of inoculation was changed to a hydrophilic one, Δ*plg1* showed germ tube swelling and appressorium development only when both cAMP and DAG inducers were added. The untreated Δ*plg1* spores, along with the spores treated with cAMP alone and DAG alone did not show some evidence of the early stages of appressorium development. They just showed vegetative growth or extensive germ tube formation on the non-inductive surface. The untreated wild type, as expected, also showed continuous germ tube elongation, but all cAMP and DAG treatments for the wild type spores allowed for appressorium formation even on the non-inductive surface. These results confirm what has been proposed for a long time, that crosstalk between the signaling pathways exist. However, not much is known about the particular points in the pathways in which the interactions converge or which molecules mediate the interactions

(Marroquin-Guzman and Wilson, 2015). cAMP and DAG provided what seemed to be a synergistic effect when surfaces are non-inductive to appressorium formation, and an important component to that synergy is PLG1. These results also strengthen the argument that PLG1 might be interacting with another receptor to trigger the signaling pathways leading to appressorium formation. The interaction may not necessarily be physical, but is most likely mediated by the secondary messengers, cAMP and DAG. On inductive surfaces, addition of either cAMP or DAG recovers appressorium formation in the Δ*plg1*mutant, but on a non-inductive surface neither of them induced appressorium formation. On barley leaves, which are presumed hydrophobic because of leaf waxes, DAG-treated Δ*plg1*mutant exhibited some disease symptoms, but not cAMP treatment. If PLG1 operated only through the DAG-mediated pathway and this pathway is sufficient to induce appressorium formation, then one would expect that addition of DAG will allow development of appressoria in the Δ*plg1* mutant on the hydrophilic surface. The same line of reasoning can be used for the cAMP response. If PLG1 transduces signals via the cAMP pathway alone, and this is sufficient for appressorium formation, then cAMP addition on a hydrophilic surface should rescue appressorium formation. However, those were not the outcomes of either cAMP or DAG addition. It required both the addition of cAMP and DAG to show appressorium formation in the Δ*plg1*mutant on the non-inductive surface. If PLG1 is a GPCR, could it be working to transduce the signals via both pathways, and both pathways are necessary for appressorium formation? Clearly, both pathways are important for appressorium differentiation, but PLG1 solely mediating both pathways at the same time seems

unlikely. One of the reasons for this is that on Teflon, which is a hydrophobic surface, either cAMP alone or DAG alone rescues appressorium formation. This suggests that there is possibly another receptor which works in conjunction with PLG1, and this receptor mainly responds to hydrophobicity. It has been established for a long time that the cAMP pathway is triggered in response to hydrophobicity. So perhaps that receptor, in addition to PLG1 works via the cAMP pathway, and that puts PLG1 as a major activator of the DAG-mediated pathways. But what is the relationship between the purported receptor and PLG1? There is a possibility that the other receptor also activates DAG-mediated pathways, and contributes some level of intracellular DAG; and PLG1 likewise can activate the cAMP-mediated pathway to produce some level of intracellular cAMP. This model definitely requires further testing, but this scenario can explain most of the observed results. First, it supports the finding that in the presence of cAMP alone, or DAG alone, the Δ*plg1*mutant forms appressoria on a hydrophobic surface. However, despite forming appressoria under both treatments, only the DAG-treated spores exhibited a considerable level of pathogenicity on barley and not the cAMP-treated spores. This suggests a condition in which the level of DAG added was sufficient to generate a response related to appressorium formation, which could have been provided if PLG1 was present. Perhaps, this response is the generation of the optimal appressorial turgor pressure either through effective glycogen and lipid mobilization, or melanin biosynthesis. It can be recalled that the cAMP-treated spores are reduced in appressorial turgor pressure, relative to wild type and the DAG-treated spores. So supplying cAMP alone, in addition to the intracellular cAMP generated by

the receptor in response to hydrophobicity, is sufficient to form the appressoria, but intracellular DAG generated by the other receptor is not sufficient to create a functional mature appressoria.

To illustrate the proposed placement of PLG1 in the signaling pathways, it is useful to look at how the GPCR signaling generally works again. In Figure 27, it is shown that GPCRs can potentially bind different Gα subunits which trigger PKA via cAMP, and PKC via the DAG. The released Gβγ can likewise trigger the DAG-mediated pathway (Ritter and Hall, 2009).

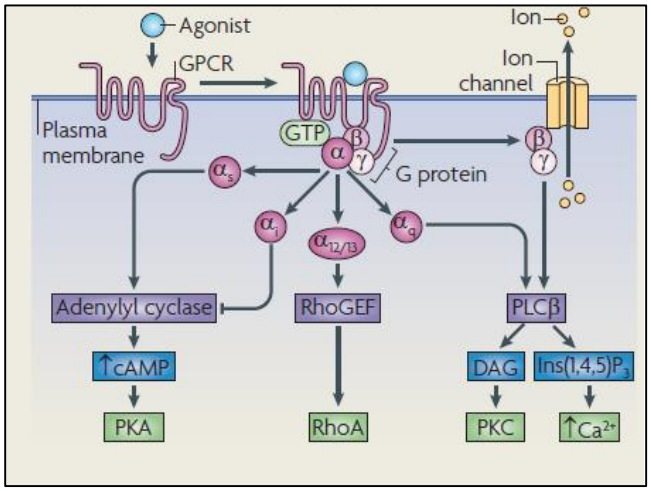

Figure 27. G Protein-Mediated Signaling by GPCRs.

Classical GPCR signaling is characterized by a seven transmembrane receptor, which responds to an extracellular stimulus. Binding triggers a conformational change that allows intracellular exchange of GDP for GTP on the Gα subunit. This then dissociates the Gα and Gβγ subunits from each other and from the GPCR. Different types of Gα can regulate the activity of effectors such as adenylyl cyclase, and phospholipase Cβ (PLCβ). The βγ subunits can also regulate certain effectors, like ion channels and PLCβ. (Reprinted with permission from Ritter, S.L. and Hall, R.A., 2009.)

Crosstalk between pathways have been suggested for a long time now, however, little is known in *M. oryzae* about the receptors and the downstream components at which they converge. The sole receptor in *M. oryzae* that is typically known in literature as the hydrophobicity sensor is PTH11. Aside from the first report on PTH11, the idea that it might be an upstream activator of cAMP-mediated signaling and of a functionally overlapping pathway, which is presumably DAG, had been emphasized in a study on the *M. oryzae CUT2* encoding cutinase (Skamnioti and Gurr, 2007). To further provide a proof of concept for the proposed signaling role involving PLG1 and another receptor, one study that was found upon literature search focused on the entomopathogenic fungi of the genus *Metarhizium* (Gao et al., 2011). *Metarhizium* is the most abundant fungi isolated in soils and is also a producer of various cell types like conidia, hyphae, and appressoria. They typically facilitate infection through adhesion and penetration of host cuticle (Driver et al., 2000). Interestingly, it has two species which emerged as models for investigating host preference, host switching and mechanisms of speciation. In the study, a comparative analysis of the genome sequences of the broad-spectrum insect pathogen *M. anisopliae* and the acridid-specific *M. acridum* was performed (Gao et al., 2011). What they found was that despite the differences in the host ranges, the developmental processes were similar for the two species. PTH11-like GPCRs were also highly represented and they posited that there is variation on the transcriptomes, specifically with respect to pathogen-host interaction (PHI) genes upon testing the different species. Moreover, they developed a model in which a single receptor modulates multiple signaling pathways, for example, the cAMP- and DAG-related

pathways (Gao et al., 2011). Perhaps the existence of numerous GPCRs or GPCR-like proteins in pathogenic fungi has something to do with host specificity, and the idea that multiple GPCRs may regulate the overall intracellular concentrations of secondary messengers, making their concentrations optimum to trigger the downstream pathways. As suggested earlier, that may be the case for PLG1, and a possible interacting receptor. Having all this information, the proposed model is shown in Figure 28 where dashed arrows show the proposed interactions. The outcomes of the cAMP and DAG treatments in relation to the model are shown in Figure 29.

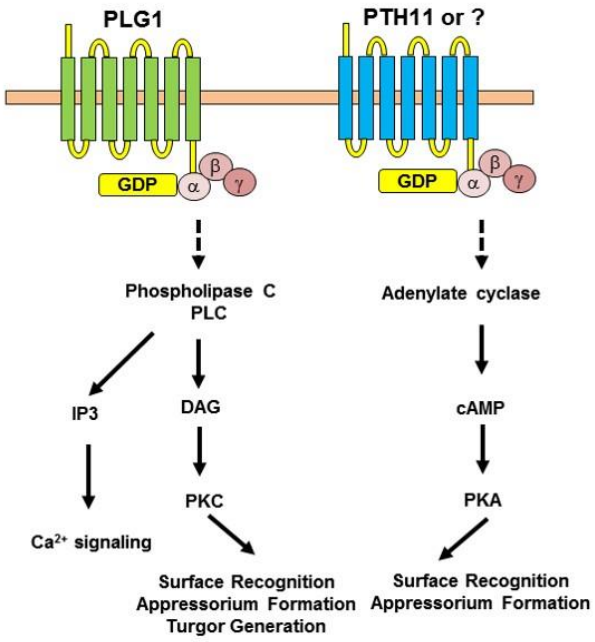

Figure 28. Proposed Model for the Signaling Role of PLG1.

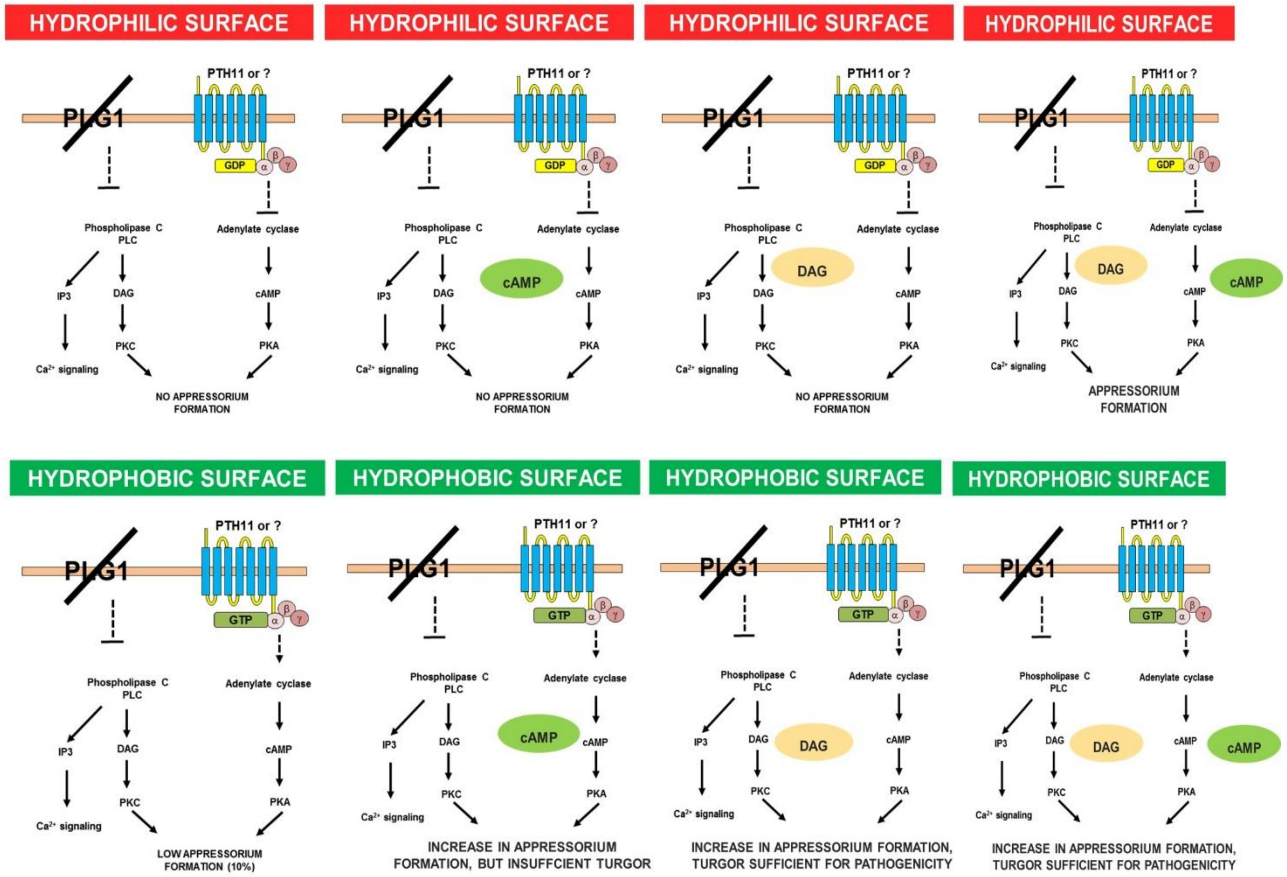

Figure 29. Summarized Outcomes of cAMP and DAG Treatments

qRT-PCR analysis was performed to further establish the relationships between PLG1 and the downstream genes such as *CPKA*, *PKC,* and *PMK1*, by examining their transcript levels in the wild type and Δ*plg1* mutant background. A significant decrease in the *PKC* transcript level was observed in the Δ*plg1* mutant at 24 hpe on Teflon, compared to wild type. This indicates a functional connection between PLG1 and the downstream components of the DAG-mediated pathway. *PMK1* expression does not seem to be affected when *PLG1* is abolished, suggesting that *PLG1* may not play a big role in the regulation of the MAP kinase pathway. Although *CPKA* seemed significantly regulated based on the graph alone, the statistical parameters that were set designated the change in expression as not significant. Perhaps more independent experiments are required to ascertain the expression of *CPKA*.

In summary, PLG1 appears to be major activator of the DAG-mediated pathway. Based on the models presented in Figure 28 and Figure 29, if PLG1 behaves as a GPCR, then it must be able to interact with the characterized G proteins in *M. oryzae*. Moreover, since it was proposed that modulation of the intracellular cAMP and DAG levels can be a function of PLG1, future experiments should be done to quantify levels of the secondary messengers in the wild type and Δ*plg1* mutant strains.

CHAPTER V

ANALYSIS OF OTHER RECEPTOR FEATURES OF PLG1

Introduction

In the past, when host-microbial pathogen interactions were being described, the microbes have always been thought as the main aggressors in the arms race, causing a disease state when they overcome the hosts' resistance (Casadevall and Pirofski, 2000). However, not all interactions with a microbe results in a disease. Thus changes in terminologies pertaining to host-pathogen interactions were proposed recently, to emphasize that outcomes of the infection process are not only dependent on the attributes of the microbe, but more importantly on host factors (Casadevall and Pirofski, 2000; Stahl and Bishop, 2000). One thing has not changed however, and that is, for such interactions to happen, cell surface receptors functioning as sensors, from both hosts and pathogens must come into play (Gruber et al., 2013). These cell surface receptors are typically transmembrane proteins which fall into three classes: ion-channel-coupled receptors, enzyme-coupled receptors, and GPCRs (Boyle, 2008).

Ion-channel-coupled receptors are also called ligand-gated channels, which undergo conformational changes upon ligand binding. They usually consist of five subunits that form a tunnel or pore which allows ions such as Na^+ and K^+ to pass through, thereby altering the membrane potential and excitability of the cell. Once the ligand dissociates,

the ion channel closes and is available to bind a new ligand (Lodish, 2008). The enzyme-coupled receptors behave either as enzymes through their intracellular catalytic domain or interact with other enzymes, and their activation is caused by signal molecules in the form of dimers. They are divided into 6 classes: tyrosine kinase receptors, tyrosine kinase-associated receptors, receptor-like tyrosine phosphatase, receptor serine/threonine kinases, receptor guanylyl cyclases and histidine kinase-associated receptors (Cuatrecasas, 1974; Alberts et al., 2013). GPCRs activate the trimeric GTP-binding proteins (G proteins) upon ligand binding, and the downstream effectors activate, either an enzyme or an ion channel in the plasma membrane (Alberts et al., 2013). For a long time, GPCRs were thought to directly interact only with G proteins. However, this would seem to limit the specificity of signal transduction via GPCRs because for a large proportion of known GPCRs, there is only a small number of identified G proteins. Lately, several interacting molecules were identified to mediate signals via GPCRs and they include arrestins, GPCR kinases, and small GTP-binding proteins (Gruber et al., 2013).

Twenty to thirty percent of most organisms' proteomes are comprised of membrane proteins (Krogh et al., 2001). Out of these, more than 40% are molecular targets of approved therapeutic drugs in humans (Overington et al., 2006). However, despite their significant representation in the proteome and importance in different biological processes, they continue to be among the most challenging targets in biology (Carpenter et al., 2008). Membrane proteins are difficult to study because the plasma membrane in

which they are localized in represent only 2%-5% of the 6%-12% lipid membrane composition of a cell's cytosolic volume (Boyle, 2008). Thus, their extraction from the membrane primarily requires the use of detergents for them to become soluble in an aqueous solution. It is thus important to select the proper set of buffers and detergents to keep the membrane proteins stable as they are being isolated and purified (Lin and Guidotti, 2009). All these challenges have slowed down the membrane protein structure identification through X-ray crystallography and nuclear magnetic resonance (NMR) spectroscopy (Babcock and Li, 2014). Moreover, building reliable models of membrane proteins based on the limited information available on protein databases is tough because of the lack of suitable templates, low sequence similarity and wide variety of ligand specificities even within the same superfamily of each transmembrane protein class (Michino et al., 2010).

A few membrane receptors have been characterized in filamentous fungi. For example in *S. cerevisiae*, the GPCR Gpr1 is responsible for sensing glucose and sucrose and interacts with the Gα protein Gpa2 to activate the cAMP pathway (Lemaire et al., 2004). In *C. albicans*, Gpr1 also activates the cAMP pathway and was shown to be important to hyphal growth regulation on solid media, in response to glucose and amino acids such as methionine (Maidan et al., 2008). In *N. crassa*, the GPCR Gpr-4 is homologous to the *S. cerevisiae* and is also required for carbon source utilization since Δ*Gpr-4* deletion mutants accumulate less biomass compared to wild type on poor carbon sources (Li and Borkovich, 2006). In *C. neoformans*, Gpr4 was shown to be a methionine sensor that

interacts with the Gα protein Gpa1 to affect mating through a cAMP/PKA-dependent signaling cascade (Xue et al., 2006).

As introduced in Chapter I, homologs of the characterized receptors in other filamentous fungi were found in *M. oryzae*, however, none of the homologs have been characterized and reported (Li et al., 2007). To date, only PTH11 is the proposed *M. oryzae* GPCR that is involved in pathogenicity, after it has been shown the Δ*pth11* mutants are defective in appressorium differentiation (DeZwaan et al., 1999). Although it has not been shown to interact directly with any known G protein in *M. oryzae*, it was shown to interact with RGS proteins (Ramanujam et al., 2013). More information however are available for the *M. oryzae* G proteins. All three *M. oryzae* Gα subunits MagA, MagB, and MagC are involved in sexual development. The Δ*magA* and Δ*magC* mutants can produce perithecia but the ascospores never reached maturity, while the Δ*magB* mutant failed to form perithecia (Liu and Dean, 1997). Furthermore, MagB was shown to regulate vegetative growth and appressorium formation via cAMP/PKA pathway (Liu and Dean, 1997). In addition to the Gα subunits, the Gβ subunit Mgb1 and the Gγ subunit Mgg1 have also been characterized, and were shown to affect appressorium penetration and infectious growth. Addition of exogenous cAMP did not rescue the phenotypic defects of the Δ*mgb1* and the *mgg1* T-DNA-disrupted mutants, indicating that the subunits may act upstream of other signaling pathways, but not the cAMP/PKA pathway (Liu and Dean, 1997; Nishimura et al., 2003; Liang et al., 2006). The targeted deletion of Mgg1 has been reported, and although the phenotypic defects were similar to

the T-DNA-disrupted *mgg1* mutants, the Δ*mgg1* mutants responded to exogenous cAMP. The Δ*mgg1* mutants formed appressoria in the presence of cAMP, but penetration and infectious growth were still defective. This thus places *Mgg1* as another GPCR-related gene that might be involved in transducing signals via the cAMP pathway, and perhaps other signaling pathways (Li et al., 2015).

In Chapter IV, it was shown that PLG1 lies upstream of the cAMP and DAG signaling pathways, as expected for a membrane protein which potentially serves as a sensor for extracellular signals. Since it was proposed that PLG1 may have GPCR properties, being similar in amino acid composition to PTH11, experiments have been done to verify such idea. Biochemically, the interaction of PLG1 with the known G proteins in *M. oryzae* can be done through protein-protein interaction assays such as the yeast two hybrid (Y2H) assay for an *in vivo* approach and co-immunoprecipitation study for an *in vitro* approach.

The basis of the conventional Y2H system is the modular property of the Gal4 transcription factor (Fields and Song, 1989). Gal4 was shown to bind to a specific DNA sequence, termed the upstream activation domain (UAS) to activate transcription in the presence of galactose. However, when Gal4 was separated into two fragments, the N-terminal fragment did still bind to the UAS, but no transcription activation was observed in the presence of galactose. This was termed the DNA binding domain (DBD). It was then found that the activation of transcription was mediated by the C-terminal fragment,

termed the activation domain (AD) (Fields and Song, 1989; Brückner et al., 2009). These features of the Gal4 transcription factor were then utilized to come up with an assay that can be used to verify protein-protein interactions. In a Y2H assay, one protein is fused to the Gal4 DBD, resulting in the bait construct while the other potential interacting protein is fused to the Gal4 AD, producing the prey construct. The bait that is introduced to yeast as a plasmid binds the UAS of the promoter. If there is an interaction between the bait and the prey, the prey with the AD which is also introduced into yeast as a plasmid, is recruited and, that allows the reconstitution of a functional Gal4 transcription factor. It then leads to the recruitment of RNA polymerase II which allows transcription of the reporter genes (Brückner et al., 2009).

Currently, there are several reporters in the Y2H system, which were made to be under the control of Gal4-responsive promoters. The most common one is the *MEL-1* reporter which encodes α-galactosidase, an enzyme that naturally occurs in many yeast strains. Due to Y2H interactions, MEL1 is expressed and secreted by yeast cells. Colonies that produce MEL1 turn blue upon addition of the chromogenic substrate 5-Bromo-4-Chloro-3-indolyl a-D-galactopyranoside (X-α-gal) on a solid medium (Aho et al., 1997). Nutritional reporters such as *HIS3* and *ADE2* are also extensively used in most Y2H kits. The yeast strain in which the bait constructs are transformed into, are usually not capable of synthesizing histidine or adenine (White, 1996). That means that in media lacking the essential amino acids histidine or adenine, the untransformed yeast cells will not be able to grow. Thus, if the bait and prey constructs interact, then Gal4-responsive His3 and

Ade2 expression takes place, and the cells will be able to grow on the minimal media lacking histidine and adenine, respectively (White, 1996). The *AUR1-C* reporter, which encodes the enzyme inositol phosphoryl ceramide synthase has also been used inY2H kits recently (Clontech Laboratories, 2013). In Y2H, the expression of *AUR1-C* resulting from interaction of the bait and prey, confers strong resistance to the highly toxic drug Aureobasidin A (AbA). AbA is a cyclic depsipeptide which is toxic to fungi, including *S. cerevisiae* at low concentrations (0.1–0.5 µg/mL) (Endo et al., 1997). AbA is a preferred reporter over nutritional markers because it offers a much more stringent selection. Non-transformed cells are killed right away rather than being retarded in growth (Clontech Laboratories, 2013).

The Y2H assay is an appealing technique for detecting protein-protein interactions for a number of reasons. First, it is an *in vivo* technique which uses the yeast system, and represents a eukaryotic system that can give results closer in reality than most *in vitro* methods or assays based on bacterial expression (Van Criekinge and Beyaert, 1999). With the commercial Y2H kits that are readily available, there are minimal requirements to begin screening such as the cDNA of interest that is properly cloned into the bait and prey vectors. Weak and transient interactions that are usually inherent in signaling cascades can also be detected in Y2H screens because the genetic reporter gene strategy leads to significant output amplification (Van Criekinge and Beyaert, 1999). However, such interactions should be verified further to eliminate false positives. The Y2H system

also allows for analysis of known interactions through identification of necessary protein domains or residues that are relevant for interactions (White, 1996).

Although the Y2H is an elegant method for detecting protein-protein interactions, it is not without limitations and disadvantages (Van Criekinge and Beyaert, 1999). For example, the proteins of interest must be able to fold correctly and exist as a stable protein inside the yeast cells. Moreover, some posttranslational modifications required for the interaction such as disulfide bond formation, glycosylation and phosphorylation that are otherwise present in the actual organism, may not necessarily take place in yeast. This is one of the main disadvantages when utilizing heterologous systems, which had been circumvented in new Y2H kits, by co-expressing the enzyme carrying out the posttranslational modifications. In some rare cases, there exists a possibility in which a third protein in yeast might bridge the two bait and prey constructs, thereby giving a positive interaction result (Van Criekinge and Beyaert, 1999). Another limitation is that the Y2H fusion proteins must be targeted to the yeast nucleus for the activation of the reporter genes and may work only for the cytoplasmic domains of the proteins. This means that the system may become problematic for transmembrane proteins, although there are several reports on the success of Y2H with transmembrane proteins (Daniel and Reynolds, 1999; Hopkinson and Jones, 2000; Traweger et al., 2003; Rochdi et al., 2004). This problem is avoided by making truncations fragments of the gene of interest, so the transmembrane regions will not be expressed. There are also some cases in which one

or both hybrid proteins may be toxic to yeast, but this can be relieved by using a vector which expresses lower levels of the fusion protein (Clontech Laboratories, 2013).

The success of an Y2H experiment depends on factors such as the choice of the bait protein, choice of cDNA library for large-scale mining of interacting partners, and the stringency of the selection which depends on the number of media components that impart selection. Bait and prey constructs should be tested individually to ensure that they do not activate transcription in the absence of the interacting partner, an outcome termed as autoactivation. Sometimes, background colonies are observed as a result of leaky expression of the nutritional reporter or overly dense plating. Autoactivation and background colonies both contribute to the number of false positives that can be seen on the test plate (Clontech Laboratories, 2013). Due to the presented limitations of the Y2H system, it is often recommended to verify positive interactions using biochemical methods like affinity chromatography and/or immunoprecipitation. Also, the strength of interactions can be verified quantitatively by monitoring the activity of the Gal-responsive *LacZ* gene encoding β-galactosidase that is integrated in some yeast strains employed in Y2H screening (Clontech Laboratories, 2013).

Since PLG1 has been proposed to be a transmembrane protein with possible GPCR properties, experiments have been put forth to determine its possible interactions with the Gα subunits MagA, MagB and MagC through Y2H and co-immunoprecipitation experiments. Since no reported information are available for the experimental methods

concerning GPCRs in *M. oryzae*, the experiments have been patterned from the most recent characterization of the GPCR Gpr4 in *C. neoformans* (Xue et al., 2006). This chapter discusses the results of the interactions studies between the truncated PLG1 cDNA fragments which does not span the membrane and the Gα subunits MagA, MagB and MagC. Moreover, an alternative model for the transmembrane topology prediction for PLG1 will be presented. In addition to the identification of the membrane-spanning domains, a pore-lining helix motif has also been identified. The pore-lining helix is commonly found in ion channels, and it is only recently that the algorithm for predicting such motif has been developed into a prediction software (Nugent and Jones, 2012). The identification of this motif in PLG1 is of particular interest, because it can provide another model as to how PLG1 triggers downstream signaling pathways in *M. oryzae*. Moreover, it can be applied to the other GPCR-like proteins in *M. oryzae* to uncover properties that were not identified by other software.

Materials and Methods

Yeast Two Hybrid Assay

cDNA was synthesized from 2 µg of total RNA extracted from germlings on Teflon at 24 hpe using the SuperScript® III RT cDNA synthesis kit (Life Technologies). cDNA sequences coding for PLG1, Gα subunits MagA, MagB and MagC were amplified by PCR using ExTaq (TaKaRa Bio Inc.) with primers listed in Appendix A. The PCR

template amount was optimized to get robust amplification, and it was found to be 2 µL of the synthesized cDNA for a 50 µL total PCR volume. Truncated fragments of PLG1 were prepared: A (*PLG1*$_{1\text{-}9}$), B (*PLG1*$_{70\text{-}87}$), C (*PLG1*$_{258\text{-}396}$), D (*PLG1*$_{258\text{-}304}$), E (*PLG1*$_{305\text{-}350}$), F (*PLG1*$_{351\text{-}396}$) by PCR amplification the full-length PLG1 fragment as template. The cDNAs of the full-length and truncated versions of PLG1 were cloned into the pGBKT7 vector, while the cDNAs of MagA, MagB and MagC were cloned into pGADT7 vector (Clontech). Each pGBKT7 and pGADT7 construct was sequenced for the in frame fusion of each cDNA to the Gal4-DNA binding domain (BD) and Gal4-DNA activating domain (AD), respectively. Each of the pGBKT7 or bait construct was transformed into the *S. cerevisiae* strain Y2H Gold, while each of the pGADT7 or prey construct was transformed into the *S. cerevisiae* Y187 (Clontech). Y2H Gold and Y187 transformants were selected on yeast dropout media lacking tryptophan (SD-Trp) and leucine (SD-Leu), respectively. Yeast plasmid DNA was extracted from the selected transformants and were screened via PCR and sequenced for the desired insert as described (Ausubel et al., 1992). Bait autoactivation test was carried out by comparing growth of selected transformants on SD-Trp, SD-Trp/X-α-gal and SD-Trp/X-α-gal/aureobasidin A (AbA), where the final concentrations of X-α-gal (GoldBio) and AbA (Clontech) were 40 µg/mL and 200 ng/mL, respectively. Prey autoactivation test was performed on SD-Trp/X-α-gal. Mating experiments were carried out according to manufacturer's instructions, and transformants which grew on SD-Trp-Leu were selected for PCR screening of the bait and prey inserts using primers indicated in Appendix A. The vector controls supplied in the kit were the pGBKT7-53, pGBKT7-

Lam and pGADT7-T plasmids, where yeast strain harboring both pGBKT7-53 and pGADT7-T served as positive interaction control, while the strain with both pGBKT7-Lam and pGADT7-T served as negative control. In addition to SD-Trp-Leu, all the resulting mated transformants with varying cell dilutions in 1X were tested on SD-Trp-Leu-His and SD-Trp-Leu-His-Ade, supplemented with either X-α-gal or AbA, or both, to assess interactions. Plates were incubated for 3-5 days at 30^{o}C.

Yeast Protein Extraction, Co-Immunoprecipitation and Western Blotting

The yeast two hybrid mated and unmated bait and prey constructs were grown for protein extraction following the methods indicated in the Clontech Yeast Protocols Handbook (Xiao, 2006). Protein extracts for co-immunoprecipitation were prepared following a protocol courtesy of Dr. Kathryn Ryan (TAMU Department of Biology). Cultures with $O.D._{600}$ between 0.4 and 0.6 were centrifuges for 5 min at 3000 rpm using a benchtop centrifuge. The cell pellets were resuspended in 1 mL sterile water and transferred to a 1.5 mL microfuge tube, prior to centrifugation for 30 s at 3000 rpm. The cell pellets were once again resuspended in 300 µL ice cold lysis buffer composed of 20 mM Tris (pH. 6.5), 5mM MgCl2, 2% Triton X-100, 150 mM NaCl supplemented with 1X protease inhibitor cocktail (Life Technologies) and 1X PMSF (Sigma Aldrich). Approximately 500 µL of autoclaved acid-washed glass beads (Sigma) was added to each tube. The suspension was vortexed 4 times, alternating between 1 min of vortex mixing and 2 min of cool down on ice. The supernatant was then transferred to a new

microfuge tube using a small gauge needle and was centrifuged for 10 min at 3000 rpm and 4^{o}C to pellet unlysed cells. The supernatant was finally transferred to a new microfuge tube, and was either frozen in liquid N_2 for -80^{o}C storage or immediately subjected to co-immunoprecipitation. Co-immunoprecipitation was performed by incubating 100 µL of the yeast protein extract to 50 µL of packed Protein G Sepharose™ beads (GE Healthcare) with the primary antibody. For the bait constructs carrying the c-myc tag, monoclonal mouse anti-c-myc (Invitrogen) served as primary antibody, while for the prey constructs carrying the HA tag, monoclonal rat anti-HA served as primary antibody. The tubes were incubated in a rotator in the cold room for 1.5 h. They were centrifuged briefly and the supernatant was collected and saved for each protein sample. The beads were washed 6X with a wash buffer composed of 0.05% tween, 150 mM NaCl, 50 mM Tris-HCl (pH. 6.5). The tubes were centrif*u*ged once again and the beads were resuspended in 25 µL 4X SDS gel loading buffer. SDS-PAGE was ran as described (Ausubel, 1992), using 12% resolving gel for the c-myc-tagged proteins, 8% for the HA-tagged proteins, and 4% stacking gel for both. Following SDS-PAGE, the gel was treated and the proteins were transferred onto the Amersham Hybond-N nylon membrane following manufacturer's instructions (GE Healthcare). A wet transfer method was performed using the Dunn carbonate buffer composed of 10 mM $NaHCO_3$, 3 mM Na_2CO_3 and 20% methanol (pH 9.9) as transfer buffer. The transfer was allowed to proceed overnight at 30V and 4^{o}C using the Mini Trans-Blot® Electrophoretic Transfer Cell (BioRad). Western blot was carried out following a modified protocol described in the Abcam website (http://www.abcam.com/ps/pdf/protocols/wb-

beginner.pdf). To check for successful transfer, the membrane was washed in TBST buffer (0.1% Tween-20 and 1X TBS from 10X TBS composed of 2.42% (w/v) Trizma base, 8% (w/v) NaCl at pH 7.6) once and incubated in 2% Ponceau S for 5 min. Once protein bands are visualized, indicating successful transfer, the membrane was washed once with TBST to remove excess stain. The membrane was then blocked with 5% BSA (Sigma) in TBST for 1 hr and 4^{o}C under agitation. After blocking the membrane, it was rinsed with TBST and incubated with the appropriate primary antibody in 2.5% BSA in TBST overnight at 4^{o}C under agitation. The membrane was washed 5 times in TBST while agitating at room temperature, incubating the membrane for 5 min per wash. The secondary antibody was diluted in 2.5% TBST (goat anti-rat antibody conjugated to HRP (Sigma) for the detection of rat anti-HA primary antibody or goat anti-mouse antibody conjugated to AP (BioRad) for the detection of the anti-c-myc primary antibody) and incubated for 2 h at room temperature with agitation. The membrane, was washed with TBST three times, incubating the membrane for 10 min per wash, while agitating at room temperature. Colorimetric detection was used for both secondary antibody conjugates: BCIP/NBT substrate solution (Life Technologies) for the AP conjugate, and the TMB chromogenic substrate solution (Life Technologies) for the HRP conjugate. Positive and negative interaction controls were included in every run.

In Vitro Translation and Autoradiography

To prepare ^{35}S-Met-labeled bait and prey proteins, the Promega TnT® T7 Coupled Reticulocyte Lysate system was used to perform *in vitro* transcription and translation, following manufacturer's instructions. Co-immunoprecipitation of the *in vitro* prepared proteins was carried out using a modified procedure as described in the user manual of the MATCHMAKER Co-IP Kit (www.ebiotrade.com/buyf/productsf/clontech/pt3323-1.pdf) (Clontech). Ten µL of the *in vitro* translated ^{35}S-methionine labeled bait protein was incubated with 10 µL of the *in vitro* translated ^{35}S-methionine labeled prey protein for 1 h at room temperature. Then 1 µg of either the anti-c-myc or anti-HA antibody was added to the respective tubes, and incubated for 1 h at room temperature. Meanwhile, the protein G sepharose beads were pre-treated following the protocol courtesy of Dr. Ana Victoria Suescun (Dr. Dorothy Shippen's lab, TAMU Department of Biochemistry and Biophysics). The protein G sepharose beads were blocked 3 times at 4°C, with 1 mL of blocking buffer for every blocking step. The blocking buffer is composed of buffer W100 (20 mM Tris-acetate pH 8.0, 10% glycerol, 1 mM EDTA, 5 mM $MgCl_2$, 0.2 M NaCl, 0.1 M potassium glutamate and 1% NP-40) with 50 µg/mL each of lysozyme, BSA and glycogen. Approximately 20 µL of the blocked beads and 240 µL of buffer W100 were added to each sample. The tubes were placed in a rotator overnight at 4°C. The tubes were centrifuged at 2500 rpm for 2 min, and 5 µL of the supernatant was saved as the "output" sample for the gel run. The beads were washed with 1 mL of buffer W300 composed of 10% (v/v) 2 M potassium glutamate, 90% (v/v)

buffer W100 and 0.1% (v/v) 1 M dithiothreitol (DTT) for a total of 7 times. All incubation and washing steps were done at 4 ^{o}C. Finally, beads were washed twice with buffer TMG composed of 1% (v/v) 1 M Tris-acetate, pH 8.0, 0.01 % (v/v) 1 M $MgCl_2$, 0.1% (v/v) 1 M DTT and 10% (v/v) 100% glycerol. After the last wash, approximately 20 µL of TMG was left behind and 7.5 µL of 4X SDS loading dye was added to the mixture. The mixture was boiled for 3 min and supernatant was loaded onto the gel for SDS-PAGE. Since the *in vitro* translated products are smaller, the tricine SDS-PAGE procedure was used where, 4% stacking gel, 10% spacer gel and 16% resolving gel were used to separate the proteins (Schagger, 2006). After electrophoresis, the gel was dried in the gel dryer at 80^{o}C for 30 min (BioRad). The dried gel was exposed to a phosphor imaging screen overnight at room temperature and was scanned using the Typhoon 9410 Variable Mode Imager under the Storage Phosphor imaging mode.

Results

PLG1 Interacts with the Gα Subunit MagB, but not with MagA and MagC in a Yeast Two Hybrid Interaction Assay

To check for potential physical interactions between PLG1 and the known Gα subunits in *M. oryzae,* yeast two-hybrid interaction assays were carried out. Since it is known that the conventional yeast two hybrid assay does not readily work with membrane-bound proteins, six truncated PLG1 constructs were made by amplifying the cDNA

fragments encoding portions of the receptor. These constructs were designated A to F, where A (*PLG1*$_{1\text{-}9}$) is the nine amino acid long N-terminal region that is predicted to be extracellular; B (*PLG1*$_{70\text{-}87}$) is the seventeen amino acid long second cytoplasmic loop which is also the longest among the three loops ; C (*PLG1*$_{258\text{-}396}$) is the full-length cytoplasmic tail; and D (*PLG1*$_{258\text{-}304}$), E (*PLG1*$_{305\text{-}350}$), and F (*PLG1*$_{351\text{-}396}$) are truncated versions of fragment C, equally composed of forty six amino acids. All fragments, including the full length PLG1 served as baits in the mating assay. The preys on the other hand were the three Gα subunits – MagA, MagB and MagC. The bait and prey constructs were transformed into yeast strains Y2H Gold and Y187, respectively. The plasmid in which the bait cDNAs were cloned has the tryptophan biosynthesis gene, allowing the positive clones to grow on medium lacking tryptophan. The prey cDNAs on the other hand, were cloned into a plasmid harboring the leucine biosynthesis gene, allowing the positive clones to grow on a medium lacking leucine. After selection of the transformants on either SD-Trp or SD-Leu media, good-growing colonies were picked and PCR-screened for the desired bait or prey cDNA insert. Positive transformants were stored as glycerol stocks and were further tested.

Prior to performing the mating assay, it is necessary to check for bait autoactivation to ensure that that the baits do not activate the *MEL1* and *AUR1-C* reporters in the absence of the possible interacting partners. The yeast two hybrid kit manufacturer suggested testing the bait constructs on SD-Trp/X-α-gal and SD-Trp/AbA. On the SD-Trp/X-α-gal plate, the bait constructs are still expected to grow but should remain white or very pale

blue in response to X-α-gal. On the SD-Trp/Aba plate, no colonies should be observed with the bait construct alone because resistance towards the AbA drug is only observed when both bait and prey constructs are present and are interacting. Results of the autoactivation test are shown in Appendix B. All bait constructs do not appear to activate the *MEL1* and *AUR1-C* reporters, hence they were used for the interaction assays.

When the MagA and MagC Gα subunits were tested, no positive interactions were detected as shown in Figure 30B and Figure 30C. As a guide to the gene fragment encoded by the truncated fragments, Figure 30A shows the predicted transmembrane topology for PLG1, alongside the identity and the amino acid lengths of the fragments. The left panel in Figure 30B shows varying dilutions of the mated strains of the MagA prey and the baits A, B, C and F, plated on the lowest stringency medium (SD-Trp-Leu) with X-α-gal. The right panel in the same figure shows mated strains on the highest stringency selection (SD-Trp-Leu-His-Ade) plate with X-α-gal and AbA. On the other hand, the right and left panels in Figure 30C show similar selection plates, but with MagC as the prey protein. PIC and NIC refer to the positive interaction and negative interaction controls, respectively. The yeast two hybrid kit came with the pGBKT7-53 (bait) and pGADT7-T (prey) vectors for the PIC mated strain, while the pGBKT7-Lam (bait) and pGADT7-T (prey) vectors were the constructs for the NIC mated strain. In both MagA and MagC hybrid tests for the two types of selection plates, the PIC showed blue growth, indicating that there is a strong positive interaction between the p53 protein

and the T antigen. NIC did not result in blue colonies for both the MagA and MagC tests. A very pale blue color was seen for the lowest dilution (1:10) for B/MagA, F/MagA and F/MagC, but it was nowhere close to the color intensity seen for PIC. All the other mated strains showed white growth on the plates. The mated strains did not grow on the SD-Trp-Leu-His-Ade/ X-α-gal/AbA, except for PIC.

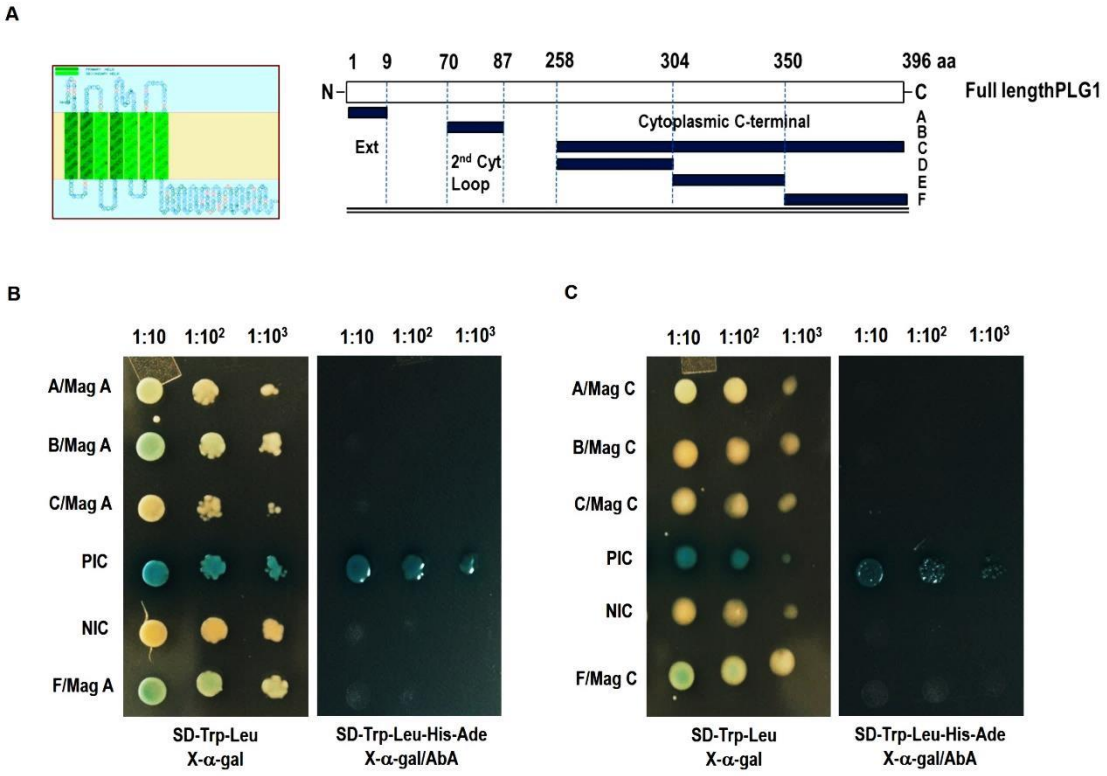

Figure 30. PLG1 Does Not Interact with the Gα subunits MagA and MagC.

(A) Schematic of the PLG1 truncated fragments which served as bait proteins in yeast two hybrid assays.
(B) Dilutions of the mated strains with MagA as the prey protein were plated on SD-Trp-Leu/X-α-gal (left panel) or on SD-Trp-Leu-His-Ade/X-α-gal/AbA (right panel). PIC and NIC were the positive and negative interaction controls, respectively. Plates were photographed 5 days after incubation at 30°C.
(C) Dilutions of the mated strains with MagC as the prey protein were plated on SD-Trp-Leu/X-α-gal (left panel) or on SD-Trp-Leu-His-Ade/X-α-gal/AbA (right panel). PIC and NIC were the positive and negative interaction controls, respectively. Plates were photographed 5 days after incubation at 30°C.

Obtaining the amplified cDNA for the MagB subunit took a little longer than for MagA and MagC. The amount of cDNA that was being obtained from the available RNA was oftentimes low and its final concentration was not sufficient for the subsequent cloning steps. So with that experimental lag, it was necessary to retest the bait constructs that were previously used with the MagA and MagC preys. As shown in Appendix B, the selected transformants were retested on either SD-Trp or SD-Leu, and the bait constructs still grow on SD-Trp, but not on SD-Leu, and the opposite growth pattern is observed for the prey constructs, which included MagB.

Once the constructs had been reconfirmed for their growth on either SD-Trp and SD-Leu, and the mated strains with MagB were obtained, tests on the different selective media were performed. Figure 31 shows the tests for the lowest stringency selective media. These included SD-Trp-Leu supplemented with X-α-gal, SD-Trp/Aba, SD-Trp-Leu/Aba. Figure 31A shows the expected appearance of PIC and NIC colonies, growing on SD-Trp-Leu. In all types of selective media supplemented with X-α-gal, PIC always grew robustly and exhibited intense blue color. NIC is not expected to grow very well when the stringency of selection is increased, and does not exhibit a blue color in the presence of X-α-gal. Once again, a guide to the truncated fragments and their compositions is shown in Figure 31B. All bait constructs mated with the MagB prey construct were tested. They all grew well on SD-Trp-Leu (Figure 31C), but upon addition of X-α-gal, only the mated strain resulting from MagB prey and F bait showed a blue color across all dilutions (Figure 31D). Although the blue color was less intense

compared to PIC, this result was promising. Upon addition of AbA on the SD-Trp-Leu medium, it can be seen in Figure 28E that PIC grew robustly and showed blue colonies across dilutions. Background colonies are believed to be observed for the NIC, since this is not expected to show growth on SD-Trp-Leu/AbA. MagB-F strain showed a decrease in growth compared to SD-Trp-Leu without AbA, but at lower dilutions, they grew well and showed blue colonies. At this point, another bait construct, EF was made and tested. Colonies were also seen for the lower dilutions, but there is a possibility that these are also background colonies. Another selective plate, SD-Trp/Aba/X-α-gal which was also one of test plates for bait autoactivation was used. As a reconfirmation of the bait autoactivation test, it can be seen that there is no growth when the baits (F or EF) alone were tested (Figure 31F). Blue colony growth was observed for PIC and F/MagB. It is worth noting that the growth of F/MagB is retarded and the blue color that the colonies exhibit is also less intense, compared to PIC. There is a possibility that only a weak interaction exists between F or EF and MagB. Both NIC and EF/MagB seemed to grow too but only at the lowest dilution. In addition, EF/MagB showed a blue tinge, which was not seen for NIC. Overall, these suggest that PLG1 might be interacting with MagB via the last 46 amino acids in the cytoplasmic domain. The bait EF was constructed to see if there will be enhanced interaction with MagB, perhaps through a different folding pattern. However, it is clear that the interaction seemed lesser compared to the F bait construct, as shown by the amount of growth on the selective plates.

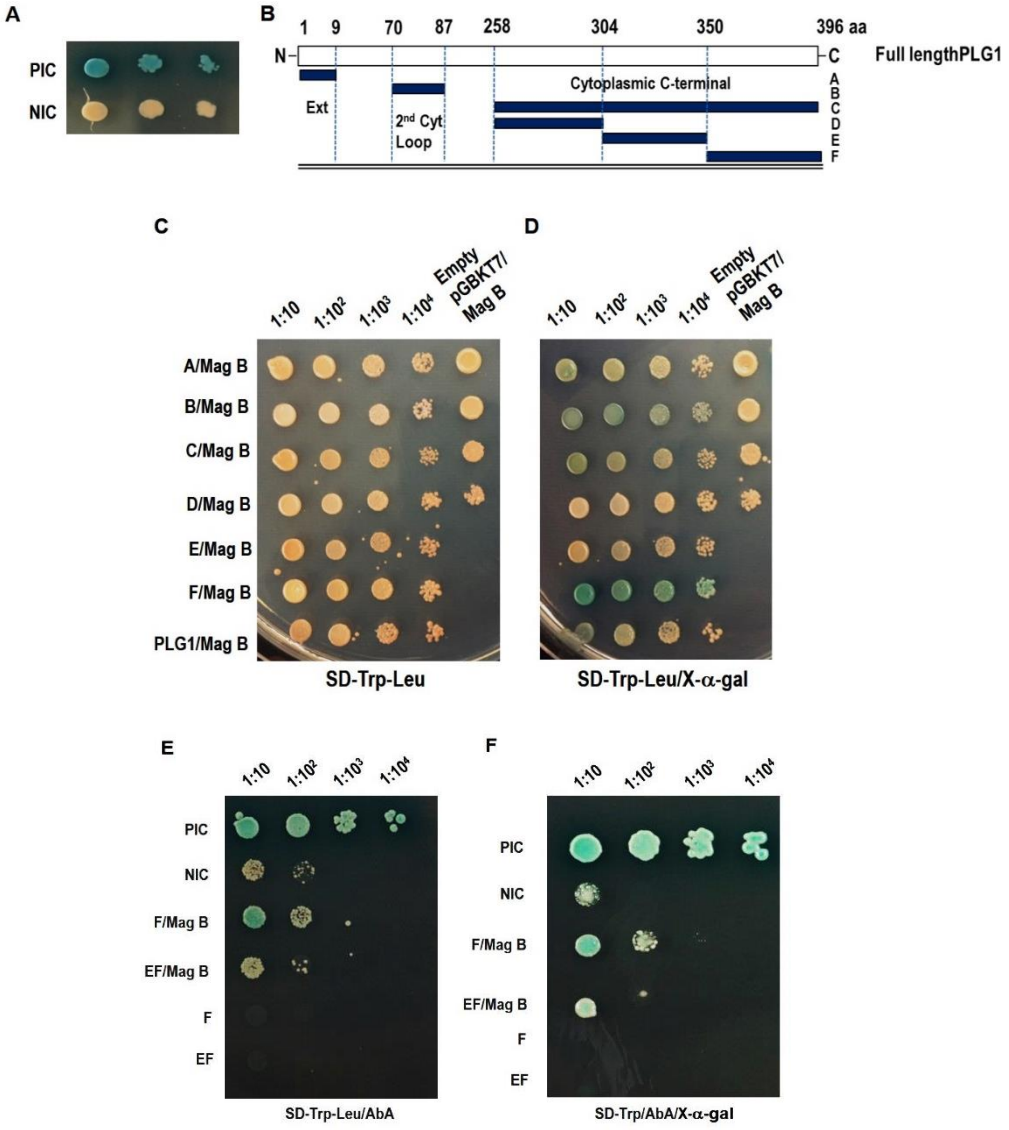

Figure 31. Yeast Two Hybrid Interaction Assays on Low Stringency Selective Media Observed After Five Days at 37 ºC.

(A) The controls, PIC and NIC were plated on SD-Trp-Leu.
(B) Schematic of the PLG1 truncated fragments which served as bait proteins in yeast two hybrid assays.
(C) Bait constructs A to F, including PLG1 were mated with MagB and spotted on SD-Trp-Leu. The strain empty pGBKT7/MagB served as a control.
(D) Bait constructs A to F, including PLG1 were mated with MagB and spotted on SD-Trp-Leu with X-α-gal. The strain empty pGBKT7/MagB served as a control.
(E) PIC, NIC, F/MagB and EF/MagB were spotted on SD-Trp-Leu/Aba.
(F) PIC, NIC, F/MagB and EF/MagB were spotted on SD-Trp/Aba with X-α-gal.

Since an interaction between F and MagB seems to exist, higher stringency selection plates were tested. Interestingly, F/MagB grew well on SD-Trp-Leu-His plates and EF/MagB grew to a lesser extent compared to F/MagB (Figure 32A). Blue color was also observed when the SD-Trp-Leu-His plate was supplemented with X-α-gal (Figure 32B). However, when the strength of selection was increased by adding AbA, F/MagB only showed growth for the lowest dilution, EF/MagB did not grow at all, while PIC grew robustly (Figure 32C). Moreover, when the strongest selection was used, SD-Tr-Leu-His-Ade, no colonies were observed for F/MagB. This suggests different possibilities: 1) that F/MagB interaction might be weak or transient, 2) the interacting domains do not readily encounter each other presumably due to protein folding patterns, and instead of MagB, the cytoplasmic region of PLG1 interacts more strongly with the Gβγ, and 3) the promoter sequences for the activation of the selective marker are not readily accessible.

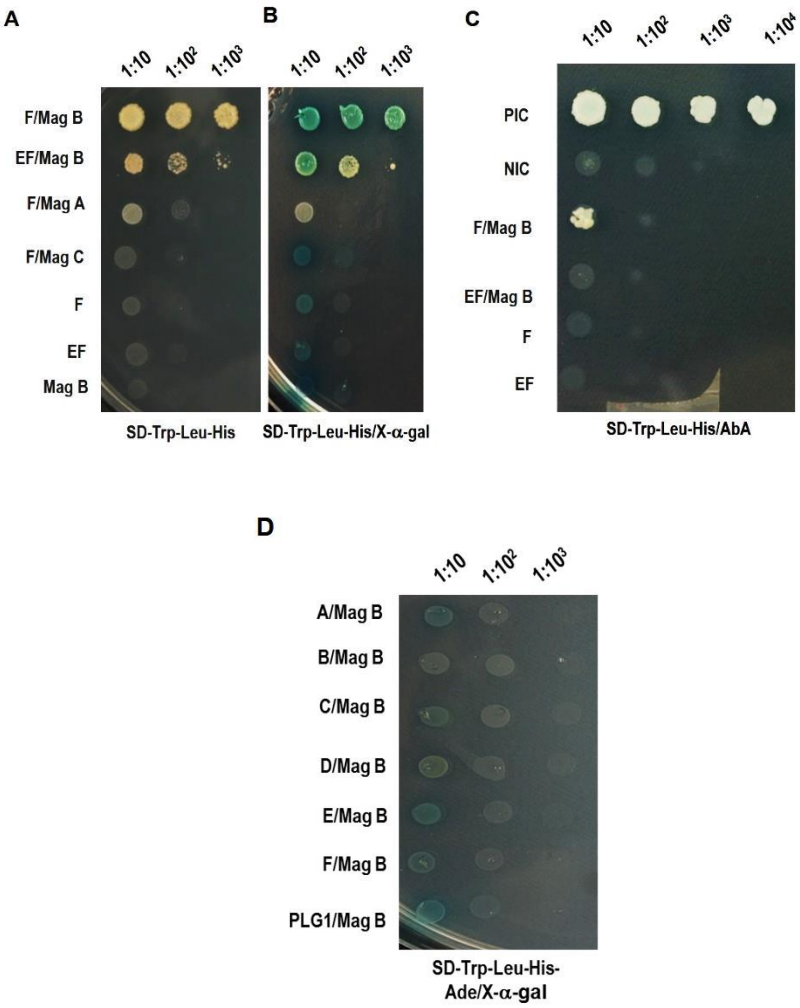

Figure 32. Yeast Two Hybrid Interaction Assays on Medium and High Stringency Selective Media Observed After Five Days at 37 ºC.

(A) Mated strains F/MagB and EF/MagB were spotted on SD-Trp-Leu-His. For comparison, F/MagA and F/MagC were also tested.
(B) Mated strains F/MagB and EF/MagB were spotted on SD-Trp-Leu-His with X-α-gal. For comparison, F/MagA and F/MagC were also tested.
(C) Bait constructs A to F, including PLG1 were mated with MagB and spotted on SD-Trp-Leu-His/Aba.
(D) Mated strains were spotted on the highest stringency selection plate, SD-Trp-Leu-His-Ade.

Co-Immunoprecipitation Assay Did not Confirm Interaction Between PLG1 Gα Subunit MagB

Since a possible interaction between F bait and MagB prey has been detected through Y2H experiments, a confirmation of this interaction was done through co-immunoprecipitation (co-IP). The first step to doing the co-IP is to confirm that the c-myc-tagged bait and the HA-tagged prey can be detected individually. Baits were detected with the monoclonal anti-c-myc antibody and preys were detected with the monoclonal rat anti-HA primary antibody. Secondary antibody conjugates for the bait and prey were detected colorimetrically with BCIP/NBT substrate solution and TMB substrate solution, respectively. Figure 33A confirms the presence of the bait proteins shown by the strong purple bands for the p53 bait coming from the positive interaction control (PIC, p53-T), the Lam bait from the negative interaction control (NIC, Lam-T), and the F fragment from the MagB-F-containing yeast cells. Y2HG and Y187 lanes correspond to the proteins extracted from the yeast cells not transformed with the vectors carrying any tagged constructs, thereby no bands are seen in those lanes. Figure 33B confirms the presence of the prey proteins: T antigen, present both in the PIC and NIC, shown by the blue bands. MagB is also detected in the MagB-F lane.

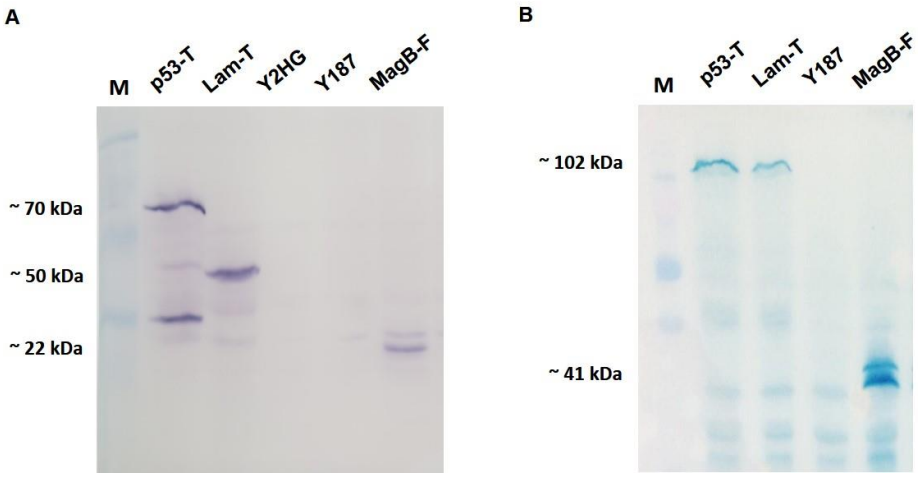

Figure 33. Confirmation of Myc-Tagged and HA-Tagged Constructs via Western Blotting.

(A) Bait proteins tagged with c-myc c show purple bands: p53 bait for PIC, p53-T, the Lam bait for the NIC, Lam-T, and the F fragment from the F/MagB mated strain.
(B) Prey proteins tagged with HA show blue bands: T antigen both for PIC and NIC, and MagB from the F/MagB mated strain.

After confirmation of the tagged-constructs, a co-IP experiment was carried out and results are shown in Figure 34. The yeast protein was extracted from the yeast cells which were allowed to grow on liquid culture imparting the selection, i.e. SD-Trp-Leu for the mated strains, SD-Trp for the strains containing the bait alone, and SD-Leu for the strains containing the prey alone. The method was done first for the positive interaction control (or PCM in Figure 34A and Figure 34B) to ensure that the conditions for the co-IP were working. However, the co-IP was not successful in detecting interaction even for the positive control. Figure 34A shows the result when the protein was pulled down with anti-c-myc, the membrane was incubated with anti-HA for the

Western blot, and the detection was done with the TMB substrate. For the output, i.e. the supernatant after the pulldown step, a band was seen for the c-myc-tagged p53, but no band is detected from the protein G sepharose beads. Ideally, if the interaction exists, then the protein G sepharose beads will be bound to the pulldown antibody, pulling with it both bait and prey. Either bait or prey should be detected from the beads, depending on the antibody used for the Western blot conditions. Figure 34B shows the result when the protein was pulled down with anti-HA, the membrane was incubated with anti-c-myc for the Western blot, and the detection was done with the BCIP/NBT substrate. Similarly, no bands were seen coming from the input protein from the beads. The same yeast growth conditions, protein extraction and co-IP methods were also tried for the MagB-F construct and the NIC. Using the c-myc detection, once again, bands are seen in the output but not from the beads. All these indicate that the possible interactions are lost during the extraction procedures, because even the positive control which clearly shows strong interaction results from the Y2H experiments, did not show pulldown of either bait or prey construct from the supposedly bound beads. The stringency of the extraction and wash buffers used were also adjusted and the several co-IP conditions were changed to preserve the interaction, but to no avail. There is a possibility that the interaction manifests only *in vivo*, but the folding patterns of the tagged proteins, since they were expressed from a vector could have been altered during the extraction steps, hence they don't interact based on the conditions used for the *in vitro* biochemical methods.

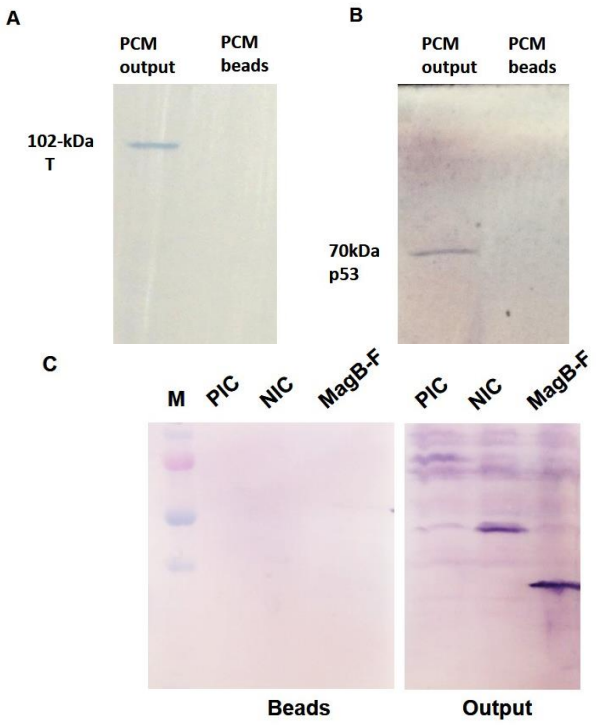

Figure 34. Co-immunoprecipitation Assay for Positive and Negative Controls, and MagB-F.

(A) PCM is the positive interaction control (p53-T). The mated yeast cells were grown in SD-Trp-Leu, followed by protein extraction, SDS-PAGE, co-IP, then the Western detection. When pulled down with anti-c-myc and detected with anti-HA, band is observed for the output, but not for the protein extract bound to the protein G sepharose beads.
(B) PCM is the positive interaction control (p53-T). The mated yeast cells were grown in SD-Trp-Leu, followed by protein extraction, SDS-PAGE, co-IP, then the Western detection. When pulled down with anti-HA and detected with anti-c-myc, band is observed for the output, but not for the protein extract bound to the protein G sepharose beads.
(C) The positive (p53-T) and negative (Lam-T) interaction controls were also tested, including the experimental yeast protein with F/MagB. Using the same procedures described for **(A)** and **(B)**, no bands are obtained from the proteins from the protein G sepharose beads, only for the output.

The manufacturer of the Y2H assay kit actually recommended performing an *in vitro* translation technique for the co-IP, so that only the desired bait or prey fragments are expressed, and no extraneous sequences from the vector can interfere with the co-IP.

This is because the T7 promoters and epitope tags in the bait and prey cloning vectors are located downstream of the Gal4 coding sequences. If the rabbit reticulocyte lysate-based translation kit is used which commonly uses RNA synthesized in vitro from the T7 RNA polymerase promoter, then proteins are translated without the Gal4 domains and this increases the specificity of the interactions, between the bait and prey proteins. Radiolabeling with ^{35}S allows for the detection of the *in vitro* transcribed and translated fragments. Figure 35A and Figure 35B show the detection of the individual bait and prey proteins prior to co-IP, to ensure that the kit worked and produced the desired products. All the fragments were necessary for the positive interaction control (p53/T) and the experimental samples (MagB-F and MagB-EF) were successfully synthesized. Once again, the co-IP step was verified first for the PIC (p53/T). This time, as shown in Figure 35C, interaction between p53 and T was seen as expected. The third and fourth lanes are for testing the individual fragments, in the presence of the relevant antibodies for pulling them down. Lanes 1 and 2, are reciprocal pull down assays, using either anti-c-myc or anti-HA, but in both cases two bands are seen, corresponding to the interacting partners. These indicate that the whole procedure works, and so it was then applied to the experimental samples. Unfortunately, no relevant interactions were detected for F/MagB under these conditions. Lanes 1 and 2 show the individual bait and prey fragments pulled down with the relevant antibodies. Lanes 3 and 4 are reciprocal pull downs for the samples containing both MagB-F. Lane 3 shows a pull down with the anti-c-myc antibody, and it strongly detected the F fragment. There is a faint band seen corresponding to the size of MagB, however upon looking at the "beads only" control

(last lane in Figure 35D), it looks like MagB interacts with the beads as well. The signal level is similar as to when the antibodies were added (Lane 3), and so this suggests that the faint band observed is most likely MagB binding to the beads. For some reason, this doesn't go away, even after changing the incubation times/temperatures with the beads, and stringency of the bead washes. Assuming that MagB indeed bind to the beads, and if F has a relevant interaction with MagB, then it would be pulled down, when anti-HA specific to MagB is used. However, this was not the case as seen in Lane 4 (Figure 35D). If a relevant interaction exists, then a band corresponding to F should be strongly seen in that lane. This is the final co-IP test which confirms that the F fragment of PLG1 does not interact with MagB *in vivo.*

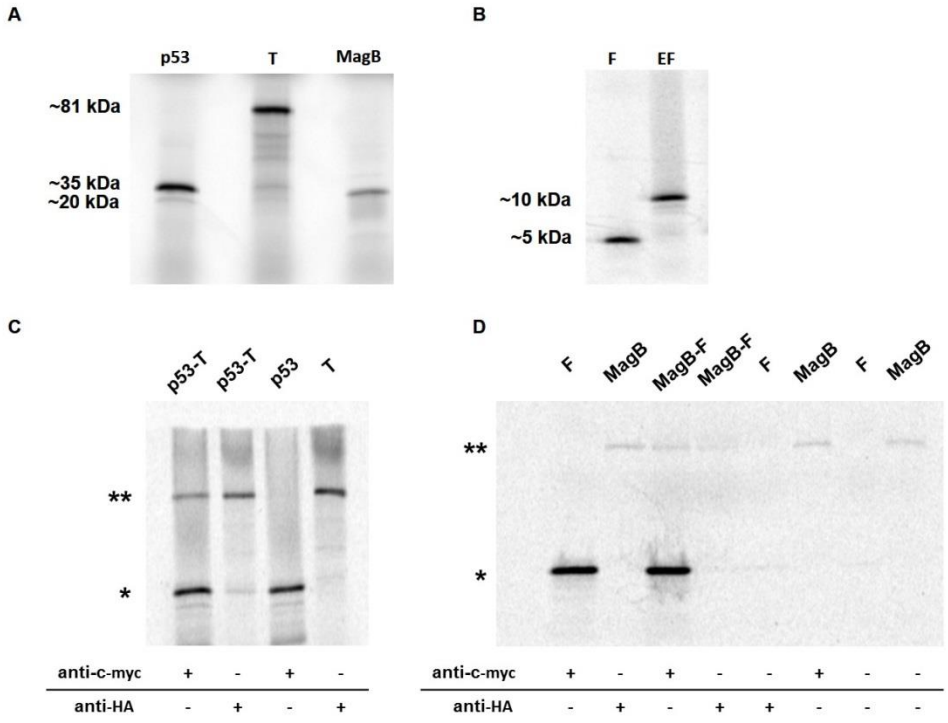

Figure 35. Co-immunoprecipitation Assay for *In* Vitro Translated Positive Interaction Control and MagB-F Experimental Construct.

(A) ^{35}S-labeled p53, T and MagB proteins are detected indicating successful *in vitro* translation
(B) ^{35}S-labeled F and EF proteins are detected indicating successful *in vitro* translation
(C) Positive control p53 shows interaction with T after pull down with either anti-c-myc or anti-HA
(D) Experimental sample MagB-F did not show relevant interaction between the MagB prey and the F bait, as shown by the third and fourth lanes were anti-c-myc and anti-HA, were used respectively for the pull down.

PLG1 is Predicted to Have a Pore Lining Helix Along One of Its Membrane-Spanning Regions

In order to mine for more information about relevant domains in PLG1 which can further shed light on its function, various protein prediction software were used. In most

cases, the software predicted what was already known, that PLG1 has transmembrane domains, but no other protein features were found. It was only in 2013, when the protein sequence analysis software PSIPRED was used (http://bioinf.cs.ucl.ac.uk/psipred/), that another possible relevant feature was identified. PSIPRED identified a pore lining helix situated between its 5th and 6th transmembrane domains (Figure 36). Interestingly, the pore lining helix was detected only for PLG1, and not for the other PTH11-like GPCRs that were downregulated in the Δ*bip1* mutant. A pore lining helix is often found running parallel to transmembrane helices, and allows an opening along which ions or molecules can pass through (Nugent and Jones, 2012). In most ion channels channel-lining transmembrane helices are enriched with charged residues, and this allows the passage of the relevant ions through the channel. The algorithm for predicting such regions were made functional in 2012, so the PSIPRED website can be a useful tool for checking for such protein regions which were most likely not identified in the past (Nugent and Jones, 2012).

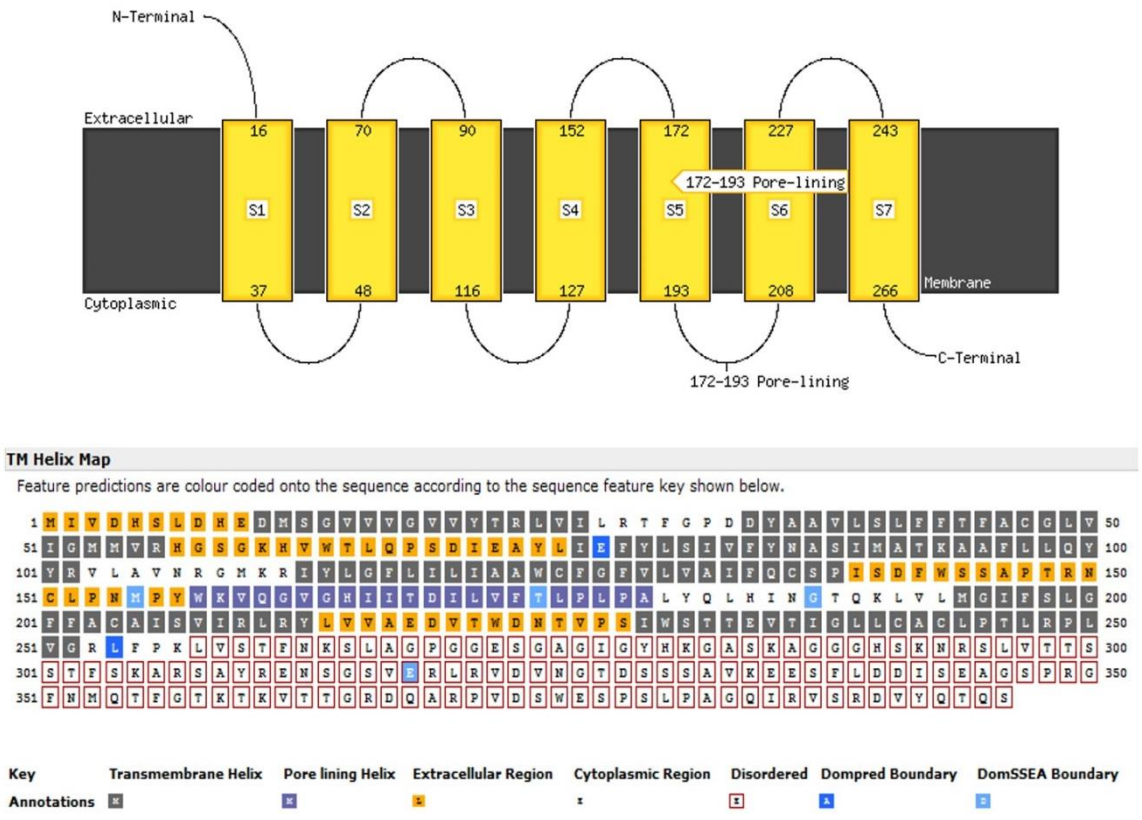

Figure 36. Identification of a Pore Lining Helix Motif in PLG1.

The amino acid sequence for PLG1 was used as an entry sequence in the PSIPRED protein sequence analysis software (http://bioinf.cs.ucl.ac.uk/psipred/).

Discussion

In an attempt to confirm the GPCR property of PLG1, protein-protein interaction assays such as yeast two hybrid and co-immunoprecipitation procedures were employed. GPCRs are known to interact with the Gα subunits. Fortunately, in *M. oryzae*, these Gα subunits namely MagA, MagB and MagC, have been identified and characterized. The

Y2H results showed that PLG1, regardless of any truncated region, did not interact with MagA and MagC, but showed interaction with MagB via its 46 amino acid cytoplasmic domain (F fragment), under low and medium stringency selection. This was an exciting and interesting result at first because the Δ*magB* mutant shares the same phenotype with the Δ*plg1*with respect to the appressorium differentiation defect, and the ability to respond to cAMP and HDD. However, in comparison to the Y2H positive interaction control, only a weak interaction seemed to exist between MagB and F because with the highest stringency selection (SD-Trp-Leu-His-Ade), the mated strain did not grow at all. To confirm whether this interaction is real or not, a co-IP assay has been performed. The co-IP method did not detect any interaction between MagB and the F fragment. There are several possible explanations for these results. In Y2H, which is an *in vivo* assay, the weak interaction is most likely preserved. However, the interaction is disrupted when *in vitro* procedures are performed, so no significant interaction is observed with the co-IP experiment. Secondly, there is a possibility that PLG1 does not really interact with MagB. As introduced earlier, one limitation of the Y2H is the presence of a possible proteins in yeast which may bridge the interaction between the bait and the prey (Van Criekinge and Beyaert, 1999). Perhaps this is the case, that is why a weak interaction is seen between MagB and F in yeast *in vivo*, but interaction may not be physiologically relevant at all in *M. oryzae*.

If PLG1 weakly interacts with MagB, does that mean that it is not a GPCR? It cannot be concluded right away, because GPCRs are also shown to interact with the Gβγ subunit.

In literature, there are various proposed models regarding the activation of G proteins. One model, the C terminus "latch" hypothesis, points to a region of the Gα subunit harboring the critical amino acid residues for the receptor-promoted activation. This assumes that the receptor-catalyzed GDP to GTP exchange is solely dependent on the receptor-Gα contact and the Gβγ merely serves for the association of the heterotrimer with the plasma membrane (Hamm et al., 1988; Marin et al., 2002). Recent studies however have implicated the Gβγ as an active participant in the guanine nucleotide exchange, and resulted in the formulation of the Gβγ "lever" hypothesis. The studies have shown direct interaction of the Gβγ subunit to the receptor (Mahon et al., 2006). Possibly, the weak association between MagB and the F fragment of PLG1 is due to conformational issues. Perhaps the Gβγ subunit is required to enhance the contact. Also, the MGG1 Gγ subunit was recently shown to have some relevance in the developmental and pathogenicity aspects of the fungus, supporting the possibility that the subunits other than Gα overall contribute to the interaction with the receptor (Li et al., 2015).

An interesting prediction was made for PLG1 using the PSIPRED prediction software. A pore lining helix was identified between the 5^{th} and 6^{th} transmembrane regions of PLG1, and suggests that PLG1 might function as an ion channel. One important feature of an ion channel is that it is not continuously open, meaning that a certain stimulus triggers a change in an ion channel's conformation, thereby switching in from a closed state to an open state. Some G proteins are known to directly activate ion channels in two ways: 1) the Gβγ subunit binds to the ion channel and 2) through GPCR-mediated

activation of PLC, from which DAG is produced which subsequently activates the PKC, which directly binds to the ion channel (Alberts et al., 2013). The latter mode thus places the ion channel downstream of the DAG-mediated pathway. If that is the case, then addition of exogenous DAG in the Δ*plg1* may not trigger downstream pathways because PLG1 is not there to be activated anyway. However, it was observed that DAG addition recovered a good number of appressoria compared to the Δ*plg1* mutant strain on Teflon. Whether or not PLG1 has some potential ion channel features, this idea remains to be tested experimentally. This finding however can provide an alternative function for the numerous GPCR-like proteins that were identified in the *M. oryzae* proteome. Considering the ratio of the G proteins to the GPCRs, there is a possibility that some of the GPCR-like proteins are other types of cell surface receptors. With the inherent difficulty of studying membrane proteins biochemically, it is perhaps useful to screen all the *M.* oryzae GPCR-like proteins with PSIPRED, to identify relevant protein regions which were not identified by other prediction software previously.

CHAPTER VI

CONCLUSIONS AND FUTURE DIRECTIONS

Summary

The purpose of this work is to understand how the expanded family of PTH11-like GPCRs in *M. oryzae* contributes to pathogenicity, through the characterization of PLG1. PLG1 was determined to be a member of the PTH11-like family of GPCRs via *in silico* analysis (Kulkarni et al., 2005). The basis for the functional analysis of PLG1 is the finding that it is one of the PTH11-like GPCR-encoding genes that was downregulated in the non-pathogenic Δ*bip1* mutant (Tag et al., in preparation).

The most straightforward way to assess gene function is to create a targeted deletion mutant for that specific gene. In Chapter III, construction of the *PLG1* deletion mutant (Δ*plg1*) was described, in which *PLG1* was replaced by the hygromycin phosphotransferase gene to allow for selection of transformants. Phenotypic analysis of the Δ*plg1* mutant revealed that it was non-pathogenic on both barley and rice because of its defect in appressorium differentiation. All of the Δ*plg1* spores which were allowed to germinate on a hydrophobic surface underwent the early stages of surface recognition such as germ tube formation and hooking stage or hyphal tip swelling, however only a few continued into developing a mature appressoria. Often times, multiple swellings are seen at the hyphal tip. The Δ*plg1* mutant formed appressoria at only 10% of wild type

frequency. These results hinted at the importance of PLG1 in completing appressorium differentiation on an inductive surface. Moreover, the results allowed for further examination of PLG1 function, because it was shown to be relevant to pathogenicity.

Since PLG1 was hypothesized to be a receptor of the GPCR type, it is possible to evaluate its role in the signaling pathways which are known to induce/mediate appressorium morphogenesis. Addition of 1,16-hexadecenediol or HDD recovered appressoria to a greater extent in the Δ*plg1* mutant. The mechanisms by which HDD trigger the signaling pathways for appressorium formation are unknown, but HDD can be considered as an extracellular signal that the fungus can respond to. If that's the case, then PLG1 might not be important in its recognition because the Δ*plg1* mutant responded to HDD treatment by way of appressorium formation. A considerable amount of information however is available for the cAMP-mediated pathway, that is primarily activated by surface contact and chemical sensing (Lee and Dean, 1993). However, far less is known about the signal pathways through protein kinase C (PKC), as mediated by diacylglycerol (Zhang et al., 2001). The connection of the cAMP and DAG pathways have been suggested for a long time but there exists a few documented reports of their functional connection (Liu and Dean, 1997; DeZwaan et al., 1999). Based on the cAMP and DAG treatment responses that Δ*plg1* mutant on both inductive and non-inductive surfaces, as described in Chapter IV, I propose that PLG1 is a potential major activator of the DAG-mediated pathways. The model that was suggested in Chapter IV (Figure 27), proposes PLG1 to be working in conjunction with another receptor, presumably

PTH11, which responds to surface cues primarily via the cAMP-mediated pathway. The suggestion that PLG1 might be a major activator of DAG-related pathways is further confirmed by expression studies on downstream genes. Upon comparison of the wild type and Δ*plg1* mutant differentiated on Teflon at 24 hpe, qRT-PCR analysis revealed that the transcript level of *PKC*, the downstream gene activated by DAG signaling is significantly reduced in the Δ*plg1* mutant. This provided a functional relationship between PLG1 and the DAG-related pathways.

If PLG1 is a GPCR, it potentially interacts with G proteins in the fungus. In Y2H assays, a weak interaction between the cytoplasmic region, F of PLG1 and the Gα subunit MagB has been identified. However, co-IP assay did not detect any interaction between PLG1 and MagB. This raises the question as to whether the interaction is real or not. Perhaps, in *M. oryzae*, PLG1 is more closely interacting with the Gβγ subunit, and given how the subunits are linked together, PLG1 may contact the Gα in a manner that is weaker compared to Gβγ.

Overall, this study contributed to the knowledge of how some of the GPCR-like proteins in *M. oryzae* may function. Clearly, crosstalk in signaling mechanisms exist in appressorium formation and one of the probable reasons that they do, as suggested in the body of this work, is the modulation of intracellular cAMP and DAG levels. This is probably one of the reasons why when a single putative receptor is taken out of the genome, as for PTH11 for example, appressorium formation is still observed, although at

very low levels. Perhaps other receptors are contributing to the levels of the secondary messengers required for appressorium formation, but are usually not enough to trigger complete appressorium differentiation.

Future Work

Expression Analysis of Other DAG-Related Genes

Although PKC has been shown to be downregulated in the Δ*plg1* mutant, a stronger evidence of the functional connection between PLG1 and DAG could be established if other known genes downstream of PKC will be analyzed. The hypothesis is that in the Δ*plg1* mutant, these genes will be downregulated as well, as a result of PKC downregulation. Unfortunately, limited information is known about these downstream effectors. Perhaps an alternative experiment is the use of next generation sequencing technologies, RNA-seq for example, to study the transcripts that are differentially expressed between the wild type and Δ*plg1* mutant strains at different time points. Then, once the genes have been identified, their expression will be verified using gene-specific primers in a qRT-PCR assay. This data mining method will allow identification of the possible downstream effectors leading to appressorium formation. This has been proposed previously, but due to time constraints and lack of current resources, it has not been pursued.

Testing the Interaction of PLG1 with Other G Protein Subunits In Vivo and In Vitro

It has been discussed that PLG1 interacts with MagB, albeit weakly in Y2H assay, hypothetically classifying it as a GPCR. Assigning PLG1 with the GPCR function may be strengthened by performing an *in vivo* experiment such as bifluorescence complementation (BiFC), wherein possible interactions are identified within the organism of interest. As indicated earlier, other proteins within the host organism might allow the proper conformation of the interacting proteins, allowing one to see a stronger interaction compared to what was seen in the Y2H results. Difficulties however exist for creating the tagged constructs of the G proteins and transforming them into *M. oryzae*, since the G proteins are essential to cell function (Ramanujam et al., 2013).

In order to look at the interactions of PLG1 with the other G protein subunits in *M. oryzae*, a Y2H assay may be performed once again. If potential interactions are detected, then it can be confirmed further with a BiFC assay. In addition to these, co-IP assays should be performed alongside to provide validation for the expression of functional constructs.

Measurement of Intracellular cAMP and DAG Levels

If the proposed model is true about PLG1 function, then the cAMP and DAG levels, mainly DAG levels, should be significantly different between the wild type and Δ*plg1* mutant. There are known methods by which cAMP levels are measured in *M. oryzae*

(Ramanujam and Naqvi, 2010). The process involves preparing mycelia or conidia under the desired growth and developmental conditions, and preparing the samples according to the methods described in the cAMP Biotrak Immuno-assay System manufactured by Amersham. DAG level measurement from cells has been described in other organisms, but none in *M. oryzae* so far. (Tewson et al., 2012). Outcomes of such experiments however, should be interpreted with caution because other receptors in the fungus may contribute to the amount of intracellular secondary messengers. One should keep in mind that measurable intracellular cAMP and DAG levels may be due to the coordinated inputs of all these pathways, and not just one receptor.

Construction of a PLG1 and PTH11 Double Deletion Mutant

During the course of this study, the deletion of PTH11 from the *M. oryzae* 70-15 genome was attempted but was not successful. Interestingly, there are no documented Δ*pth11* mutants in the wild type 70-15 background. The original Δ*pth11* mutant was constructed under the 4091-8-5 wild type background. It would be of interest to find out if the phenotypes will be similar if the *PTH11* deletion is done in the 70-15 background. Moreover, if the proposed model is true, then a double deletion mutant will perhaps lead to more severe phenotypes than the single deletion mutants, and the cAMP and DAG responses will be different in both hydrophobic and hydrophilic surfaces.

REFERENCES

Adachi, K., and Hamer, J.E. (1998). Divergent cAMP signaling pathways regulate growth and pathogenesis in the rice blast fungus Magnaporthe grisea. The Plant Cell **10,** 1361-1374.

Affeldt, K.J., Carrig, J., Amare, M., and Keller, N.P. (2014). Global survey of canonical Aspergillus flavus G protein-coupled receptors. mBio **5,** e01501-01514.

Aho, S., Arffman, A., Pummi, T., and Uitto, J. (1997). A novel reporter gene MEL1 for the yeast two-hybrid system. Analytical Biochemistry **253,** 270-272.

Alberts, B., Bray, D., Hopkin, K., Johnson, A., Lewis, J., Raff, M., Roberts, K., and Walter, P. (2013). Cell communication. In Essential Cell Biology, Fourth Edition (Taylor & Francis Group: New York), p. 561-566.

Babcock, J.J., and Li, M. (2014). Deorphanizing the human transmembrane genome: A landscape of uncharacterized membrane proteins. Acta Pharmacol Sin **35,** 11-23.

Bae, C.Y., Kim, S., Choi, W.B., and Lee, Y.H. (2007). Involvement of extracellular matrix and integrin-like proteins on conidial adhesion and appressorium differentiation in Magnaporthe oryzae. Journal of Microbiology and Biotechnology **17,** 1198-1203.

Beckerman, J.L., and Ebbole, D.J. (1996). MPG1, a gene encoding a fungal hydrophobin of Magnaporthe grisea, is involved in surface recognition. Molecular Plant-Microbe Interactions : MPMI **9,** 450-456.

Boyle, J. (2008). Molecular biology of the cell, Biochemistry and Molecular Biology Education **36,** 317-318.

Brand, A., and Gow, N.R. (2012). Tropic orientation responses of pathogenic fungi. In Morphogenesis and Pathogenicity in Fungi (Springer Berlin: Heidelberg), p. 21-41.

Brenner, S., Johnson, M., Bridgham, J., Golda, G., Lloyd, D.H., Johnson, D., Luo, S., McCurdy, S., Foy, M., Ewan, M., Roth, R., George, D., Eletr, S., Albrecht, G., Vermaas, E., Williams, S.R., Moon, K., Burcham, T., Pallas, M., DuBridge, R.B., Kirchner, J., Fearon, K., Mao, J., and Corcoran, K. (2000). Gene expression analysis by massively parallel signature sequencing (MPSS) on microbead arrays. Nature Biotechnology **18,** 630-634.

Breth, B., Odenbach, D., Yemelin, A., Schlinck, N., Schröder, M., Bode, M., Antelo, L., Andresen, K., Thines, E., and Foster, A.J. (2013). The role of the Tra1p transcription factor of Magnaporthe oryzae in spore adhesion and pathogenic development. Fungal Genetics and Biology **57,** 11-22.

Brückner, A., Polge, C., Lentze, N., Auerbach, D., and Schlattner, U. (2009). Yeast two-hybrid, a powerful tool for systems biology. International Journal of Molecular Sciences **10,** 2763-2788.

Bush, D.S. (1993). Regulation of cytosolic calcium in plants. Plant Physiology **103,** 7-13.

Cargnello, M., and Roux, P.P. (2011). Activation and function of the MAPKs and their substrates, the MAPK-activated protein kinases. Microbiology and Molecular Biology Reviews : MMBR **75,** 50-83.

Carpenter, E.P., Beis, K., Cameron, A.D., and Iwata, S. (2008). Overcoming the challenges of membrane protein crystallography. Current Opinion in Structural Biology **18,** 581-586.

Casadevall, A., and Pirofski, L.A. (2000). Host-pathogen interactions: basic concepts of microbial commensalism, colonization, infection, and disease. Infection and Immunity **68,** 6511-6518.

Castroagudín, V.L., Ceresini, P.C., de Oliveira, S.C., Reges, J.T.A., Maciel, J.L.N., Bonato, A.L.V., Dorigan, A.F., and McDonald, B.A. (2014). Resistance to QoI fungicides is widespread in Brazilian populations of the wheat blast pathogen Magnaporthe oryzae. Phytopathology **105,** 284-294.

Catlett, N.L., Lee, B.-N., Yoder, O.C., and Turgeon, B.G. (2003). Split-marker recombination for efficient targeted deletion of fungal genes. Fungal Genet. Newsl. **50,** 9-11.

Chen, D., Wang, Y., Zhou, X., Wang, Y., and Xu, J.R. (2014). The Sch9 kinase regulates conidium size, stress responses, and pathogenesis in Fusarium graminearum. PloS One **9,** e105811.

Cho, Y.-C., Suh, J.-P., Jeung, J.-U., Roh, J.-H., Yang, C.-I., Oh, M.-K., Jeon, J.-S., Choi, I.-S., Hwang, H.-G., Yang, S.-J., and Kim, Y.-G. (2009). Resistance genes and their effects to blast in Korean rice. In Advances in Genetics, Genomics and Control of Rice Blast Disease (Springer: Netherlands), p. 291-304.

Choi, W., and Dean, R.A. (1997). The adenylate cyclase gene MAC1 of Magnaporthe grisea controls appressorium formation and other aspects of growth and development. The Plant Cell **9,** 1973-1983.

Clifton, M.C., Abendroth, J., Edwards, T.E., Leibly, D.J., Gillespie, A.K., Ferrell, M., Dieterich, S.H., Exley, I., Staker, B.L., Myler, P.J., Van Voorhis, W.C., and Stewart, L.J. (2011). Structure of the cystathionine gamma-synthase MetB from Mycobacterium ulcerans. Acta Crystallographica **67,** 1154-1158.

Clontech Laboratories, I. (2013). Matchmaker® gold yeast two-hybrid system user manual. PT4084-1 version PR742227.

Couch, B.C., and Kohn, L.M. (2002). A multilocus gene genealogy concordant with host preference indicates segregation of a new species, Magnaporthe oryzae, from M. grisea. Mycologia **94,** 683-693.

Couch, B.C., Fudal, I., Lebrun, M.H., Tharreau, D., Valent, B., van Kim, P., Notteghem, J.L., and Kohn, L.M. (2005). Origins of host-specific populations of the blast pathogen Magnaporthe oryzae in crop domestication with subsequent expansion of pandemic clones on rice and weeds of rice. Genetics **170,** 613-630.

Cserzo, M., Wallin, E., Simon, I., von Heijne, G., and Elofsson, A. (1997). Prediction of transmembrane alpha-helices in prokaryotic membrane proteins: the dense alignment surface method. Protein Eng **10,** 673-676.

Cuatrecasas, P. (1974). Membrane receptors. Annual Review of Biochemistry **43,** 169-214.

Dagdas, Y.F., Yoshino, K., Dagdas, G., Ryder, L.S., Bielska, E., Steinberg, G., and Talbot, N.J. (2012). Septin-mediated plant cell invasion by the rice blast fungus, Magnaporthe oryzae. Science **336,** 1590-1595.

Daniel, J.M., and Reynolds, A.B. (1999). The catenin p120(ctn) interacts with Kaiso, a novel BTB/POZ domain zinc finger transcription factor. Molecular and Cellular Biology **19,** 3614-3623.

de Castro, E., Sigrist, C.J., Gattiker, A., Bulliard, V., Langendijk-Genevaux, P.S., Gasteiger, E., Bairoch, A., and Hulo, N. (2006). ScanProsite: detection of PROSITE signature matches and ProRule-associated functional and structural residues in proteins. Nucleic Acids Research **34,** W362-365.

de Jong, J.C., McCormack, B.J., Smirnoff, N., and Talbot, N.J. (1997). Glycerol generates turgor in rice blast. Nature **389,** 244-244.

Deacon, E.M., Pettitt, T.R., Webb, P., Cross, T., Chahal, H., Wakelam, M.J., and Lord, J.M. (2002). Generation of diacylglycerol molecular species through the cell cycle: a role for 1-stearoyl, 2-arachidonyl glycerol in the activation of nuclear protein kinase C-betaII at G2/M. Journal of Cell Science **115,** 983-989.

Dean, R., Van Kan, J.A., Pretorius, Z.A., Hammond-Kosack, K.E., Di Pietro, A., Spanu, P.D., Rudd, J.J., Dickman, M., Kahmann, R., Ellis, J., and Foster, G.D. (2012). The top 10 fungal pathogens in molecular plant pathology. Molecular Plant Pathology **13,** 414-430.

Dean, R.A. (1997). Signal pathways and appressorium morphogenesis. Annual Review of Phytopathology **35,** 211-234.

Dean, R.A., Talbot, N.J., Ebbole, D.J., Farman, M.L., Mitchell, T.K., Orbach, M.J., Thon, M., Kulkarni, R., Xu, J.R., Pan, H., Read, N.D., Lee, Y.H., Carbone, I., Brown, D., Oh, Y.Y., Donofrio, N., Jeong, J.S., Soanes, D.M., Djonovic, S., Kolomiets, E., Rehmeyer, C., Li, W., Harding, M., Kim, S., Lebrun, M.H., Bohnert, H., Coughlan, S., Butler, J., Calvo, S., Ma, L.J., Nicol, R., Purcell, S., Nusbaum, C., Galagan, J.E., and Birren, B.W. (2005). The genome sequence of the rice blast fungus Magnaporthe grisea. Nature **434,** 980-986.

DeZwaan, T.M., Carroll, A.M., Valent, B., and Sweigard, J.A. (1999). Magnaporthe grisea pth11p is a novel plasma membrane protein that mediates appressorium differentiation in response to inductive substrate cues. The Plant Cell **11,** 2013-2030.

Dixon, K.P., Xu, J.R., Smirnoff, N., and Talbot, N.J. (1999). Independent signaling pathways regulate cellular turgor during hyperosmotic stress and appressorium-mediated plant infection by Magnaporthe grisea. The Plant Cell **11,** 2045-2058.

Douliez, J.-P. (2004). Cutin and suberin monomers are membrane perturbants. Journal of Colloid and Interface Science **271,** 507-510.

Driver, F., Milner, R.J., and Trueman, J.W.H. (2000). A taxonomic revision of Metarhizium based on a phylogenetic analysis of rDNA sequence data. Mycological Research **104,** 134-150.

Ebata, Y., Yamamoto, H., and Uchiyama, T. (1998). Chemical Composition fo the Glue From Appressoria of Magnaporthe grisea. Bioscience, Biotechnology, and Biochemistry **62,** 672-674.

Eierhoff, T., Hrincius, E.R., Rescher, U., Ludwig, S., and Ehrhardt, C. (2010). The Epidermal Growth Factor Receptor (EGFR) Promotes Uptake of Influenza A Viruses (IAV) into Host Cells. PLoS Pathogens **6,** e1001099.

Emmett, R.W., and Parbery, D.G. (1975). Appressoria. Annual Review of Phytopathology **13,** 147-165.

Endo, M., Takesako, K., Kato, I., and Yamaguchi, H. (1997). Fungicidal action of aureobasidin A, a cyclic depsipeptide antifungal antibiotic, against Saccharomyces cerevisiae. Antimicrobial Agents and Chemotherapy **41,** 672-676.

Endo, T., Nakamura, T., Yonemaru, J., Ishikawa, G., Yamaguchi, M., Kataoka, T., Nakagomi, K., and Yokogami, N. (2009). Genetic Analysis of Resistance Against Bacterial Leaf Blight and Leaf Blast Disease in the Japanese Rice Cultivar Asominori. In Advances in Genetics, Genomics and Control of Rice Blast Disease (Springer: Netherlands), p. 305-313.

Farman, M.L. (2002). Meiotic deletion at the BUF1 locus of the fungus Magnaporthe grisea is controlled by interaction with the homologous chromosome. Genetics **160,** 137-148.

Fields, S., and Song, O. (1989). A novel genetic system to detect protein-protein interactions. Nature **340,** 245-246.

Forrest, G.C. (1990). Genetic Analysis of Melanin-Deficient, Nonpathogenic Mutants of Magnaporthe grisea. Molecular Plant-Microbe Interactions : MPMI **3,** 135-135.

Fredriksson, R., Lagerstrom, M.C., Lundin, L.G., and Schioth, H.B. (2003). The G-protein-coupled receptors in the human genome form five main families. Phylogenetic analysis, paralogon groups, and fingerprints. Molecular Pharmacology **63,** 1256-1272.

Gao, Q., Jin, K., Ying, S.-H., Zhang, Y., Xiao, G., Shang, Y., Duan, Z., Hu, X., Xie, X.-Q., Zhou, G., Peng, G., Luo, Z., Huang, W., Wang, B., Fang, W., Wang, S., Zhong, Y., Ma, L.-J., St. Leger, R.J., Zhao, G.-P., Pei, Y., Feng, M.-G., Xia, Y., and Wang, C. (2011). Genome sequencing and comparative transcriptomics of the model entomopathogenic fungi Metarhizium anisopliae and M. acridum. PLoS Genetics **7,** e1001264.

Gilbert, M.J., Thornton, C.R., Wakley, G.E., and Talbot, N.J. (2006). A P-type ATPase required for rice blast disease and induction of host resistance. Nature **440,** 535-539.

Gilbert, R.D., Johnson, A.M., and Dean, R.A. (1996). Chemical signals responsible for appressorium formation in the rice blast fungus Magnaporthe grisea. Physiological and Molecular Plant Pathology **48,** 335-346.

Gogvadze, E., Barbisan, C., Lebrun, M.-H., and Buzdin, A. (2007). Tripartite chimeric pseudogene from the genome of rice blast fungus Magnaporthe grisea suggests double template jumps during long interspersed nuclear element (LINE) reverse transcription. BMC Genomics **8,** 360.

Gowda, M., Jantasuriyarat, C., Dean, R.A., and Wang, G.L. (2004). Robust-LongSAGE (RL-SAGE): a substantially improved LongSAGE method for gene discovery and transcriptome analysis. Plant Physiology **134,** 890-897.

Gowda, M., Nunes, C.C., Sailsbery, J., Xue, M., Chen, F., Nelson, C.A., Brown, D.E., Oh, Y., Meng, S., Mitchell, T., Hagedorn, C.H., and Dean, R.A. (2010). Genome-wide characterization of methylguanosine-capped and polyadenylated small RNAs in the rice blast fungus Magnaporthe oryzae. Nucleic Acids Research **38,** 7558-7569.

Gowda, M., Venu, R.C., Raghupathy, M.B., Nobuta, K., Li, H., Wing, R., Stahlberg, E., Couglan, S., Haudenschild, C.D., Dean, R., Nahm, B.H., Meyers, B.C., and Wang, G.L. (2006). Deep and comparative analysis of the mycelium and appressorium transcriptomes of Magnaporthe grisea using MPSS, RL-SAGE, and oligoarray methods. BMC Genomics **7,** 310.

Gruber, S., Omann, M., and Zeilinger, S. (2013). Comparative analysis of the repertoire of G protein-coupled receptors of three species of the fungal genus Trichoderma. BMC Microbiology **13,** 1-14.

Gruenheid, S., and Finlay, B.B. (2003). Microbial pathogenesis and cytoskeletal function. Nature **422,** 775-781.

Guo, M., Guo, W., Chen, Y., Dong, S., Zhang, X., Zhang, H., Song, W., Wang, W., Wang, Q., Lv, R., Zhang, Z., Wang, Y., and Zheng, X. (2010). The basic leucine zipper transcription factor Moatf1 mediates oxidative stress responses and is necessary for full virulence of the rice blast fungus Magnaporthe oryzae. Molecular Plant-Microbe Interactions : MPMI **23,** 1053-1068.

Hamer, J.E., and Talbot, N.J. (1998). Infection-related development in the rice blast fungus Magnaporthe grisea. Current Opinion in Microbiology **1,** 693-697.

Hamer, J.E., Howard, R.J., Chumley, F.G., and Valent, B. (1988). A mechanism for surface attachment in spores of a plant pathogenic fungus. Science **239,** 288-290.

Hamm, H., Deretic, D., Arendt, A., Hargrave, P., Koenig, B., and Hofmann, K. (1988). Site of G protein binding to rhodopsin mapped with synthetic peptides from the alpha subunit. Science **241,** 832-835.

Hardham, A.R. (1992). Cell biology of pathogenesis. Annual Review of Plant Physiology and Plant Molecular Biology **43,** 491-526.

Hasegawa, E., Ota, Y., Hattori, T., and Kikuchi, T. (2010). Sequence-based identification of Japanese Armillaria species using the elongation factor-1 alpha gene. Mycologia **102,** 898-910.

Hegde, Y., and Kolattukudy, P.E. (1997). Cuticular waxes relieve self-inhibition of germination and appressorium formation by the conidia of Magnaporthe grisea. Physiological and Molecular Plant Pathology **51,** 75-84.

Herbst, R.S. (2004). Review of epidermal growth factor receptor biology. International Journal of Radiation Oncology, Biology, Physics **59,** 21-26.

Heredia, A. (2003). Biophysical and biochemical characteristics of cutin, a plant barrier biopolymer. Biochimica et Biophysica Acta **1620,** 1-7.

Hirokawa, T., Boon-Chieng, S., and Mitaku, S. (1998). SOSUI: classification and secondary structure prediction system for membrane proteins. Bioinformatics **14,** 378-379.

Hoch, H.C., and Staples, R.C. (1987). Structural and chemical changes among the rust fungi during appressorium development. Annual Review of Phytopathology **25,** 231-247.

Hoch, H.C., and Staples, R.C. (1991). Signaling for infection structure formation in fungi. In The Fungal Spore and Disease Initiation in Plants and Animals (Springer: US), p. 25-46.

Hofmann. (1993). TMbase - A database of membrane spanning proteins segments. Biol. Chem. Hoppe-Seyler **374**.

Holm, S. (1979). A simple sequentially rejective multiple test procedure. Scandinavian Journal of Statistics **6,** 65-70.

Holmberg, S., and Petersen, J.G. (1988). Regulation of isoleucine-valine biosynthesis in Saccharomyces cerevisiae. Current Genetics **13,** 207-217.

Hopkinson, S.B., and Jones, J.C. (2000). The N terminus of the transmembrane protein BP180 interacts with the N-terminal domain of BP230, thereby mediating keratin cytoskeleton anchorage to the cell surface at the site of the hemidesmosome. Molecular Biology of the Cell **11,** 277-286.

Howard, R.J., and Ferrari, M.A. (1989). Role of melanin in appressorium function. Experimental Mycology **13,** 403-418.

Howard, R.J., and Valent, B. (1996). Breaking and entering: host penetration by the fungal rice blast pathogen Magnaporthe grisea. Annual Review of Microbiology **50,** 491-512.

Howard, R.J., Ferrari, M.A., Roach, D.H., and Money, N.P. (1991). Penetration of hard substrates by a fungus employing enormous turgor pressures. Proceedings of the National Academy of Sciences **88,** 11281-11284.

Jansson, H.-B., and Åkesson, H. (2003). Extracellular matrix, esterase and the phytotoxin prehelminthosporol in infection of barley leaves by bipolaris sorokiniana. European Journal of Plant Pathology **109,** 599-605.

Jelitto, T., Page, H., and Read, N. (1994). Role of external signals in regulating the pre-penetration phase of infection by the rice blast fungus, Magnaporthe grisea. Planta **194,** 471-477.

Jeon, J., Choi, J., Lee, G.W., Dean, R.A., and Lee, Y.H. (2013). Experimental evolution reveals genome-wide spectrum and dynamics of mutations in the rice blast fungus, Magnaporthe oryzae. PloS One **8,** e65416.

Kamakura, T., Yamaguchi, S., Saitoh, K.-i., Teraoka, T., and Yamaguchi, I. (2002). A novel gene, CBP1, encoding a putative extracellular chitin-binding protein, may play an important role in the hydrophobic surface sensing of Magnaporthe grisea during appressorium differentiation. Molecular Plant-Microbe Interactions **15,** 437-444.

Kankanala, P. (2007). Cell Biology and Gene Expression Profiling During the Early Biotrophic Invasion by the Rice Blast Fungus Magnaporthe Oryzae. (Kansas State University).

Kankanala, P., Czymmek, K., and Valent, B. (2007). Roles for rice membrane dynamics and plasmodesmata during biotrophic invasion by the blast fungus. The Plant Cell **19,** 706-724.

Kato, H., Yamamoto, M., Yamaguchi-Ozaki, T., Kadouchi, H., Iwamoto, Y., Nakayashiki, H., Tosa, Y., Mayama, S., and Mori, N. (2000). Pathogenicity, mating ability and DNA restriction fragment length polymorphisms of Pyricularia populations isolated from Gramineae, Bambusideae and Zingiberaceae plants. J Gen Plant Pathol **66,** 30-47.

Kershaw, M.J., Wakley, G., and Talbot, N.J. (1998). Complementation of the mpg1 mutant phenotype in Magnaporthe grisea reveals functional relationships between fungal hydrophobins. The EMBO Journal **17,** 3838-3849.

Khang, C.H., Berruyer, R., Giraldo, M.C., Kankanala, P., Park, S.Y., Czymmek, K., Kang, S., and Valent, B. (2010). Translocation of Magnaporthe oryzae effectors into rice cells and their subsequent cell-to-cell movement. The Plant Cell **22,** 1388-1403.

Klotz, S.A., and Smith, R.L. (1991). A fibronectin receptor on Candida albicans mediates adherence of the fungus to extracellular matrix. The Journal of Infectious Diseases **163,** 604-610.

Koga, H., and Nakayachi, O. (2004). Morphological studies on attachment of spores of Magnaporthe grisea to the leaf surface of rice. J Gen Plant Pathol **70,** 11-15.

Kolattukudy, P.E. (1980). Biopolyester membranes of plants: cutin and suberin. Science **208,** 990-1000.

Kolattukudy, P.E. (1985). Enzymatic Penetration of the Plant Cuticle by Fungal Pathogens. Annual Review of Phytopathology **23,** 223-250.

Kolattukudy, P.E., Ettinger, W., and Sebastian, J. (1987). Cuticular lipids in plant-microbe interactions. In The Metabolism, Structure, and Function of Plant Lipids (Springer New York), p. 473-480.

Kolattukudy, P.E., Rogers, L.M., Li, D., Hwang, C.S., and Flaishman, M.A. (1995). Surface signaling in pathogenesis. Proceedings of the National Academy of Sciences **92,** 4080-4087.

Krogh, A., Larsson, B., von Heijne, G., and Sonnhammer, E.L. (2001). Predicting transmembrane protein topology with a hidden Markov model: application to complete genomes. Journal of Molecular Biology **305,** 567-580.

Kulkarni, R.D., Kelkar, H.S., and Dean, R.A. (2003). An eight-cysteine-containing CFEM domain unique to a group of fungal membrane proteins. Trends in Biochemical Sciences **28,** 118-121.

Kulkarni, R.D., Thon, M.R., Pan, H., and Dean, R.A. (2005). Novel G-protein-coupled receptor-like proteins in the plant pathogenic fungus Magnaporthe grisea. Genome Biology **6,** 24.

Kumamoto, C.A. (2008). Molecular mechanisms of mechanosensing and their roles in fungal contact sensing. Nat Rev Micro **6,** 667-673.

Kwon, L.J., Seo, H.J., Kim, E.O., Medyani. (2006). Identification of anti-angiogenic and anti-cell adhesion materials from halophilic enterobacteria of the Trachurus japonicus. Journal of Microbiology and Biotechnology **16,** 1544-1553 .

Lee, S.C., and Lee, Y.H. (1998). Calcium/calmodulin-dependent signaling for appressorium formation in the plant pathogenic fungus Magnaporthe grisea. Molecules and Cells **8,** 698-704.

Lee, Y.H., and Dean, R.A. (1993). cAMP regulates infection structure formation in the plant pathogenic fungus Magnaporthe grisea. The Plant Cell **5,** 693-700.

Lemaire, K., Van de Velde, S., Van Dijck, P., and Thevelein, J.M. (2004). Glucose and sucrose act as agonist and mannose as antagonist ligands of the G protein-coupled receptor Gpr1 in the yeast Saccharomyces cerevisiae. Molecular Cell **16,** 293-299.

Leung, H., Lehtinen, U., Karjalainen, R., Skinner, D., Tooley, P., Leong, S., and Ellingboe, A. (1990). Transformation of the rice blast fungus Magnaporthe grisea to hygromycin B resistance. Current Genetics **17,** 409-411.

Li, L., and Borkovich, K.A. (2006). GPR-4 is a predicted G-protein-coupled receptor required for carbon source-dependent asexual growth and development in Neurospora crassa. Eukaryotic Cell **5,** 1287-1300.

Li, L., Xue, C., Bruno, K., Nishimura, M., and Xu, J.R. (2004). Two PAK kinase genes, CHM1 and MST20, have distinct functions in Magnaporthe grisea. Molecular Plant-Microbe Interactions : MPMI **17,** 547-556.

Li, L., Wright, S.J., Krystofova, S., Park, G., and Borkovich, K.A. (2007). Heterotrimeric G Protein Signaling in Filamentous Fungi. Annual Review of Microbiology **61,** 423-452.

Li, Y., Que, Y., Liu, Y., Yue, X., Meng, X., Zhang, Z., and Wang, Z. (2015). The putative Gγ subunit gene MGG1 is required for conidiation, appressorium formation, mating and pathogenicity in Magnaporthe oryzae. Current Genetics**,** 1-11.

Liang, S., Wang, Z., Liu, P., and Li, D. (2006). A Gγ subunit promoter T-DNA insertion mutant—A1-412 of Magnaporthe grisea is defective in appressorium formation, penetration and pathogenicity. Chinese Science Bull **51,** 2214-2218.

Lin, S.H., and Guidotti, G. (2009). Purification of membrane proteins. Methods in Enzymology **463,** 619-629.

Liu, H., Suresh, A., Willard, F.S., Siderovski, D.P., Lu, S., and Naqvi, N.I. (2007a). Rgs1 regulates multiple Gα subunits in Magnaporthe pathogenesis, asexual growth and thigmotropism. The EMBO Journal **26,** 690-700.

Liu, S., and Dean, R.A. (1997). G protein alpha subunit genes control growth, development, and pathogenicity of Magnaporthe grisea. Molecular Plant-Microbe Interactions : MPMI **10,** 1075-1086.

Liu, T.-b., Lu, J.-p., Liu, X.-h., Min, H., and Lin, F.-c. (2008). A simple and effective method for total RNA isolation of appressoria in Magnaporthe oryzae. Journal of Zhejiang University. Science. B **9,** 811-817.

Liu, W., Zhou, X., Li, G., Li, L., Kong, L., Wang, C., Zhang, H., and Xu, J.R. (2011a). Multiple plant surface signals are sensed by different mechanisms in the rice blast fungus for appressorium formation. PLoS Pathogens **7,** e1001261.

Liu, W., Zhou, X., Li, G., Li, L., Kong, L., Wang, C., Zhang, H., and Xu, J.-R. (2011b). Multiple plant surface signals are sensed by different mechanisms in the rice blast fungus for appressorium formation. PLoS Pathogens **7,** e1001261.

Liu, X.-H., Lu, J.-P., Zhang, L., Dong, B., Min, H., and Lin, F.-C. (2007b). Involvement of a Magnaporthe grisea serine/threonine kinase gene, MgATG1, in appressorium turgor and pathogenesis. Eukaryotic Cell **6,** 997-1005.

Liu, X., Yue, Y., Li, B., Nie, Y., Li, W., Wu, W.-H., and Ma, L. (2007c). A G protein-coupled receptor is a plasma membrane receptor for the plant hormone abscisic acid. Science **315,** 1712-1716.

Livak, K.J., and Schmittgen, T.D. (2001). Analysis of relative gene expression data using real-time quantitative PCR and the 2(-Delta Delta C(T)) Method. Methods **25,** 402-408.

Lodish, H. (2008). G Protein –coupled receptors and their effectors. In Molecular Cell Biology (W. H. Freeman: New York).

Lu, Q., Lu, J.-p., Li, X.-d., Liu, X.-h., Min, H., and Lin, F.-c. (2008). Magnaporthe oryzae MTP1 gene encodes a type III transmembrane protein involved in conidiation and conidial germination. Journal of Zhejiang University. Science. B **9,** 511-519.

Macko, V., Staples, R.C., Allen, P.J., and Renwick, J.A.A. (1971). Identification of the germination self-inhibitor from wheat stem rust Uredospores. Science **173,** 835-836.

Mahon, M.J., Bonacci, T.M., Divieti, P., and Smrcka, A.V. (2006). A docking site for G protein βγ subunits on the parathyroid hormone 1 receptor supports signaling through multiple pathways. Molecular Endocrinology **20,** 136-146.

Maidan, M.M., De Rop, L., Relloso, M., Diez-Orejas, R., Thevelein, J.M., and Van Dijck, P. (2008). Combined inactivation of the Candida albicans GPR1 and TPS2 genes results in avirulence in a mouse model for systemic infection. Infection and Immunity **76,** 1686-1694.

Marin, E.P., Krishna, A.G., and Sakmar, T.P. (2002). Disruption of the α5 helix of transducin impairs rhodopsin-catalyzed nucleotide exchange. Biochemistry **41,** 6988-6994.

Marroquin-Guzman, M., and Wilson, R.A. (2015). GATA-dependent glutaminolysis drives appressorium formation in Magnaporthe oryzae by suppressing TOR inhibition of cAMP/PKA signaling. PLoS Pathogens **11,** e1004851.

Mathioni, S.M., Patel, N., Riddick, B., Sweigard, J.A., Czymmek, K.J., Caplan, J.L., Kunjeti, S.G., Kunjeti, S., Raman, V., Hillman, B.I., Kobayashi, D.Y., and Donofrio, N.M. (2013). Transcriptomics of the rice blast fungus Magnaporthe oryzae in response to the bacterial antagonist Lysobacter enzymogenes reveals candidate fungal defense response genes. PloS One **8,** e76487.

McBeath, J.H., McBeath, J., and McBeath, J. (2010). Plant diseases, pests and food security. In Environmental Change and Food Security in China. (Springer: Netherlands), p. 117-156.

Mehrabi, R., Ding, S., and Xu, J.R. (2008). MADS-box transcription factor mig1 is required for infectious growth in Magnaporthe grisea. Eukaryotic Cell **7,** 791-799.

Mendgen, K., and Deising, H. (1993). Infection structures of fungal plant pathogens – a cytological and physiological evaluation. New Phytologist **124,** 193-213.

Meng, S., Brown, D.E., Ebbole, D.J., Torto-Alalibo, T., Oh, Y.Y., Deng, J., Mitchell, T.K., and Dean, R.A. (2009). Gene Ontology annotation of the rice blast fungus, Magnaporthe oryzae. BMC Microbiology **9 Suppl 1,** S8.

Michino, M., Chen, J., Stevens, R.C., and Brooks, C.L. (2010). Fold GPCR: structure prediction protocol for the transmembrane domain of G protein-coupled receptors from class A. Proteins **78,** 2189-2201.

Mitchell, A., Chang, H.Y., Daugherty, L., Fraser, M., Hunter, S., Lopez, R., McAnulla, C., McMenamin, C., Nuka, G., Pesseat, S., Sangrador-Vegas, A., Scheremetjew, M., Rato, C., Yong, S.Y., Bateman, A., Punta, M., Attwood, T.K., Sigrist, C.J., Redaschi, N., Rivoire, C., Xenarios, I., Kahn, D., Guyot, D., Bork, P., and Letunic, I. (2015). The InterPro protein families database: the classification resource after 15 years. Nucleic Acids Res **43,** D213-221.

Mitchell, T.K., and Dean, R.A. (1995). The cAMP-dependent protein kinase catalytic subunit is required for appressorium formation and pathogenesis by the rice blast pathogen Magnaporthe grisea. The Plant Cell **7,** 1869-1878.

Mosquera, G., Giraldo, M.C., Khang, C.H., Coughlan, S., and Valent, B. (2009). Interaction transcriptome analysis identifies Magnaporthe oryzae BAS1-4 as

Biotrophy-associated secreted proteins in rice blast disease. The Plant Cell **21,** 1273-1290.

Nakamura, N. (2011). The role of the transmembrane RING finger proteins in cellular and organelle function. Membranes **1,** 354-393.

Neves, S.R., Ram, P.T., and Iyengar, R. (2002). G protein pathways. Science **296,** 1636-1639.

Nguyen, Q.B., Kadotani, N., Kasahara, S., Tosa, Y., Mayama, S., and Nakayashiki, H. (2008). Systematic functional analysis of calcium-signalling proteins in the genome of the rice-blast fungus, Magnaporthe oryzae, using a high-throughput RNA-silencing system. Molecular Microbiology **68,** 1348-1365.

Nishimura, M., Park, G., and Xu, J.R. (2003). The G-beta subunit MGB1 is involved in regulating multiple steps of infection-related morphogenesis in Magnaporthe grisea. Molecular Microbiology **50,** 231-243.

Nugent, T., and Jones, D. (2012). Detecting pore-lining regions in transmembrane protein sequences. BMC Bioinformatics **13,** 169.

Odenbach, D., Breth, B., Thines, E., Weber, R.W., Anke, H., and Foster, A.J. (2007). The transcription factor Con7p is a central regulator of infection-related morphogenesis in the rice blast fungus Magnaporthe grisea. Molecular Microbiology **64,** 293-307.

Oh, H.-S., and Lee, Y.-H. (2000). A target-site-specific screening system for antifungal compounds on appressorium formation in Magnaporthe grisea. Phytopathology **90,** 1162-1168.

Oh, Y., Donofrio, N., Pan, H., Coughlan, S., Brown, D.E., Meng, S., Mitchell, T., and Dean, R.A. (2008). Transcriptome analysis reveals new insight into appressorium formation and function in the rice blast fungus Magnaporthe oryzae. Genome Biology **9,** R85.

Osherov, N., and May, G. (2000). Conidial germination in Aspergillus nidulans requires RAS signaling and protein synthesis. Genetics **155,** 647-656.

Osherov, N., and May, G.S. (2001). The molecular mechanisms of conidial germination. FEMS Microbiology Letters **199,** 153-160.

Ou, S. (1980). Pathogen variability and host resistance in rice blast disease. Annual Review of Phytopathology **18,** 167-187.

Overington, J.P., Al-Lazikani, B., and Hopkins, A.L. (2006). How many drug targets are there? Nature reviews. Drug Discovery **5,** 993-996.

Pavesi, G., Mereghetti, P., Mauri, G., and Pesole, G. (2004). Weeder Web: discovery of transcription factor binding sites in a set of sequences from co-regulated genes. Nucleic Acids Research **32,** W199-W203.

Plotnikov, A., Zehorai, E., Procaccia, S., and Seger, R. (2011). The MAPK cascades: signaling components, nuclear roles and mechanisms of nuclear translocation. Biochimica et Biophysica Acta **1813,** 1619-1633.

Qi, Z., Wang, Q., Dou, X., Wang, W., Zhao, Q., Lv, R., Zhang, H., Zheng, X., Wang, P., and Zhang, Z. (2012). MoSwi6, an APSES family transcription factor, interacts with MoMps1 and is required for hyphal and conidial

morphogenesis, appressorial function and pathogenicity of Magnaporthe oryzae. Molecular Plant Pathology **13,** 677-689.

Ramanujam, R., and Naqvi, N.I. (2010). PdeH, a high-Affinity cAMP phosphodiesterase, is a key regulator of asexual and pathogenic differentiation in Magnaporthe oryzae. PLoS Pathogens **6,** e1000897.

Ramanujam, R., Calvert, M.E., Selvaraj, P., and Naqvi, N.I. (2013). The late endosomal HOPS complex anchors active G-protein signaling essential for pathogenesis in Magnaporthe oryzae. PLoS Pathogens **9,** e1003527.

Rho, H.-S., Jeon, J., and Lee, Y.-H. (2009). Phospholipase C-mediated calcium signalling is required for fungal development and pathogenicity in Magnaporthe oryzae. Molecular Plant Pathology **10,** 337-346.

Ritter, S.L., and Hall, R.A. (2009). Fine-tuning of GPCR activity by receptor-interacting proteins. Nat Rev Mol Cell Biol **10,** 819-830.

Rochdi, M.D., Laroche, G., Dupré, É., Giguère, P., Lebel, A., Watier, V., Hamelin, É., Lépine, M.-C., Dupuis, G., and Parent, J.-L. (2004). Nm23-H2 interacts with a G protein-coupled receptor to regulate its endocytosis through an Rac1-dependent mechanism. Journal of Biological Chemistry **279,** 18981-18989.

Rossman, A.Y., Howard, R.J., and Valent, B. (1990). Pyricularia grisea, the correct name for the rice blast disease fungus. Mycologia **82,** 509-512.

Sadat, M.A., Jeon, J., Mir, A.A., Choi, J., Choi, J., and Lee, Y.-H. (2014). Regulation of cellular diacylglycerol through lipid phosphate phosphatases is required for pathogenesis of the rice blast fungus, Magnaporthe oryzae. PloS One **9,** e100726.

Sambrook, J., and Russell, D.W. (2006). Purification of nucleic acids by extraction with phenol:chloroform. Cold Spring Harbor Protocols **2006,** pdb.prot4455.

Saunders, D.G.O. (2015). Hitchhiker's guide to multi-dimensional plant pathology. New Phytologist **205,** 1028-1033.

Schagger, H. (2006). Tricine-SDS-PAGE. Nat. Protocols **1,** 16-22.

Schweizer, P., Felix, G., Buchala, A., Müller, C., and Métraux, J.P. (1996). Perception of free cutin monomers by plant cells. Plant Journal **10,** 331-341.

Sesma, A., and Osbourn, A.E. (2004). The rice leaf blast pathogen undergoes developmental processes typical of root-infecting fungi. Nature **431,** 582-586.

Skamnioti, P., and Gurr, S.J. (2007). Magnaporthe grisea cutinase2 mediates appressorium differentiation and host penetration and is required for full virulence. The Plant Cell **19,** 2674-2689.

Smékalová, V., Doskočilová, A., Komis, G., and Šamaj, J. (2014). Crosstalk between secondary messengers, hormones and MAPK modules during abiotic stress signalling in plants. Biotechnology Advances **32,** 2-11.

Soanes, D.M., Kershaw, M.J., Cooley, R.N., and Talbot, N.J. (2002). Regulation of the MPG1 hydrophobin gene in the rice blast fungus Magnaporthe grisea. Molecular Plant-Microbe Interactions : MPMI **15,** 1253-1267.

Soanes, D.M., Chakrabarti, A., Paszkiewicz, K.H., Dawe, A.L., and Talbot, N.J. (2012). Genome-wide transcriptional profiling of appressorium development by the rice blast fungus Magnaporthe oryzae. PLoS Pathogens **8,** e1002514.

Stahl, E.A., and Bishop, J.G. (2000). Plant-pathogen arms races at the molecular level. Current Opinion in Plant Biology **3,** 299-304.

Stull, J.T. (2001). Ca2+-dependent cell signaling through calmodulin-activated protein phosphatase and protein kinases minireview series. Journal of Biological Chemistry **276,** 2311-2312.

Tag, A., Lambou, K., Collemare, J., Clergeot, P.H., Barbisan, C., Perret, P., Beffa, R., Thomas, T., and Lebrun, M.H. (in preparation). The rice blast fungus Magnaporthe grisea transcription factor BIP1 is required for pathogenesis and regulates a distinct set of appressorium specific genes.

Talbot, N.J. (1995). Having a blast: exploring the pathogenicity of Magnaporthe grisea. Trends in Microbiology **3,** 9-16.

Talbot, N.J., Ebbole, D.J., and Hamer, J.E. (1993). Identification and characterization of MPG1, a gene involved in pathogenicity from the rice blast fungus Magnaporthe grisea. The Plant Cell **5,** 1575-1590.

Talbot, N.J., Kershaw, M.J., Wakley, G.E., De Vries, O., Wessels, J., and Hamer, J.E. (1996). MPG1 encodes a fungal hydrophobin involved in surface interactions during infection-related development of Magnaporthe grisea. The Plant Cell **8,** 985-999.

Tewson, P., Westenberg, M., Zhao, Y., Campbell, R.E., Quinn, A.M., and Hughes, T.E. (2012). Simultaneous detection of Ca2+ and diacylglycerol signaling in living cells. PloS One **7,** e42791.

Thines, E., Weber, R.W., and Talbot, N.J. (2000). MAP kinase and protein kinase A-dependent mobilization of triacylglycerol and glycogen during appressorium turgor generation by Magnaporthe grisea. The Plant Cell **12,** 1703-1718.

Thines, E., Eilbert, F., Sterner, O., and Anke, H. (1997). Signal transduction leading to appressorium formation in germinating conidia of Magnaporthe grisea: effects of second messengers diacylglycerols, ceramides and sphingomyelin. FEMS Microbiology Letters **156,** 91-94.

Traweger, A., Fuchs, R., Krizbai, I.A., Weiger, T.M., Bauer, H.C., and Bauer, H. (2003). The tight junction protein ZO-2 localizes to the nucleus and interacts with the heterogeneous nuclear ribonucleoprotein scaffold attachment factor-B. The Journal of Biological Chemistry **278,** 2692-2700.

Uchiyama, T., and Okuyama, K. (1990). Participation of Oryza sativa leaf wax in appressorium formation by Pyricularia oryzae. Phytochemistry **29,** 91-92.

Valent, B., and Chumley, F.G. (1991). Molecular genetic analysis of the rice blast fungus, Magnaporthe grisea. Annual Review of Phytopathology **29,** 443-467.

Valent, B., and Khang, C.H. (2010). Recent advances in rice blast effector research. Current Opinion in Plant Biology **13,** 434-441.

Van Criekinge, W., and Beyaert, R. (1999). Yeast two-hybrid: state of the art. Biological Procedures Online **2,** 1-38.

Van Dijck, P. (2009). Nutrient sensing G protein-coupled receptors: interesting targets for antifungals? Medical Mycology **47,** 671-680.

Velculescu, V.E., Vogelstein, B., and Kinzler, K.W. (2000). Analysing uncharted transcriptomes with SAGE. Trends in Genetics : TIG **16,** 423-425.

Veneault-Fourrey, C., Barooah, M., Egan, M., Wakley, G., and Talbot, N.J. (2006). Autophagic fungal cell death is necessary for infection by the rice blast fungus. Science **312,** 580-583.

Vidhyasekaran, P. (2007). Fungal Pathogenesis in Plants and Crops: Molecular Biology and Host Defense Mechanisms, Second Edition (CRC Press: USA).

White, M.A. (1996). The yeast two-hybrid system: forward and reverse. Proceedings of the National Academy of Sciences of the United States of America **93,** 10001-10003.

Widawsky, D.A., and O'Toole, J.C. (1990). Prioritizing the rice biotechnology research agenda for Eastern India (Rockefeller Foundation: New York).

Wilson, R.A., and Talbot, N.J. (2009). Under pressure: investigating the biology of plant infection by Magnaporthe oryzae. Nature Reviews. Microbiology **7,** 185-195.

Wösten, H.A., Schuren, F.H., and Wessels, J.G. (1994). Interfacial self-assembly of a hydrophobin into an amphipathic protein membrane mediates fungal attachment to hydrophobic surfaces. The EMBO Journal **13,** 5848-5854.

Xiao, J.Z., Watanabe, T., Kamakura, T., Ohshima, A., and Yamaguchi, I. (1994). Studies on cellular differentiation of Magnaporthe grisea: physicochemical aspects of substratum surfaces in relation to appressorium formation. Physiological and Molecular Plant Pathology **44,** 227-236.

Xiao, W. (2006). Yeast Protocols. (Humana Press: USA).

Xu, J.R. (2000). Map kinases in fungal pathogens. Fungal genetics and biology : FG & B **31,** 137-152.

Xu, J.R., and Hamer, J.E. (1996). MAP kinase and cAMP signaling regulate infection structure formation and pathogenic growth in the rice blast fungus Magnaporthe grisea. Genes & Development **10,** 2696-2706.

Xu, J.R., Staiger, C.J., and Hamer, J.E. (1998). Inactivation of the mitogen-activated protein kinase Mps1 from the rice blast fungus prevents penetration of host cells but allows activation of plant defense responses. Proceedings of the National Academy of Sciences of the United States of America **95,** 12713-12718.

Xu, J.R., Zhao, X., and Dean, R.A. (2007). From genes to genomes: a new paradigm for studying fungal pathogenesis in Magnaporthe oryzae. Advances in Genetics **57,** 175-218.

Xu, X.-H., Su, Z.-Z., Wang, C., Kubicek, C.P., Feng, X.-X., Mao, L.-J., Wang, J.-Y., Chen, C., Lin, F.-C., and Zhang, C.-L. (2014). The rice endophyte Harpophora oryzae genome reveals evolution from a pathogen to a mutualistic endophyte. Scientific Reports **4,** 5783.

Xue, C., Bahn, Y.S., Cox, G.M., and Heitman, J. (2006). G protein-coupled receptor Gpr4 senses amino acids and activates the cAMP-PKA pathway in Cryptococcus neoformans. Molecular biology of the Cell **17,** 667-679.

Yong-Hwan, L., and Dean, R.A. (1994). Hydrophobicity of contact surface induces appressorium formation in Magnaporthe grisea. FEMS Microbiology Letters **115,** 71-75.

Zeigler, R.S., Leong, S.A., Teng, P.S., International, C.A.B., and Institute, I.R.R. (1994). Rice Blast Disease. (CAB International).

Zhang, N., Zhao, S., and Shen, Q. (2011). A six-gene phylogeny reveals the evolution of mode of infection in the rice blast fungus and allied species. Mycologia **103,** 1267-1276.

Zhang, S., and Xu, J.-R. (2014). Effectors and Effector Delivery in Magnaporthe oryzae. PLoS Pathogens **10,** e1003826.

Zhang, Z., Priddey, G., and Gurr, S.J. (2001). The barley powdery mildew protein kinase C gene, pkc1 and pkc-like gene, are differentially expressed during morphogenesis. Molecular Plant Pathology **2,** 327-337.

Zheng, W., Zhao, Z., Chen, J., Liu, W., Ke, H., Zhou, J., Lu, G., Darvill, A.G., Albersheim, P., Wu, S., and Wang, Z. (2009). A Cdc42 ortholog is required for penetration and virulence of Magnaporthe grisea. Fungal Genetics and Biology : FG & B **46,** 450-460.

APPENDIX A

PRIMERS USED IN THIS STUDY

All sequences are written in the 5’ to 3’ direction.

Primers for generating gene replacement construct via split-marker approach	
M13F	GTCACGACGTTGTAAAACGACGGCCAGT
M13R	CAATTTCACACAGGAAACAGCTATGACC
HY	GTTGGTCAAGACCAATGCGGAGCA
YG	CGACAGCGTCTCCGACCTGATG
P1	GCAACTGTCACAGTCAATG
P2	ACTGGCCGTCGTTTTACAACGTCGTGACTCTTGGTGCGACTGTCCTTG
P3	GGTCATAGCTGTTTCCTGTGTGAAATTGTGATGATGATTATATGGCTG
P4	TGACTGGCCCTCCTCATATC
Primers for validation of gene replacement	
3’-PLG1	TCATGATTGTGTCTGGTAGA
5’-PLG1	TGATCGTAGACCACTCTCTA
3’-HYG	CTATTCCTTTGCCCTCG
5’-HYG	CTATTCCTTTGCCCTCG
3’- DOWNFAR	AGAGGTTCTGGCAAAACTCG
5’- UPFAR	GAATCTTGAACTCAATCGGT
UP-03584 JXN	CAAGGACAGTCGCACCAAGATGATCG
DOWN-03584 JXN	CAGCCATATAATCATCATCATCATGAT
UP-HYG JXN	CAAGGACAGTCGCACCAAGAGTCAC
DOWN-HYG JXN	CAGCCATATAATCATCATCACAATTTC
5’-UPnearHYG	GCAATATAAACAGAGCGGCT
3’-DOWNnearHYG	CAACTGGTCCTTGGAGTGTC
Primers for construction and validation of complementation vector	
3’- DOWNFAR	AGAGGTTCTGGCAAAACTCG
5’- UPFAR	GAATCTTGAACTCAATCGGT

Table (continued)

Primers for construction and validation of complementation vector	
5'-innerPLG1	TGTACTGATCACGTTGGCTG
3'-innerPLG1	CAGCAATCCGACGTACGGTA
5'-BAR	TGCACCATCGTCAACCACTA
3'-BAR	ACAGCGACCACGCTCTTGAA
5'-CA_XhoI	TCCGGAGAGAGTCTCAATCT
5'-CA_XhoI	GGTCTACGATCATCTTGGTG
Primers for construction of GFP-tagged construct	
5'-GFP_Inframe_EcoRI	GGCCGAATTCCATGGTGAGCAAGGG
3'-GFP_Inframe_EcoRI	GGCGAATTCCCTTGTACAGCTCGTC
5'-UP5_GFPjxn	CCAAGGCCGAATTCCATGGTG
3'-PLG1_GFPjxn	TCATGAATTCTTGTACAGCTC
5'-SDM_EcoRI	GACAGTCGCACCAAGGAATTCATGAT
3'-SDM_EcoRI	GTGGTCTACGATCATGAATTCCTTGG
Primers for qRT-PCR assay	
5'-EF1α_qPCR	GCCCGGTATGGTCGTTACCT
3'-EF1α_qPCR	AGCTGCTGGTGGTGCATCTC
5'-ILV5_qPCR	CCAGCTCTACGACTCGGTCAA
3'-ILV5_qPCR	AGTCGGGCTGGCTGTTGTAGT
5'-PLG1_qPCR	TCATTGGCATGATGGTTCGT
3'-PLG1_qPCR	CGATATCACTGGGCTGCAAA
5'-cPKA_qPCR	CCAACGACGAGCGCAAA
3'-cPKA_qPCR	CAACGTAATCAGGAACGGATTCT
5'-PKC_qPCR	GGAAGACATGTGGTACGGCTCTA
3'-PKC_qPCR	GCAAAATTTCTGGTGCCATAAAC
5'-PMK1_qPCR	GCGAGGGCGCTTATGGA
3'-PMK1_qPCR	TCTTCTTTATGGCAACCTTTTGG

Table (continued)

Primers for the yeast two hybrid constructs	
5’-PLG1_EcoRI	CCGGGAATTC ATCGTAGACCACTCT
3’-PLG_SalI	CCGGGTCGACTGATTGTGTCTGGTA
5’-Nterm45bp_EcoRI	CCGGGAATTCATCGTAGACCACTCT
3’-Nterm45bp_SalI	CCGGGTCGACGACGCCGCTCAT
5’-2ndcytloop_EcoRI	CCGGGAATTC TTTTTGCTCCAA
3’-2ndcytloop_SalI	CCGGGTCGACGCGCTTCATCCC
5’-PLG1fullCterm_EcoRI	CCGGGAATTC GTATCTACATTCAAC
3’-PLG1fullCterm_SalI	CCGGGTCGACTGATTGTGTCTGGT
5’-V-S1Cterm_EcoRI	CCGGGAATTC GTATCTACATTCAAC
3’-V-S1Cterm_SalI	CCGGGTCGACGGAGAAGGTCGAAG
5’-K-GCterm_EcoRI	CCGGGAATTC AAGGCTCGCTCCGC
3’-K-GCterm_SalI	CCGGGTCGACCCCACGAGGCGATC
5’-F-S2Cterm_EcoRI	CCGGGAATTC TTCAACATGCAGAC
3’-F-S2Cterm_SalI	CCGGGTCGACTGATTGTGTCTGGT
5’-Mag_SmaI	CCGGGAATTCATGGGCGCTTGCATG
3’-MagA_EcoRI	CCCGGGCAGAATACCTGAG
5’-MagB_NdeI	ATCGGCATATGCGGCAGCACCCTATT
3’-MagB_BamHI	CCGGGGATTCTGATAACCGAAGGAT
5’-MagC_NdeI	CATATGCAAGCACTCAGTTG
3’-MagC_BamHI	GGATCCCAAGATGAGTTG
5’-DNA-BD_T7	GTAATACGACTCACTATAGGGCGA
3’-DNA-BD_T7	TACCTGAGAAAGCAACCTGACCTACAGG
5’-AD_T7	GTAATACGACTCACTATAGGGCGA
3’-AD_T7	ACTTGCGGGGTTTTTCAGTATCTACGAT

APPENDIX B

VALIDATION OF Y2H CONSTRUCTS

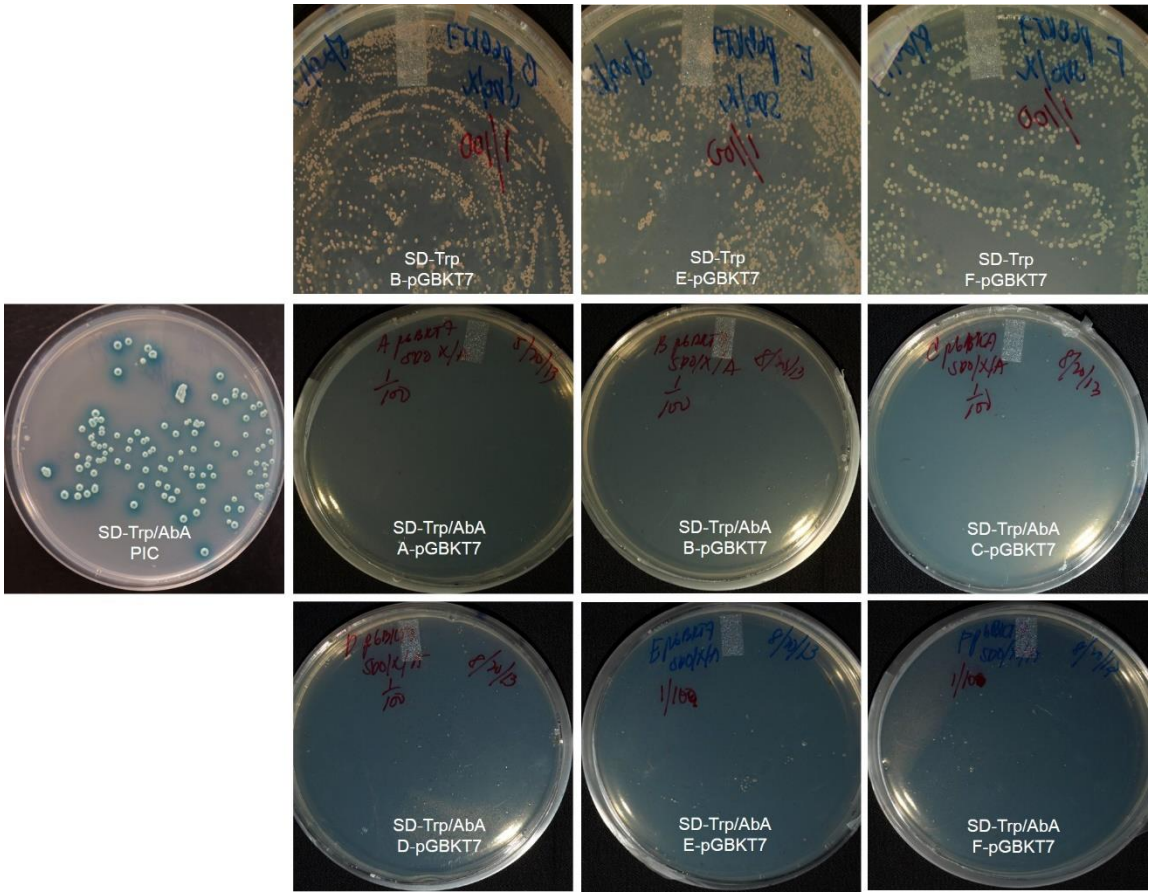

Bait Autoactivation Test on Minimal Media Lacking Tryptophan or on Minimal Media Lacking Tryptophan and Supplemented with AbA

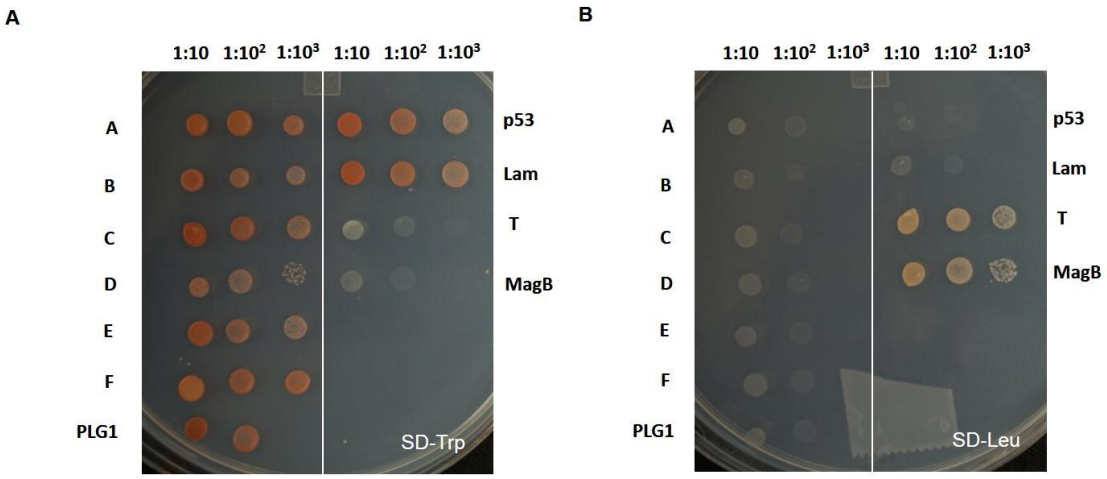

Validation of the PLG1 and Control Baits and MagB and Control Prey Constructs on Minimal Media Lacking Either Tryptophan **(A)** or Leucine **(B)**